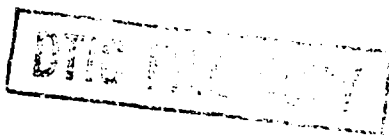


AD-A234 242



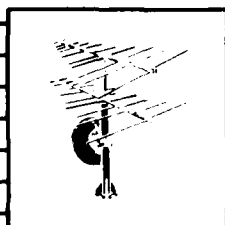
ARO 27981.1-EG-SBI

FINAL REPORT  
PHASE I SBIR

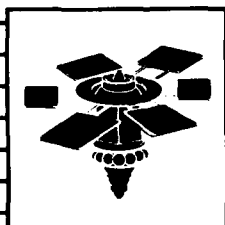
USE OF PROPERTY RESTORAL ALGORITHMS FOR BLIND  
ADAPTATION OF RECEIVE-PATH AND TRANSMIT-PATH  
ANTENNA ARRAYS IN A GROUND-BASED COMMUNICATION SYSTEM



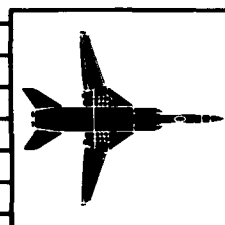
FEBRUARY 22, 1991



C3CM Systems



Decoys



Threat Simulators



Advanced  
CounterMeasure  
Systems

REPORT DOCUMENTATION PAGE

1a. REPORT SECURITY CLASSIFICATION <i>Unclassified</i>		1b. RESTRICTIVE MARKINGS	
2a. SECURITY CLASSIFICATION AUTHORITY		3. DISTRIBUTION/AVAILABILITY OF REPORT  Approved for public release; distribution unlimited.	
2b. DECLASSIFICATION/DOWNGRADING SCHEDULE			
4. PERFORMING ORGANIZATION REPORT NUMBER(S)		5. MONITORING ORGANIZATION REPORT NUMBER(S)  <i>ARO 27981.1-EL-SBI</i>	
6a. NAME OF PERFORMING ORGANIZATION <i>Advanced CounterMeasure Systems</i>	6b. OFFICE SYMBOL <i>(if applicable)</i>	7a. NAME OF MONITORING ORGANIZATION  <i>U. S. Army Research Office</i>	
6c. ADDRESS (City, State, and ZIP Code) <i>9838 Old Placerville Road Sacramento, CA 95827</i>		7b. ADDRESS (City, State, and ZIP Code)  <i>P. O. Box 12211 Research Triangle Park, NC 27709-2211</i>	
8a. NAME OF FUNDING/SPONSORING ORGANIZATION <i>U. S. Army Research Office</i>	8b. OFFICE SYMBOL <i>(if applicable)</i>	9. PROCUREMENT INSTRUMENT IDENTIFICATION NUMBER  <i>DAAL03-90-C-0025</i>	
8c. ADDRESS (City, State, and ZIP Code)  <i>P. O. Box 12211 Research Triangle Park, NC 27709-2211</i>		10. SOURCE OF FUNDING NUMBERS	
		PROGRAM ELEMENT NO.	PROJECT NO.
		TASK NO.	WORK UNIT ACCESSION NO.

11. TITLE (Include Security Classification) *Use of Property Restoral Algorithms for blind adaption of receive-path and transmit-path antenna arrays in a ground-based communication system. (unclassified)*

12. PERSONAL AUTHOR(S)  
*Dean W. Minster*

13a. TYPE OF REPORT <i>Final</i>	13b. TIME COVERED <i>FROM Sept 90 TO Feb 91</i>	14. DATE OF REPORT (Year, Month, Day) <i>22 February 1991</i>	15. PAGE COUNT <i>130</i>
-------------------------------------	--	--	------------------------------

16. SUPPLEMENTARY NOTATION  
*The view, opinions and/or findings contained in this report are those of the author(s) and should not be construed as an official Department of the Army position, policy, or decision, unless so designated by other documentation.*

17. COSATI CODES			18. SUBJECT TERMS (Continue on reverse if necessary and identify by block number)
FIELD	GROUP	SUB-GROUP	

19. ABSTRACT (Continue on reverse if necessary and identify by block number)

A receive adaptation algorithm which is tailored for spread spectrum communications, frequency hopping and direct sequence, has been developed. A receive architecture which is compatible with existing Army radios, yet flexible enough to accomodate a variety of algorithms, using commercially available and proven components, and with minimum complexity to allow size and power reductions in future designs to result in compatibility with the Army's mobile applications, has been developed. The performance of the algorithm and limitations of the architecture have been simulated, and the expected performance is evaluated.

In addition, the possibility of using the information acquired during receive adaptation to steer transmit beams in either retrodirective or directive fashion was explored. Two applications in particular are addressed: Low Probability of Intercept (LPI) and Anti-Jam (A/J) communications. The concepts for application of an Adaptive Array Processor (AAP) to LPI and A/J communications is presented, and the expected performance is simulated and evaluated.

20. DISTRIBUTION/AVAILABILITY OF ABSTRACT <input type="checkbox"/> UNCLASSIFIED/UNLIMITED <input type="checkbox"/> SAME AS RPT. <input type="checkbox"/> UTK USERS		21. ABSTRACT SECURITY CLASSIFICATION <i>Unclassified</i>	
22a. NAME OF RESPONSIBLE INDIVIDUAL <i>Richard M. Denison, CFO</i>		22b. TELEPHONE (Include Area Code) <i>(916) 362-9226</i>	22c. OFFICE SYMBOL

## 1. FORWARD

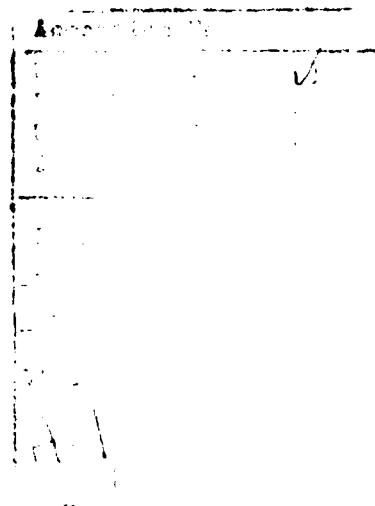
Advanced Countermeasure Systems (ACM Systems) has completed the Phase I SBIR awarded on August 6, 1990 under the U.S. Army Research Office contract number DAAL03-90-C-0025. This document is the final report of this Phase I study effort.

The original RFP solicitation, A90-099 Adaptive Antennas and Processing, stated the objective to be "Perform research to provide technology for adaptive antenna arrays and processing for Army tactical ground radio communications." The solicitation went on to describe the general requirements to be "Army tactical ground radio systems operate in an environment of strong and complex interference. Adaptive antennas have the potential to provide 20-30 db gain. However the systems must have the ability to converge rapidly in the presence of worst case countermeasures and must be small since Army communication terminals need to be mobile. Research is also needed on the operation of such antennas in wideband systems such as spread spectrum, frequency hopping and direct sequence. Techniques must also be found for the utilization and integration of adaptive antennas in Army networks." The specific Phase I goal was stated to be "... demonstrate the feasibility of small adaptive antennas under conditions of high interference (jamming)."

These objectives and goals of Phase I have been met and exceeded by ACM Systems, as is evident in the final report which follows. A receive adaptation algorithm which is tailored for spread spectrum communications, frequency hopping and direct sequence, has been developed. A receive architecture which is compatible with existing Army radios, yet flexible enough to accomodate a variety of algorithms, using commercially available and proven components, and with minimum complexity to allow size and power reductions in future designs to result in compatibility with the Army's mobile applications, has been developed. The performance of the algorithm and limitations of the architecture have been simulated, and the expected performance is evaluated.

In addition, as part of our Phase I effort, ACM Systems explored the possibility of using the information acquired during receive adaptation to steer transmit beams in either retrodirective or directive fashion. Two applications in particular are addressed: Low Probability of Intercept (LPI) and Anti-Jam (A/J) communications. The concepts for application of an Adaptive Array Processor (AAP) to LPI and A/J communications is presented, and the expected performance is simulated and evaluated.

The goal for Phase II of this SBIR, as stated in the original solicitation, is "... demonstrate hardware implementation of small adaptive antennas." ACM Systems' response to this Phase II goal is the recently submitted proposal, dated January 7, 1991, and entitled A Multi-Purpose Adaptive Array Processor Hardware Development for Frequency Hopped, Direct Sequence Spread Spectrum Radios. This proposal addresses and exceeds the Government's expectations for Phase II of this SBIR program.



## 2. TABLE OF CONTENTS

<u>Section</u>	<u>Title</u>	<u>Page</u>
1.	Foward	1
2.	Table of Contents	2
3.	List of Appendixes, Illustrations and Tables	3
4.	Body of Report	4
4.1	Statement of the Problem Studied	4
4.2	Summary of the Most Important Results	5
4.3	Work Carried Out / Results Obtained	6
4.3.1	Introduction	6
4.3.2	Algorithm Development	7
4.3.2.1	Introduction	7
4.3.2.2	Reveive Algorithms Investigated	8
4.3.2.3	Baseline: Dominant Mode Maximin Algorithm	13
4.3.2.4	Dominant Mode Derivation	15
4.3.2.5	Adaptation Convergence and Stability Analysis	17
4.3.2.6	Receive Adaptation Performance Analysis	24
4.3.2.7	Directive / Retrodirective Communication	32
4.3.2.8	Directive Communications Performance Analysis	34
4.3.3	Architecture Development	39
4.3.3.1	Introduction	39
4.3.3.2	Data Collection and Top Level Architecture	41
4.3.3.3	Complex Weighting	46
4.3.3.4	Statistical Measurements	51
4.3.3.5	Weight Calculations	56
4.3.3.6	Baseline AAP Architecture	59
4.3.3.7	Calibration	74
4.3.3.8	Complete Baseline Receive AAP Architecture	84
4.3.3.9	Transmit Architecture	86
4.3.4	Computer Modeling and Simulations	88
4.3.4.1	Introduction	88
4.3.4.2	Simulation Descriptions	88
4.3.4.3	Simulation Results	99
4.3.5	Documentation	123
4.4	Technical Feasibility (Evaluation of Results)	123
4.4.1	Introduction	123
4.4.2	Algorithm Technical Feasibility	123
4.4.3	Architecture Technical Feasibility	124
4.4.4	Simulated Performance Evaluation	124
4.4.5	Summary / Conclusions	126
4.5	List of All Technical Publications	126
4.6	Personnel Earning Advanced Degrees While on Project	127
5.	Bibliography	128
6.	Appendixes	130

## 3. LIST OF APPENDIXES, ILLUSTRATIONS AND TABLES

<u>Figure</u>	<u>Title</u>	<u>Page</u>
1	Collision Threshold Values	31
2	Data Collection Timing	40
3	Block Diagram, Spectral Separation Off Time Data	42
4	Block Diagram, Anticipative Off Time Data	44
5	Complex Weighting Options	47
6	Statistical Measurement Options	53
7	Analog Calculator Block Diagram	55
8	Digital Controller Block Diagram	58
9	Block Diagram, Baseline Choice # 1	60
10	Block Diagram, Baseline Choice # 2	63
11	RF Assembly Block Diagram	64
12	IF Assembly Block Diagram	66
13	Synthesizer Block Diagram	70
14	Calibration of Complex Weights	75
15	Calibration of Statistical Measurements	77
16	Calibration of Baseband Data Collection	79
17	Calibration of IF Correlation Data, Step 1	81
18	Calibration of IF Correlation Data, Step 2	83
19	Complete Baseline Receive AAP Block Diagram	85
20	Transmit Considerations	87
21	Algorithm Flow Chart	96
22	Baseline Jammer Scenario	100
23	SINR Convergence	101
24	Baseline Receive Antenna Patterns	104
25	Changing SOI DOA Receive Antenna Patterns	105
26	Antenna Pattern Drift in Absence of SOI	106
27	SINR Drift in Absence of SOI	107
28	Antenna Array Geometries	109
29	Receive Antenna Patterns vs. Number of Elements	111
30	Receive Antenna Patterns vs. Array Diameter	112
31	Convergence Time vs. Jammer Level	114
32	Retrodirective Antenna Patterns	116
33	Smoothing Aperature Estimates	117
34	Directivity vs. Number of Elements	118
35	LPI - Directive Comm Intercept Footprints	120
36	Intercept Footprint Reduction vs. # of Elements	121
37	A/J - Directive Comm Jammer Footprints	122

<u>Table</u>	<u>Title</u>	<u>Page</u>
1	Bin Center Frequencies	88
2	SOI Parameters	89
3	System Parameters	90
4	Jammer Parameters	90
5	User Specified Processing Parameters	95
6	Algorithm Variables	95
7	Output SINR for Initial Visits	102
8	Output SINR for Various Jammer Levels	113

## 4. BODY OF REPORT

### 4.1 STATEMENT OF PROBLEM STUDIED

The Phase I technical objectives were stated in the proposal as follows:

*The goal of Phase I is to determine the ability of property restoral algorithms to be used for blind signal extraction and directive/retrodirective transmission, and to develop low-cost architectures for performing this processing. This goal is accomplished using the following procedure.*

- *Identify realistic test cases for developing and evaluating the blind directive / retrodirective communication system.*

- *Design a candidate property restoral algorithm that is best able to blindly adapt the receive-path array weights in the environment identified above, and develop methods for using the receive-path weights to compute the transmit-path array weights that maximizes the transmitted signal energy in the direction of the received signal communicator.*

- *Develop a realistic architecture for performing the signal reception and directive / retrodirective transmission using the algorithm designed above, and determine the cost / performance tradeoffs for each of these structures under realistic dynamic range / noise conditions.*

- *Evaluate the performance of the processing algorithm and reception / transmission system developed above, using theoretical analysis and computer simulation.*

*Two primary approaches are to be considered for performing the blind emitter reception: LSCMA adaptation, with initialization / recapture via transience exploitation; and spectral self-coherence restoral.*

Rather than proceeding blindly towards the stated objectives of the proposal, ACM Systems contacted several interested Government technical representatives early in the Phase I program, to ascertain the areas of greatest interest for investigation and development under this contract. The stated objectives of the proposal were widely accepted and encouraged, with the following points of emphasis suggested as well:

- Any receive adaptation algorithm would need to be optimized for application to spread spectrum communication systems, both frequency hopped and direct sequence.

- Previous Government studies and independent research efforts have yielded many receive adaptation algorithms. An effort which addresses architectural implementations of these various algorithms, as well future algorithms, was needed.

- The architectures developed as part of this study must consider the intended application: existing Army tactical ground based communication systems. This implies low cost, small size, low power dissipation, and of course frequency hopping, direct sequence spread spectrum signal compatibility.

The objectives as stated in the proposal, modified to emphasize the areas suggested by concerned technical representatives from the Government, were accomplished via a Phase I Work Plan which included the following tasks: 1) Algorithm Development, 2) Architecture Development, 3) Performance Evaluation and 4) Documentation. Detailed descriptions of the results of this study are organized according to these tasks within section 4.3.

## 4.2 SUMMARY OF THE MOST IMPORTANT RESULTS

The most important results obtained in the course of this Phase I study are stated briefly below. Detailed descriptions and explanations are provided in section 4.3.

○ A realistic computer model of jammers, signals of interest, AAP front end processing, dynamic range constraints, the antenna array, directions of arrival, etc. has been established. Many key parameters are selectable variables, thereby allowing flexibility to study a variety of factors associated with each of these topics.

○ A new receive adaptation algorithm has been developed which is tailored for frequency hopped applications, the Dominant Mode Block Update algorithm. A derivation is provided, along with formal analysis of the algorithm's convergence, stability, and steady state performance. A proof indicating this algorithm to be a maximum likelihood estimator was begun and will be submitted for publication at a later date. Acknowledgement to this project for its contribution to the paper will be made at that time.

○ The algorithm was modeled on the computer and its performance was simulated for various signal, antenna array, and timing conditions. The simulated performance results are encouraging:

- Frequency hopped performance is verified, with convergence the maximum attainable SINR within a fraction of a timeslot (EPLRS timing assumed).
- The antenna patterns were generated, revealing simultaneous nulls in the direction of jammers and a beam in the direction of the desired signal.
- The number of host radio data samples required for integration by the AAP is investigated by simulation; 16 is sufficient.
- The impact of a desired signal not being present during a timeslot in which it is expected was explored; there is little degraded performance, and is easily adjusted for in the architecture. This is likely in network communications.
- The algorithm converges to the maximum SINR in response to changing desired signal directions of arrival within a fraction of a timeslot.
- Several architectural limitations were identified and simulated; most proved not to impact AAP performance, while one result caused redesign of the off time data collection scheme.
- Performance for varying jammer conditions were simulated, including directions of arrival, number of simultaneous jammers, jammer power levels, and types of jammer waveforms. The AAP performance was successful and consistent for all conditions studied.
- Antenna array parameters were investigated for their impact on AAP performance, including the number of elements, the geometry of the array, and the spacing of the elements.

## 4.2 SUMMARY OF THE MOST IMPORTANT RESULTS, (continued)

o A receive AAP architecture was developed which is compatible with existing Army tactical radios and is capable of supporting the Dominant Mode Block Update algorithm as well as many others. The features of this architecture include:

- Complex weights can be implemented at RF if required by the host Army radio, but additional flexibility is available if IF may be used. Either implementation is supported by the architecture.
- The statistical measurements required for adaptation are made directly at IF for on time processing, and at baseband for off time data collection. This combination is optimal for fast adaptation while allowing a variety of algorithms to be implemented.
- The weights are calculated digitally, allowing maximum flexibility in algorithm selection. This also allows for storage and retrieval of weights, thereby greatly enhancing performance in frequency hopped systems.
- Techniques for correcting or calibrating all significant sources of error are identified.
- Options for all circuits required for hardware development of the AAP are identified and discussed.

o Methods for generating antenna beams for transmission were developed. Both directive and retrodirective techniques were investigated. Of particular interest is applications to Low Probability of Intercept (LPI) and Anti-Jam (A/J) communications. Techniques for smoothing aperture estimates, proven by simulation to be necessary, are suggested.

o Both LPI and A/J scenarios are simulated and evaluated, showing significant system performance improvements. Antenna patterns and areas exceeding critical power levels in the vicinity of the transmitter are generated to support the evaluations.

## 4.3 WORK CARRIED OUT / RESULTS OBTAINED

### 4.3.1 INTRODUCTION

The details of the work carried out for this Phase I SBIR and the results obtained are presented in this section. The work is divided into four primary efforts: Algorithm Development, Architecture Development, Computer Modeling and Simulations, and Documentation. The work carried out and the results obtained for each of these efforts are included in the following sections.

## 4.3.2 ALGORITHM DEVELOPMENT

### 4.3.2.1 INTRODUCTION

Receive adaptation algorithms have been customized for a variety of applications. An Army mobile tactical ground based communication system requires that the algorithm include:

- Compatibility with spread spectrum techniques, both frequency hopping (FH) and direct sequence (DSSS). Most Army radios employ FH, some use DSSS techniques; these are definitely the trends for future radios.

- Fast adaptation times are desired for compatibility with FH systems, preferably providing convergence in a fraction of the transmit time period of the network radios. If this is not achieved, the adaptation must occur over several timeslots. In a network communication system, the radio attempts to receive signals from several other radios in the network, many having different directions of arrival (DOAs). In this case, steering a beam as well as nulls over several timeslots is difficult since the DOA of the desired signal changes during adaptation.

- Steering nulls in the directions of interferers is required. Reduced interference output power will generally improve the SINR provided to the host radio, but not necessarily. The desired signal may have a DOA which is in the direction of an inadvertent null formed by minimizing the interference output power. Simultaneously steering a beam in the desired signal's DOA assures the SINR will be improved, and is therefore highly desirable.

- Ease of implementation, thereby resulting in a design which minimizes the amount of hardware required. This requirement reflects the need for the AAP to be small and mobile.

- Tolerance to the severe multi-path conditions associated with ground communications.

- Frequency compensation or memory of previous, frequency dependent weights, necessary to support the wide operating bandwidths of the FH systems.

- Capability to support the wide cancellation bandwidths required for DSSS signals.

- Capable of performing blind adaptation - without special purpose antennas, special sensor geometries, matched receiver to array calibrations, or special training signals.

- Optimized for operation in severe jamming environments.

A brief summary of the receive adaptation algorithms considered as part of this study is provided in this section. A baseline algorithm is selected for focus in the architecture development and computer modeling and performance simulations. This selection is justified and further developed to meet the specific requirements of this application. An overview of the selected algorithm is provided, followed by its derivation, an analysis of its convergence and stability properties, and an analysis of its expected performance.

The concepts of directive and retrodirective communications are addressed as well. The algorithms for generating the transmit weights based on receive adaptation information is described, with emphasis on two applications: Low Probability of Intercept (LPI) communications and purely anti-jam (A/J) capabilities. Figures of merit for evaluating the directive communication system's performance are established, and the optimal transmit weights for both cases of interest are calculated.

#### 4.3.2.2 RECEIVE ALGORITHM INVESTIGATION

Several approaches were considered in this Study for adapting the receive-site antenna array, based on the possible attributes of the modulation format to be employed by the communication link. These algorithms can be grouped into five basic classes of techniques:

- *nonblind techniques*, which adapt the processor using a nonblind steepest-descent or least-squares acquisition algorithm [1], followed by a post-acquisition tracking algorithm such as a decision-direct [2] or pilot-directed [3,4] algorithm;
- *coherence-exploiting techniques*, such as the Griffiths P-vector and Frost algorithms [5,6], the self-coherence restoral (SCORE) algorithms [7,8], and higher-order cumulant and spectral analysis techniques [9,10], which adapt the processor to exploit or restore known spatial, spectral, conjugate, or higher-order self-coherence of the transmitted signal waveforms;
- *modulus-restoral (MORE) techniques*, such as the constant-modulus algorithm (CMA) [11,12], known modulus algorithm [13], multiple-modulus algorithm [14], and adaptive modulus algorithm [7], which adapt the processor to restore known or estimable modulus properties of the transmitted signal waveform to the processor output signal;
- *regenerative techniques*, such as the regenerative DSSS acquisition algorithms developed in [15,16] and the more general reference-directed adaptation techniques developed in [17,18,19], all of which exploit the known spectral, temporal or statistical structure of the transmitted signal to generate a reference signal for use in a conventional steepest-descent or least-squares adaptation algorithm; and
- *Maximin techniques*, such as the steepest-ascent Maximin algorithms developed in [20,21,22] and the dominant-mode Maximin algorithm developed in [23,24] (referred to as the *burst acquisition* algorithm in those reports), and the adaptive detection and DSSS acquisition algorithms developed in [25,26] (which can be interpreted as *rank-1* Maximin algorithms), all of which adapt the processor to restore known or estimable temporal, spectral, or spreading support of the transmitted signal to the processor output signal.

However, it is possible to quickly narrow these techniques to a few obvious choices after considering the stringent communication system requirements described in the previous section. The requirement that the communication link be secure and LPI immediately precludes nonblind techniques, which require transmission of a known (and therefore easily detectable) preamble signal in order to acquire the communication signal at the beginning of the transmission. The requirement that the techniques, since the preamble signal must then be retransmitted at the beginning of every frequency hop to track the frequency-dependent variation of the dehopped transmission channel.

These requirements also preclude a number of the blind adaptation algorithms. The SCORE algorithms are precluded for LPI modulation formats, since these formats must exhibit a very low degree of spectral or conjugate self-coherence to prevent detection by conventional feature detection technique. In particular, the convergence time of the SCORE algorithms would exceed the hop duration of most practical frequency-agile communication waveforms at the receiver SINRs likely to be encountered by such systems. Higher order spectral analysis techniques are inapplicable to this communication waveform for similar reasons. The requirement that the processor operate without knowledge of the transmit signal DOA, special

#### 4.3.2.2 RECEIVE ALGORITHM INVESTIGATION (continued)

array geometries, or array calibration data precludes the remaining coherence exploiting techniques, all of which rely on this information.

The additional requirement that the AAP be small and low-cost mitigates against the majority of modulus restoral techniques. MORE techniques have been developed that can adapt quickly enough to track frequency agile communication signals [27,28], and to operate in the presence of multiple interferers [23,29,30]. However, this capability comes at the cost of increased computational complexity. In particular, the multitarget MORE algorithm described in [23,29,30] requires (and achieves) simultaneous capture and separation of all of the signals received at the transmit signal frequency. This capability is excessive in the radios of interest here<sup>1</sup>, which only require extraction of the intended transmit signal from the receive environment.

The regenerative and Maximin techniques can provide a simpler means for satisfying these requirements if the communication signal has a DSSS and/or frequency agile modulation format. All of these techniques are extremely robust, requiring only knowledge of the spreading code or hopping sequence to train the receiver processor<sup>2</sup>. In addition, the techniques are inherently selective providing only the intended transmit signal at the processor output.

Of these techniques, the Maximin approach is superior from robustness, performance and implementation viewpoints, particularly if the communication signal has a frequency agile communication format. The Maximin approach assumes *no* knowledge of the baseband signal structure, and can operate effectively if the baseband signal has *no* discernable (or exploitable) structure, e.g., if the baseband signal is a stationary Gaussian-distributed random process. Consequently, the approach is inherently less sensitive to error in the baseband signal model, for example, if the transmit signal is subjected to over modulation, bandlimiting or clipping operations over the communication channel. Moreover, the Maximin approach is insensitive to many commonly occurring errors in the *spreading* format used to modulate the baseband signal, such as sub-hop timing error or frequency offset in FH spreading formats [23,24].

In fact, the Maximin approach can usually outperform regenerative techniques under even ideal conditions where the transmitted signal waveform is not subject to modelling error. The ability of Maximin-adapted antenna arrays to capture frequency agile signals with nearly the maximum-attainable signal-to-noise ratio (SINR) of the array has been demonstrated via both theoretical analysis [23,24] and computer simulation [20]-[24], and for exceptionally severe interference powers and reception geometries. No similarly powerful result has been reported in the literature for any of the regenerative techniques developed to date.

---

<sup>1</sup>However, this capability may be of interest in some specialized applications, e.g., if the radio is a transponder or central node in a combat net radio system.

<sup>2</sup>The regenerative techniques reported in [15]-[19] also employ nonlinearities that all (at least implicitly) assume additional information about transmitted signal baseband, for example, that it has a low modulus variation or a known modulation format.

### 4.3.2.2 RECEIVE ALGORITHM INVESTIGATION (continued)

Moreover, it can be shown [31] that the Maximin approach can be derived from the *maximum-likelihood (ML) estimate* of the baseband (dehopped) data signal, given simple regularizing conditions on the transmitted and received signal waveforms. Specifically, if the received signal data signal  $x(n)$  can be modelled by

$$x(n) = as(n) + i(n)$$

over discrete time interval  $\{1, \dots, N\}$ , where  $i(n)$  is a white circularly-symmetric complex Gaussian (CSCG) interference waveform with mean zero and unknown autocorrelation matrix  $R_{ii}$ , and where  $s(n)$  has limited statistical support, such that a linear thinning operator  $P_s$  exists that satisfies

$$P_s(s(n)) = s(n)$$

over  $\{1, \dots, N\}$ , then the joint ML estimate of  $s(n)$ ,  $a$ , and  $R_{ii}$  is given by

$$\begin{aligned} \hat{s}_{ML}(n) &= w_{ML}^H x_{pass}(n) \\ \hat{a}_{ML} &= \hat{R}_{x_{reject} x_{reject}} / \sqrt{w_{ML}^H \hat{R}_{x_{reject} x_{reject}} w_{ML}} \\ \hat{R}_{ii} &= \hat{R}_{xx} - \hat{a}_{ML} \hat{a}_{ML}^H \hat{R}_{s_{ML} s_{ML}} \\ x_{pass}(n) &= P_s(x(n)) \\ x_{reject}(n) &= x(n) - x_{pass}(n) \\ \hat{R}_{x_{(\cdot)} x_{(\cdot)}} &= \langle x_{(\cdot)}(n) x_{(\cdot)}^H(n) \rangle_N \end{aligned}$$

where  $(\cdot)^H$  denotes the conjugate-transpose (Hermitian) operation and  $\langle \cdot \rangle_N$  denotes time averaging over the reception interval, and where  $w_{ML}$  is the maximal point of the *Maximin objective function*

$$F_{ML}(w) = \frac{w^H \hat{R}_{x_{pass} x_{pass}} w}{w^H \hat{R}_{x_{reject} x_{reject}} w}$$

The thinning operator  $P_s$  can be interpreted as a generalized bandpass operation that passes the region of statistical support containing  $s(n)$  and rejects the remaining data in the environment. Example thinning operators include:

- *bandlimiting operators*, applicable to environments where  $s(n)$  has limited spectral support, i.e., where  $s(n)$  exists over a narrow frequency band within the overall received data passband (for example, if  $s(n)$  is a CW tone);
- *time-limiting operators*, applicable to environments where  $s(n)$  has limited temporal support, i.e., where  $s(n)$  exists over a narrow subset of the overall reception interval (for example, if  $s(n)$  is a burst, pulsed, or time-hopped waveform); and

#### 4.3.2.2 RECEIVE ALGORITHM INVESTIGATION (continued)

- dehop-rehop operators, applicable to environments where  $s(n)$  has limited and time-varying spectral support, i.e., where  $s(n)$  exists over a narrow "instantaneous" frequency band that hops over the receive data passband during the reception interval.

Other thinning operators that can be postulated for different signal modulation formats include: *despread-respread operators*, applicable to DSSS signals; and generalized despread-respread operators, applicable to hybrid FH/DS modulation formats.

Given this derivation, the following four-step procedure can be used to determine the ML estimate of the transmitted signal waveform:

1. pass each element of  $x(n)$  through the generalized bandpass and complementary bandreject filter that is matched to  $s(n)$ , to form thinned signal-plus-interference data signal  $x_{\text{pass}}(n)$  and signal-free data signal  $x_{\text{reject}}(n)$ ;
2. compute the sample autocorrelation of  $x_{\text{pass}}(n)$  and  $x_{\text{reject}}(n)$  over the reception interval;
3. compute the maximal value of the Maximin objective function  $F_{\text{ML}}(w)$  defined above; and
4. compute the transmitted signal estimate from the *thinned* data signal  $x_{\text{pass}}(n)$ , using the formula given above.

From this procedure, it can be seen that the Maximin algorithms reported in [20,21,22] provide the ML estimate of an FH signal using a steepest-descent algorithm<sup>3</sup>. Similarly, it can be seen that the burst-acquisition algorithm reported in [23,24] provides the estimate of a burst signal<sup>4</sup> using the exact solution to  $F_{\text{ML}}(w)$ , given by the *dominant mode* (eigenvector with maximum eigenvalue) of the *Maximin* eigenequation

$$\lambda \hat{R}_{x_{\text{reject}} x_{\text{reject}}} w = \hat{R}_{x_{\text{pass}} x_{\text{pass}}} w$$

With some additional effort, the adaptive detection algorithm reported in [25] and the DSSS acquisition algorithm reported in [26] can also be interpreted as *rank-1* approximations to the ML estimator of a burst or DSSS signal, where the statistical support for  $x_{\text{pass}}(n)$  is so sparse that the autocorrelation of  $x_{\text{pass}}(n)$  has rank 1. In this environment, Kelly and Dlugos have independently derived statistical models for  $w_{\text{ML}}$ ,  $s_{\text{ML}}(n)$  and  $F_{\text{ML}}(w_{\text{ML}})$  based on Wishart distribution of the ACMs of  $x_{\text{pass}}(n)$  and  $x_{\text{reject}}(n)$ .

<sup>3</sup>More exactly, the Maximin algorithms provide a close approximation to the ML estimate of the FH signal, since the algorithm computes  $x_{\text{reject}}(n)$  using narrowband and causal processor operations, and updates  $w$  using a stochastic steepest-ascent algorithm.

<sup>4</sup>More exactly, the burst acquisition algorithm provides a close approximation to the ML estimate of the FH signal, since the algorithm estimates  $x_{\text{pass}}(n)$  and  $x_{\text{reject}}(n)$  using the optimal value of  $F_{\text{ML}}(w)$  as an ON-time detection statistic, and almost certainly estimates  $w_{\text{ML}}$  using an estimator with significant timing error.

#### 4.3.2.2 RECEIVE ALGORITHM INVESTIGATION (continued)

This result has an important bearing on the performance of the Maximin approach. The strong link between this approach and the ML estimator indicates that the Maximin approach should provide the best possible estimate of the transmitted signal waveform over a given reception interval<sup>5</sup>. Consequently, the Maximin approach should provide faster convergence than the regenerative approaches in environments where the structure of the transmitted signal is completely characterized by its statistical support<sup>6</sup>. This prediction is borne out by the computer simulations conducted to date for all of these techniques.

The analytical tractability of the Maximin approach (relative to the regenerative approaches) also has an important bearing on the reliability of these techniques. The ability to analyze the convergent behavior of the adaptation algorithm prior to actual hardware, by allowing the system engineers to predict system performance for a variety of errors scenarios, and to design reliable safeguards against any failure modes detected during this analysis. This design philosophy is demonstrated in Section 4.3.2.6, where performance predictions are made for a number of error scenarios in addition to the nominal reception scenario.

This analytical tractability also extends to the *convergence* performance of certain of the Maximin algorithms. In particular, the convergence speed of the dominant-mode Maximin algorithm described in [23,24] and developed on this Study can be expressed in terms of the eigenstructure of the Maximin eigenequation, and related to key environment parameters such as the maximum-attainable SINR of the array. This analysis is demonstrated in Section 4.3.2.5-4.3.2.6, where it provides a powerful estimate of the convergence speed of the processor, as well as important information for further improving the performance of the processor. In particular, the modified dominant-mode Maximin algorithm described in Section 4.3.2.5 is a direct result of this analysis.

In addition to the performance advantages described above, the Maximin algorithm possesses important *implementation* advantages over the regenerative techniques developed to date. Almost all of the regenerative techniques developed to date impose a nonlinearity of some sort on the beamformer output signal during the adaptation process<sup>7</sup>. This nonlinearity complicates

---

<sup>5</sup>Of course a better estimator can be devised if additional information about the transmitted signal is incorporated into the received data model. For example, in [31] it is shown that the ML estimator reduces to a hybrid Maximin/MORE algorithm if additional knowledge of the transmitted signal modulus is incorporated into the received data model. In fact, this processor can bear a close resemblance to the regenerative processors for some transmitted signal types.

<sup>6</sup>However, the regenerative techniques may have some performance advantages (under ideal conditions) if additional information about the transmitted signal is incorporated into the received data model. Even then, the robustness and implementation advantages of the Maximin approach will mitigate against the regenerative techniques in the application of interest here.

<sup>7</sup>A notable exception is [18] which expressly removes the limiting operation from the regenerative processor in order to remove the undesirable effects imposed by this limiter. However, the resultant processor structure is still more complex than the equivalent Maximin processor structure, and does not converge to the maximum-attainable SINR solution in most environments.

#### 4.3.2.2 RECEIVE ALGORITHM INVESTIGATION (continued)

the implementation of the resultant processor, and can result in hysteresis effects such as oscillatory weight instability in the processor weights [17,32].

In contrast, the Maximin algorithms do not impose a nonlinearity on the beamformer output signal, and are consequently not subject to the hysteresis effects experienced by the regenerative techniques. In addition, the computational complexity of these techniques can be much lower than the complexity of *any* of the other candidate algorithms considered on this Study (including the regenerative techniques).

Most notably, the computational complexity of the dominant mode Maximin algorithm is lower than any of the "rapidly-converging" algorithms considered on this Study, including the cross-SCORE and least-squares MORE algorithms, the least-square extensions of the regenerative techniques developed to date, and the *nonblind* least-squares algorithm. This complexity savings results from two sources:

- the dominant mode Maximin algorithm does not require cross-correlation data to operate, only autocorrelation data (which is being collected by other algorithms as well as the Maximin algorithm); and
- the signal-free autocorrelation matrix is only inverted once per hop) rather than every block as is required in all of the other algorithms).

Together with the performance and robustness features of the Maximin algorithms, these implementation features provide the Maximin algorithms (and particularly the dominant mode Maximin algorithm) with formidable advantages over the competing approaches.

#### 4.3.2.3 BASELINE: DOMINANT MODE MAXIMIN ALGORITHM

The history of the Dominant Mode (Block Update) Maximin algorithm was presented in the previous section, and its choice as the baseline algorithm for this study was justified. The basic operation of the algorithm is explained in this section using three steps: 1) an introduction to dominant mode eigenvectors, 2) a description of the power method of determining eigenvectors, and 3) a discussion of how the eigenvector estimates are updated using blocks of stochastic data.

##### Dominant Mode Eigenvectors -

The Dominant Mode Block Update algorithm attempts to maximize the SINR at the output of the AAP. The relevant equation is  $F(\mathbf{w}) = \text{SINR} + 1 = \mathbf{w}^H \mathbf{R}_1 \mathbf{w} / \mathbf{w}^H \mathbf{R}_0 \mathbf{w}$ . Obviously, maximizing this function also maximizes the SINR. The weight vector which gives the maximum SINR is the solution  $(\lambda_{\max}, \mathbf{w}_{\max})$  to the generalized eigenequation  $\lambda \mathbf{R}_0 \mathbf{w} = \mathbf{R}_1 \mathbf{w}$ . It is proved in section 4.3.2.4 that the eigenvector solution to this eigenequation with the largest eigenvalue (the eigenequation's dominant mode) maximizes the function  $F(\mathbf{w})$ . This vector  $\mathbf{w}_{\max}$  gives the complex weights which should be applied to the input signals from the antenna array elements to provide the maximum output SINR. Note: Complete descriptions of these variables and the derivations are presented in section 4.3.2.4.

### 4.3.2.3 BASELINE: DOMINANT MODE BLOCK UPDATE (continued)

#### Power Method -

There are many ways to determine the eigenvalues of a matrix. One method that is particularly easy to implement and will converge quickly if there is one dominant eigenvalue is the power method [33]. It starts with an initial guess  $w_0$  and successively calculates better estimates by multiplying the last estimate by the same original matrix  $A$ :  $w_{k+1} = Aw_k$ . After  $k$  iterations, the estimate is  $w_k = A^k w_0$ . Assuming  $A$  has a full set of eigenvectors  $x_k$ , the vector  $w_k$  is given by the formula for a difference equation:

$$w_k = c_1 \lambda_1^k x_1 + \dots + c_n \lambda_n^k x_n.$$

If the eigenvalues are numbered according to increasing magnitude, and the maximum eigenvalue is much larger than any of the others, then

$$w_k / \lambda_n^k = c_1 (\lambda_1 / \lambda_n)^k x_1 + \dots + c_{n-1} (\lambda_{n-1} / \lambda_n)^k x_{n-1} + c_n x_n.$$

As long as the initial guess  $w_0$  has some component of  $x_n$ , so that  $c_n$  is not 0, the  $c_n x_n$  term will dominate. Since  $\lambda_n$  is larger than any other  $\lambda_k$ , the terms  $(\lambda_1 / \lambda_n)^k$  are less than 1; as the number of iterations increase,  $(\lambda_1 / \lambda_n)^k$  approaches 0. The process converges to provide an estimate of  $w$  which is proportional to the maximum eigenvector  $x_n$ . A scaling factor must be introduced in the iterations to avoid  $u_{k+1}$  from growing very large or very small;  $u_k$  should be divided by its first component  $u_{k1}$  before taking the next step. This results in a power method iteration which gives  $u_{k+1} = Au_k / u_{k1}$ , which has  $u_{k+1}$  converging to  $w_{max}$  and  $u_{k1}$  converging to  $\lambda_{max}$ .

The power method generates  $A^k$ , when  $A = R_0^{-1} R_1$  as defined above,  $A^k$  approaches a diagonal matrix with the first diagonal element approaching the SINR + 1, and all other diagonal elements approaching 1 in nominal communication environments. For large values of maximum attainable SINR this procedure should converge very quickly. Conditions may arise in which the eigenvalue spreads are not conducive to fast convergence in some cases (see section 4.3.2.6 for transient interference "collision" analysis). To speed the convergence in a transient interference environment, or for other such conditions, a factor  $u$  is introduced as follows:  $A = R_0^{-1} R_1 - uI$ . In this case,  $A^k$  approaches a diagonal matrix with the first diagonal element approaching the SINR -  $u$ , and all other diagonal elements approaching 1 -  $u$ . Selection of  $u$  can be customized for a specific jammer threat or conditions. Under normal conditions the algorithm may converge slightly more quickly than with  $u = 0$ ; for certain special cases the algorithm will converge much more quickly. Further discussion of convergence time is provided in section 4.3.2.5.

#### Stochastic Block Updates -

In the actual implementation of this algorithm,  $A = R_0^{-1} R_1$ ; data for  $R_0^{-1}$  is collected during an entire timeslot which is different than the timeslot used to collect data for  $R_1$ . Furthermore, the data for  $R_1$  is collected over several blocks of data samples within one timeslot. The data collection process is described in detail in the Architecture section of this report, section 4.3.3. The impact to the power method is that the matrix  $A$  changes slightly with each block update, even though the input signals have not changed statistically between blocks. If the integration time for each block is long enough, the deviation between sequential  $A$  matrices will be negligible. Even with modest integration times (16 samples), the affect to the performance of

### 4.3.2.3 BASELINE: DOMINANT MODE BLOCK UPDATE (continued)

#### Stochastic Block Updates (continued) -

the algorithm is negligible (verified by simulation, see section 4.3.4.). This is because multiple iterations of  $u_{k+1} = Au_k/v$  smooths the variances of the A matrix from block to block. The power method does not require a deterministic A matrix without change, but will converge with a stochastic A matrix taken from a statistically unchanging RF environment.

### 4.3.2.4 DOMINANT MODE DERIVATION

The objective of the Dominant Mode Block Update algorithm is to maximize the Signal to Interference plus Noise Ratio (SINR) at the output of the AAP. The AAP output signal is  $y(t)$ , and is equal to the sum of the weighted input signals. Therefore,

$$y = \sum w_k * x_k(t) = w^H x(t)$$

where  $()^H$  denotes Hermitian (conjugate transpose) operation.

The AAP output power may be written as  $P_{out} = \langle |y(t)|^2 \rangle_T = w^H \langle x(t)x^H(t) \rangle_T w = w^H R_{xx}' w$  where  $\langle \rangle_T$  denotes time averaging over an interval of duration T and  $R_{xx}'$  is the sample autocorrelation of  $x(t)$ . If the time interval is long and  $x(t)$  is stationary over the time interval, then  $R_{xx}'$  can be approximated by its expected value  $R_{xx} = E[R_{xx}']$ .

Since the AAP output is merely a weighted summation of all the input signals, the components of the AAP output depends on the signals present at the input when the measurements are taken. Let S represent the desired signal, or Signal Of Interest (SOI), I represent the total interference, or Signals Not Of Interest (SNOI), and N represent the noise generated internally by the AAP circuits. In an RF environment with active jammers, it is assumed there are always interferers present. When the AAP is operational, its internal noise will always be present. The SOI, however, may or may not be present. Two general output power equations may be written which describe these conditions:

$$P_{out0} = I + N, \text{ and } P_{out1} = S + I + N.$$

The subscript 1 or 0 designates whether the SOI is present or not. Forming the ratio  $P_{out1}/P_{out0}$  gives  $(S + I + N) / (I + N)$ , which is equal to the SINR + 1. Obviously, the weights which maximize SINR + 1 will result in a maximum SINR.

The presence or absence of signals is included in the variable  $x$ , so the covariance matrix  $R_{xx}$  will depend on whether the SOI is present or not. Representing  $R_{xx}$  as  $R_0$  when the SOI is not present, and as  $R_1$  when the SOI is present, the power ratio can be written as

$$F(w) = \text{SINR} + 1 = w^H R_1 w / w^H R_0 w.$$

The objective of the adaptation algorithm is to maximize this ratio. The weight vector for which this function is a maximum can be designated  $w_{max}$ , and has the following solution:

$$\lambda_{max} w_{max} = R_0^{-1} R_1 w_{max}$$

This solution can be found by setting the gradient of  $F(w)$  equal to zero and solving for  $w$ . [20]

#### 4.3.2.4 DOMINANT MODE DERIVATION (continued)

The same solution is obtained by manipulating  $F(w)$  into a ratio of quadratics, specifically the Rayleigh's Quotient, then applying Rayleigh's Principle to find the maximum and minimum eigenvalues and corresponding eigenvectors.[33]

Allowing the following change of variables:

$$z = R_0^{-1/2}w \text{ and } A = R_0^{-1/2}R_1R_0^{-1/2} \text{ (Note: } w = R_0^{-1/2}z\text{),}$$

$F(w)$  takes the form of the Rayleigh's quotient  $R(z)$ :

$$\begin{aligned} F(w) &= w^H R_1 w / w^H R_0 w \\ &= (R_0^{-1/2}z)^H R_1 (R_0^{-1/2}z) / (R_0^{-1/2}z)^H R_0 (R_0^{-1/2}z) \\ &= z^H R_0^{-1/2} R_1 R_0^{-1/2} z / z^H R_0^{-1/2} R_0 R_0^{-1/2} z \\ &= z^H A z / z^H z = R(z). \end{aligned}$$

A singular value decomposition of  $A$  simplifies the quadratic expressions in  $R(z)$ . The decomposition sets  $A = U\Lambda U^H$ , where  $\Lambda$  is a diagonal matrix whose diagonal elements are the eigenvalues of  $A$  and  $U$  is a matrix whose columns are the orthonormal eigenvectors corresponding to those eigenvalues. The corresponding eigenequation is  $\lambda_k u_k = A u_k$ . Applying this singular value decomposition, the ratio of quadratics  $R(z)$  takes the form:

$$\begin{aligned} R(p) &= p^H U^H A U p / p^H U^H U p \\ &= p^H U^H U \Lambda U^H U p / p^H U^H U p \\ &= p^H \Lambda p / p^H p \\ &= (\lambda_1 p_1^2 + \lambda_2 p_2^2 + \dots + \lambda_m p_m^2) / (p_1^2 + p_2^2 + \dots + p_m^2) \\ &\text{where } z = U p. \end{aligned}$$

The Rayleigh principle states that the Rayleigh quotient is never below  $\lambda_1$  and never above  $\lambda_m$ ; its minimum is at the eigenvector  $z_1$  and its maximum is at  $z_m$ . Intermediate eigenvectors are saddle points. The eigenvalues are ordered:  $z_m > \dots > z_2 > z_1$ .

Working backwards to return to the original variables, the equivalent eigenequation which results is  $\lambda_k R_0 w_k = R_1 w_k$ . These transformations require that  $R_0$  be positive definite such that  $R_0^{-1/2}$  exists and is Hermitian. Then, the maximum value of  $F(w)$  is equal to  $\lambda_m$  and is achieved by setting  $w$  proportional to  $w_m$ .

This result can also be achieved by noting that the non-Hermitian matrix  $B = R_0^{-1}R_1$  also has a singular value decomposition given by  $W\Lambda A$ .  $W$  is a matrix comprised of the vectors  $w_k$ ,  $A$  is a matrix comprised of the vectors  $a_k$ , and they are a pair of reciprocal basis vectors which satisfy the relationships that  $a_k = R_0 w_k$ ,  $w_k^H a_1 = 1$  when  $k = 1$  and  $w_k^H a_1 = 0$  when  $k \neq 1$ . These results imply that  $W^H R_0 W = I_m$  and  $W^H R_1 W = \Lambda$ . The diagonal of  $\Lambda$  are the real eigenvalues  $\lambda_k$ .

#### 4.3.2.4 DOMINANT MODE DERIVATION (continued)

Substituting  $w = Wp$  into  $F(w)$  gives

$$\begin{aligned} F(w) &= (Wp)^H R_1 (Wp) / (Wp)^H R_0 (Wp) \\ &= p^H (W^H R_1 W) p / p^H (W^H R_0 W) p \\ &= p^H \Delta p / p^H p \end{aligned}$$

which has an unambiguous maximum at  $p = e_1$ , yielding  $w_{\max} = w_1$  and  $F_{\max} F(w_{\max}) = \lambda_1$ .

#### 4.3.2.5 ADAPTATION CONVERGENCE AND STABILITY ANALYSIS

Note: This analysis uses slightly different notations than is used elsewhere in this report.

A convergence analysis for the actual (stochastic) dominant-mode algorithm is beyond the scope of this report. However, a convergence proof is obtainable for the nonstochastic algorithm that maximizes the power ratio

$$F(w) = \frac{w^H \underline{R} w}{w^H \underline{C} w} \quad (1)$$

where  $\underline{R}$  and  $\underline{C}$  do not change between iterations ( $\underline{R}$  corresponds to the on time autocorrelation matrix,  $\underline{C}$  corresponds to the off time). The nonstochastic update procedure is as follows:

Initialization:

$$\hat{d}(0) = \underline{R} \hat{w}(0) \quad (2)$$

$$g(0) = \hat{w}^H(0) \hat{d}(0) \quad (3)$$

$$\hat{w}(0) \leftarrow \frac{\hat{w}(0)}{\sqrt{g(0)}} \quad (4)$$

$$\hat{d}(0) \leftarrow \frac{\hat{d}(0)}{\sqrt{g(0)}} \quad (5)$$

Update  $k - k+1$ :

$$\underline{u} = \underline{C}^{-1} \hat{d}(k) \quad (6)$$

$$\underline{v} = \underline{R} \underline{u} \quad (7)$$

$$\hat{w}(k+1) = \underline{u} - \mu \hat{w}(k) \quad (8)$$

## 4.3.2.5 ADAPTATION CONVERGENCE AND STABILITY ANALYSIS (continued)

$$\hat{a}(k+1) = \gamma - \mu \hat{a}(k) \quad (9)$$

$$g(k+1) = \hat{w}^H(k+1) \hat{a}(k+1) \quad (10)$$

$$\hat{w}(k+1) = \frac{\hat{w}(k+1)}{\sqrt{g(k+1)}} \quad (11)$$

$$\hat{a}(k+1) = \frac{\hat{a}(k+1)}{\sqrt{g(k+1)}} \quad (12)$$

$$\hat{\lambda}(k+1) = \sqrt{\mu^H \gamma} \quad (13)$$

The objective of the algorithm is to set  $\hat{w}(k)$  equal to the dominant mode of the eigen-equation

$$\lambda \underline{C} \underline{w} = \underline{R} \underline{w} \quad (14)$$

as  $k \rightarrow \infty$ , without instability ( $|\hat{w}(k)| < \infty \forall k$ ). In particular, the algorithm is designed to yield

$$\hat{w}(k) \rightarrow \frac{w_1}{\sqrt{\lambda_1}}$$

$$\hat{a}(k) \rightarrow a_1 \times \sqrt{\lambda_1}$$

$$\hat{\lambda}(k) \rightarrow \lambda_1$$

as  $k \rightarrow \infty$ , where  $(\lambda_m, \underline{w}_m, \underline{a}_m)_1^M$  are the eigenvalues and corresponding right-hand and left-hand eigenvectors of the new matrix  $\hat{\underline{T}} = \underline{C}^{-1} \underline{R}$ .

$$\left. \begin{aligned} \lambda_k \underline{w}_k &= \hat{\underline{T}} \underline{w}_k \\ \lambda_k \underline{a}_k &= \hat{\underline{T}}^H \underline{a}_k \end{aligned} \right\} \underline{w}_k^H \underline{a}_k = \delta_{k-1}$$

This choice of normalization is made to ensure that the output signal power is normalized to unity over the signal on time ( $\underline{w}^H \underline{R} \underline{w}$ ).

$$\rightarrow \hat{\underline{T}} = \underline{W} \underline{\Delta} \underline{\Delta}^H, \quad \underline{W}^H \underline{\Delta} = \underline{\Delta} \underline{W}^H = \underline{I}_M$$

$$\underline{W} = [w_1 \cdots w_M]$$

## 4.3.2.5 ADAPTATION CONVERGENCE AND STABILITY ANALYSIS (continued)

$$\underline{a} = [a_1 \cdots a_M]$$

$$\underline{\Delta} = \begin{bmatrix} \lambda_1 & & 0 \\ & \ddots & \\ 0 & & \lambda_M \end{bmatrix}$$

and where  $\lambda_m$  are real and ordered, with distinct maximum, such that  $\lambda_1 > \lambda_2 \geq \cdots \geq \lambda_M$ . As shown in section 4.3.2.4, the power ratio,  $F(\underline{w})$ , is maximized at  $F(\underline{w}_{\max}) = \lambda_1$  for  $\underline{w}_{\max} = \underline{w}_1$ .

The convergence proof is facilitated by proving the following lemma:

**Lemma:** Given  $\{\hat{\lambda}(k), \hat{a}(k), \hat{w}(k)\}$  in the equations above,

1.  $\hat{a}(k) = \underline{R}\hat{w}(k)$  for every  $k \geq 0$
2.  $\hat{w}^H(k)\hat{a}(k) = 1$  for every  $k \geq 0$

Proof by induction:

1. Both properties are true for  $k=0$

$$\hat{w}(0) = \frac{\hat{w}(0)}{\sqrt{\hat{w}^H(0)\hat{a}(0)}}$$

$$\hat{a}(0) = \frac{\hat{a}(0)}{\sqrt{\hat{w}^H(0)\hat{a}(0)}} = \underline{R}\hat{w}(0)$$

$$\rightarrow \hat{w}^H(0)\hat{a}(0) = 1$$

2. Assume both properties are true for  $k$ , then show they must be true for  $k+1$

- a) Equations (6)-(7) and property 1 of the lemma yield

$$\begin{aligned} \underline{u} &= \underline{C}^{-1}\hat{a}(k) \\ &= \underline{C}^{-1}\underline{R}\hat{w}(k) \\ &= \underline{\hat{T}}\hat{w}(k) \end{aligned} \tag{15}$$

$$\begin{aligned} \underline{y} &= \underline{RC}^{-1}\hat{a}(k) \\ &= \underline{R}\underline{\hat{T}}\hat{w}(k) \end{aligned} \tag{16}$$

## 4.3.2.5 ADAPTATION CONVERGENCE AND STABILITY ANALYSIS (continued)

b) Equations (8)-(12) and (15)-(16) yield

$$\begin{aligned}\hat{\underline{w}}(k+1) &= \alpha(k+1)[\underline{\mu} - \mu \hat{\underline{w}}(k)], \quad \alpha(k+1) = \frac{1}{\sqrt{g(k+1)}} \\ &= \alpha(k+1)[\hat{\underline{T}} - \mu \underline{D}] \hat{\underline{w}}(k)\end{aligned}\tag{17}$$

$$\begin{aligned}\hat{\underline{a}}(k+1) &= \alpha(k+1)[\underline{y} - \mu \hat{\underline{a}}(k)] \\ &= \alpha(k+1)[\underline{R} \hat{\underline{T}} \hat{\underline{w}}(k) - \mu \underline{R} \hat{\underline{w}}(k)] \\ &= \underline{R} \alpha(k+1)[\hat{\underline{T}} - \mu \underline{D}] \hat{\underline{w}}(k) \\ &= \underline{P} \hat{\underline{w}}(k+1)\end{aligned}\tag{18}$$

c) Equations (11)-(12) yield condition 2 for any choice of  $\hat{\underline{w}}(k+1)$  and  $\hat{\underline{a}}(k+1)$ , as long as  $\hat{\underline{w}}^H(k+1) \hat{\underline{a}}(k+1) \neq 0$ , which holds for any positive definite  $\underline{R}$ , since  $\underline{w}$  and  $\hat{\underline{a}}$  satisfy condition 1.

Given this Lemma, then (17)-(18) can be used to express  $\hat{\underline{w}}(k)$  and  $\hat{\underline{a}}(k)$  directly in terms of  $\hat{\underline{w}}(0)$ ,

$$\hat{\underline{w}}(k) = \frac{(\hat{\underline{T}} - \mu \underline{D})^k \hat{\underline{w}}(0)}{\sqrt{\hat{\underline{w}}^H(0) (\hat{\underline{T}}^H - \mu \underline{D}^k \underline{R} (\hat{\underline{T}} - \mu \underline{D})^k \hat{\underline{w}}(0))}}\tag{19}$$

$$\hat{\underline{a}}(k) = \underline{R} \hat{\underline{w}}(k)\tag{20}$$

$$\begin{aligned}\rightarrow \hat{\lambda}(k) &= \sqrt{\hat{\underline{a}}^H(k-1) \underline{C}^{-1} \underline{R} \underline{C}^{-1} \hat{\underline{a}}(k-1)} \\ &= \sqrt{\frac{\hat{\underline{w}}^H(0) (\hat{\underline{T}}^H - \mu \underline{D}^{k-1} \hat{\underline{T}}^H \underline{R} \hat{\underline{T}} (\hat{\underline{T}} - \mu \underline{D})^{k-1} \hat{\underline{w}}(0))}{\hat{\underline{w}}^H(0) (\hat{\underline{T}}^H - \mu \underline{D}^{k-1} \underline{R} (\hat{\underline{T}} - \mu \underline{D})^{k-1} \hat{\underline{w}}(0))}}\end{aligned}\tag{21}$$

Equations (19)-(21) can be expressed in terms of the eigenvalues and eigenvectors of  $\hat{\underline{T}}$ , by setting

$$\hat{\underline{w}}(k) = \underline{W} \underline{p}(k)\tag{22}$$

using the identities

$$\underline{W}^H \underline{A} = \underline{\Delta} \underline{W}^H = \underline{I}\tag{23}$$

$$\underline{\Delta}^H \hat{\underline{T}} \underline{W} = \underline{\Delta}; \quad \underline{\Delta} = \underline{C} \underline{W}\tag{24}$$

## 4.3.2.5 ADAPTATION CONVERGENCE AND STABILITY ANALYSIS (continued)

$$\rightarrow \underline{\hat{A}}^H (\underline{\hat{T}} - \mu \underline{D} \underline{W}) = \underline{\Delta} - \mu \underline{I} \quad (25)$$

$$\underline{W}^H \underline{R} \underline{W} = \underline{\Delta} \quad (26)$$

then (19)-(21) reduce to

$$\underline{W} \underline{p}(k) = \frac{\underline{W} (\underline{\Delta} - \mu \underline{D}^k \underline{p}(0))}{\sqrt{\underline{p}^H(0) \underline{\Delta} (\underline{\Delta} - \mu \underline{D}^{2k} \underline{p}(0))}} \quad (27)$$

$$\underline{\hat{a}}(k) = \underline{\Delta} \underline{p}(k) \quad (28)$$

$$\hat{\lambda}(k) = \sqrt{\frac{\underline{p}^H(0) \underline{\Delta}^3 (\underline{\Delta} - \mu \underline{D}^{2k-2} \underline{p}(0))}{\underline{p}^H(0) \underline{\Delta} (\underline{\Delta} - \mu \underline{D}^{2k-2} \underline{p}(0))}} \quad (29)$$

Correct convergence is demonstrated by  $\underline{p}(k) \rightarrow \alpha \underline{e}_1$  as  $k \rightarrow \infty$ .

Algorithm convergence can be measured<sup>8</sup> using the generalized correlation coefficient

$$S(k) = \frac{|\underline{\hat{y}}^H(k) \underline{R} \underline{w}_1|^2}{[\underline{\hat{y}}^H(k) \underline{R} \underline{\hat{y}}(k)] [\underline{w}_1^H \underline{R} \underline{w}_1]} \quad (30)$$

<sup>8</sup> Note that stability is guaranteed at every value of  $k$ , since

$$\underline{w}^H(k) \underline{R} \underline{w}(k) = 1 \quad \forall k$$

## 4.3.2.5 ADAPTATION CONVERGENCE AND STABILITY ANALYSIS (continued)

$$\begin{aligned}
&= \frac{1}{\lambda_1} |\hat{\mathbf{w}}^H(k) \underline{\mathbf{R}} \mathbf{w}_1|^2 \\
&= \lambda_1 |\mathbf{p}^H(k) \mathbf{e}_1|^2 \\
&= \lambda_1 \frac{|\mathbf{p}^H(0) (\underline{\Delta} - \mu \underline{D})^k \mathbf{p}_1|^2}{\mathbf{p}^H(0) \underline{\Delta} (\underline{\Delta} - \mu \underline{D})^{2k} \mathbf{p}(0)} \\
&= \frac{\lambda_1 (\lambda_1 - \mu)^{2k} |\mathbf{p}_1(0)|^2}{\sum_1^M \lambda_m (\lambda_m - \mu)^{2k} |\mathbf{p}_m(0)|^2} \\
&= \left[ 1 + \sum_{m=2}^M \left( \frac{|\mathbf{p}_m(0)|}{|\mathbf{p}_1(0)|} \right)^2 \left( \frac{\lambda_m}{\lambda_1} \right) \left( \frac{\lambda_m - \mu}{\lambda_1 - \mu} \right)^{2k} \right]^{-1} \quad (31)
\end{aligned}$$

Equation (31) is monotonically convergent to unity as long as  $|\mathbf{p}_1(0)| > 0$  (i.e., as long as  $\hat{\mathbf{w}}(0)$  and  $\mathbf{w}_1$  are not orthogonal) and

$$\left( \frac{\lambda_m - \mu}{\lambda_1 - \mu} \right)^2 < 1 \quad \forall m = 2, \dots, M \quad (32)$$

$$\Rightarrow \frac{\lambda_1 + \lambda_m}{2} > \mu \quad \text{and} \quad \lambda_1 > \lambda_m \quad \forall m > 1 \quad (33)$$

The speed of this convergence is also given by the ratio

$$r_{conv} = \max \left[ \left( \frac{\lambda_2 - \mu}{\lambda_1 - \mu} \right)^2, \dots, \left( \frac{\lambda_m - \mu}{\lambda_1 - \mu} \right)^2 \right] \quad (34)$$

which constitutes the largest of the  $M-1$  decay constants in (31).

Similarly, the eigenvalue estimate  $\hat{\lambda}(k)$  also converges to  $\lambda_1$  as  $k \rightarrow \infty$ , since

$$\hat{\lambda}(k) = \sqrt{\frac{\sum_1^M |\mathbf{p}_m(0)|^2 \lambda_m^3 (\lambda_m - \mu)^{2k-2}}{\sum_1^M |\mathbf{p}_m(0)|^2 \lambda_m (\lambda_m - \mu)^{2k-2}}}$$

## 4.3.2.5 ADAPTATION CONVERGENCE AND STABILITY ANALYSIS (continued)

$$= \lambda_1 \times \sqrt{\frac{1 + \sum \frac{|p_m(0)|^2}{2 |p_1(0)|^2} \left(\frac{\lambda_m}{\lambda_1}\right)^3 \left(\frac{\lambda_m - \mu}{\lambda_1 - \mu}\right)^{2k-2}}{1 + \sum \frac{|p_m(0)|^2}{2 |p_1(0)|^2} \left(\frac{\lambda_m}{\lambda_1}\right) \left(\frac{\lambda_m - \mu}{\lambda_1 - \mu}\right)^{2k-2}}} \quad (35)$$

$\rightarrow \lambda_1 \text{ as } k \rightarrow \infty$

if  $(\lambda_m)_1^M$  satisfies (33). However, this estimate is not monotonically convergent in general, since the numerator and denominator of (35) converge at slightly different rates.

It can also be shown that the power ratio  $F(\underline{w})$  converges to  $\lambda_1$  as  $k \rightarrow \infty$ , since

$$\begin{aligned} F[\underline{w}(k)] &= \frac{\hat{\underline{w}}^H(k) \underline{R} \hat{\underline{w}}(k)}{\hat{\underline{w}}^H(k) \underline{C} \hat{\underline{w}}(k)} \\ &= \frac{\underline{p}^H(k) \underline{R} \underline{p}(k)}{\|\underline{p}(k)\|^2} \\ &= \frac{\underline{p}^H(0) (\underline{\Delta} - \mu \underline{D})^{2k} \underline{p}(0)}{\underline{p}^H(0) (\underline{\Delta} - \mu \underline{D})^{2k} \underline{p}(0)} \\ &= \lambda_1 \times \left[ \frac{1 + \sum \frac{|p_m(0)|^2}{2 |p_1(0)|^2} \left(\frac{\lambda_m}{\lambda_1}\right) \left(\frac{\lambda_m - \mu}{\lambda_1 - \mu}\right)^{2k}}{1 + \sum \frac{|p_m(0)|^2}{2 |p_1(0)|^2} \left(\frac{\lambda_m - \mu}{\lambda_1 - \mu}\right)^{2k}} \right] \\ &= \lambda_1 \times \left[ 1 - \frac{\sum \frac{|p_m(0)|^2}{2 |p_1(0)|^2} \left(1 - \frac{\lambda_m}{\lambda_1}\right) \left(\frac{\lambda_m - \mu}{\lambda_1 - \mu}\right)^{2k}}{1 + \sum \frac{|p_m(0)|^2}{2 |p_1(0)|^2} \left(\frac{\lambda_m - \mu}{\lambda_1 - \mu}\right)^{2k}} \right] \\ &\leq \lambda_1 \end{aligned}$$

with equality achieved as  $k \rightarrow \infty$  if  $(\lambda_m)_1^M$  satisfies (33).

#### 4.3.2.5 ADAPTATION CONVERGENCE AND STABILITY ANALYSIS (continued)

As shown in the next section, the convergence factor given in (34) can be strongly affected by the choice of  $\mu$ . In particular, if the  $(\lambda_m)_1^M$  are given by

$$\lambda_m = \begin{cases} 1 + \gamma_{\max} & m = 1 \\ 1 & m > 1 \end{cases}$$

where  $\gamma_{\max}$  is the maximum attainable SINR of the array, then setting  $\mu = 1$  can greatly reduce the ratio given in (34).

#### 4.3.2.6 RECEIVE ADAPTATION PERFORMANCE ANALYSIS

It is beyond the scope of this report to determine the performance of the Dominant Mode algorithm under finite time conditions. However, useful results can be obtained by replacing sample autocorrelation matrices in the true algorithm with idealized (infinite time average) statistics. The discrepancy between the actual and idealized quantities should be small if the averaging times are long in the actual algorithm.

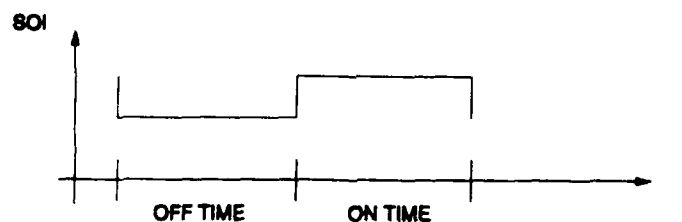
The analysis conducted here is limited to determination of the dominant mode of the generalized eigenequation  $\lambda w = R_0^{-1} R_1 w$  where  $R_0^{-1}$  is the autocorrelation of the received data measured over the off interval and  $R_1$  is the data autocorrelation measured over the on interval. This analysis is conducted for the following scenarios:

- o The nominal scenario, where both  $R_0^{-1}$  and  $R_1$  are properly computed.
- o Timing error scenarios, where the on and off time data collection intervals are out of synch with actual SOI timing.
- o Collision scenarios, where the undesired signals, signals not of interest (SNOIs), turn on or off during the data collection intervals.

The analysis which follows will show the dominant mode eigenvalues to converge to the maximum attainable SINR beamformer in all the nominal and timing error scenarios, and in many of the collision scenarios. Consequently, the algorithm is expected to be very robust in actual practice.

##### Nominal Scenario -

The instantaneous SOI power is illustrated below for the nominal communication scenario.



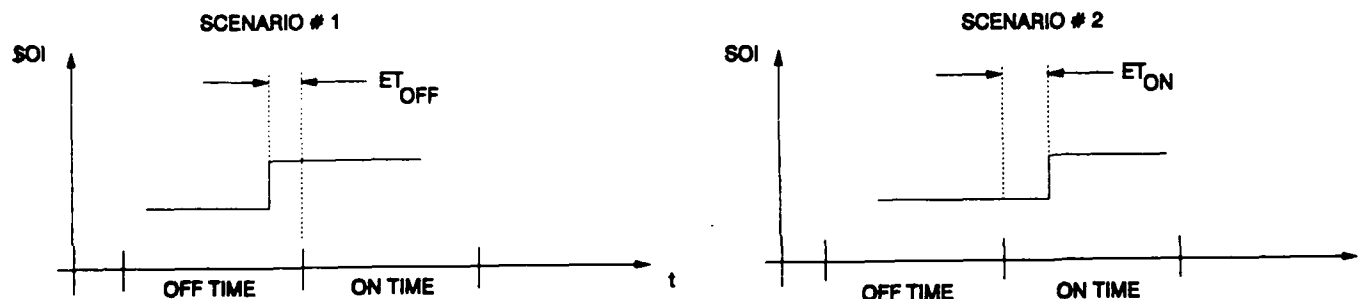
#### 4.3.2.6 RECEIVE ADAPTATION PERFORMANCE ANALYSIS (continued)

The off time and on time measurements are made over the correct intervals, yielding the relations  $x_{\text{off}}(t) = i_{\text{off}}(t)$  and  $x_{\text{on}}(t) = i_{\text{on}}(t) + as(t)$ , where  $i_{\text{off}}(t)$  and  $i_{\text{on}}(t)$  have identical autocorrelation data  $R_{ii}$ . The off time and on time autocorrelation matrices are therefore given by  $R_0 = R_{ii}$  and  $R_1 = R_{ii} + aa^H R_{ss}$ . Substituting these relations into the generalized eigenequation yields  $m-1$  solutions with  $a^H w_k = 0$  and  $\lambda_k = 1$ , and one solution with  $w_1 \propto R_{ii}^{-1} a R_{ss} = w_{\text{max}}$  and  $\lambda_1 = 1 + a^H R_{ii}^{-1} a R_{ss} = 1 + \gamma_{\text{max}}$ . The maximum SINR beamformer is  $w_{\text{max}}$  and the maximum attainable SINR of the array is  $\gamma_{\text{max}}$ .

From the preceding section (4.3.2.5), it can be seen that the Dominant Mode algorithm should converge quickly for  $u = 0$  and  $\gamma_{\text{max}}$  large, or for  $u = 1$  and virtually any value of  $\gamma_{\text{max}}$ . Furthermore, this mode shall correspond closely to the maximum SINR beamformer. The dominant mode can also be used as a quality statistic, to determine whether or not the algorithm has successfully captured the SOI.

#### Timing Error Scenarios -

The instantaneous SOI power is illustrated below for the timing error scenarios.



These figures show the off and on time data collection intervals to be out of synch with the true SOI on time. If the on time data collection interval is enabled late, some of the on time data is collected during the off interval; if its enabled early, the SOI is absent over part of the on interval.

In the first timing error scenario, the off and on autocorrelation matrices are approximated by  $R_0 = R_{ii} + \epsilon aa^H R_{ss}$  and  $R_1 = R_{ii} + aa^H R_{ss}$ . The eigenequation has  $m-1$  solutions with  $a^H w_k = 0$  and  $\lambda_k = 1$ , and one solution with  $w_1 \propto w_{\text{max}}$  and  $\lambda_1 = (1 + \gamma_{\text{max}})/(1 + \epsilon \gamma_{\text{max}})$ . For very large SINRs,  $\lambda_1$  approaches  $1/\epsilon$ .

The second scenario gives autocorrelation matrices  $R_0 = R_{ii}$  and  $R_1 = R_{ii} + (1-\epsilon)aa^H R_{ss}$ . The eigenequation also has  $m-1$  solutions with  $a^H w_k = 0$  and  $\lambda_k = 1$ , and one solution with  $w_1 \propto w_{\text{max}}$  and  $\lambda_1 = 1 + (1-\epsilon)\gamma_{\text{max}}$ .

As demonstrated above, in both cases the dominant mode of  $\lambda w = R_0^{-1} R_1 w$  corresponds to the maximum SINR beamformer. These calculations can be verified by substitution of the applicable autocorrelation matrices into the general eigenequation.

These results have important ramifications for the Dominant Mode algorithm. The performance of the algorithm is nearly independent of the synchronization error in the receiver. The algorithm should be able to capture the SOI even with very large errors in timing. A simple post-capture synchronization circuit can then be designed to remove this timing error and optimize performance after the removal of the other stationary interference.

#### 4.3.2.6 RECEIVE ADAPTATION PERFORMANCE ANALYSIS (continued)

##### Timing Error Scenarios (continued) -

Timing error can affect the convergence speed of the algorithm. The spread between the dominant eigenvalue and the lesser eigenvalues is reduced when timing errors exist. The effect is especially pronounced in the first case:  $\lambda_1$  is limited by  $1/\epsilon$  as the SINR approaches infinity. The Dominant Mode algorithm should therefore converge much more slowly in this case. However, it is expected that the convergence of this algorithm can be accelerated by setting  $u = 1$  in the algorithm since this can yield an arbitrarily low value of  $r_{conv}$  as the averaging time grows to infinity.

In a ground based Army tactical radio application the timing errors analyzed above would occur only before the host radio has been acquired by the network. Once in the network the host radio would provide the necessary timing information to the AAP to allow it to collect off time and on time data as required by its adaptation algorithm. When the host radio is not in the network it monitors the activity on a guard band channel specifically designated for acquiring synchronization with the network. The AAP could easily alter its adaptation algorithm to improve the host radio's likelihood of acquiring synchronization if the AAP is informed by the host that it is not synchronized. The AAP could even determine this condition on its own if it monitored the consecutive revisits to the same guard band frequency. Once the AAP knows the host radio is not in the network, it could increase its adaptation time: this would provide rejection of stationary jammers and have less affect on the SOIs. The jammers would continuously be received from the same directions, so a long adaptation time would suffice. The SOIs, however, would be coming from different directions, or would occur infrequently, so they would not be rejected as quickly. Jammer rejection would provide less interference output power; SOIs from various directions would decrease the likelihood that they all fall in the directions of inadvertant nulls. Therefore, the AAP would be providing improvement of the SINR available to the host radio relative to operation without the AAP most of the time.

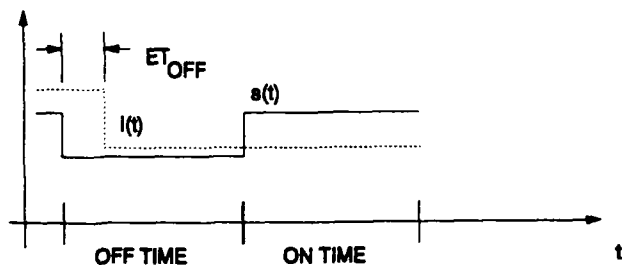
An extension of the timing error scenario is the condition that an expected SOI is not present. The AAP expects a SOI during an on time data collect, but in network communications this is not guaranteed to occur. The reasons are many and varied: All of the transmit time periods available may not be used by the network; the radio transmitting during a specific timeslot may be so far away from the radio which is host to the AAP that the received signal level is too low to be detected; or the AAP may be shielded from some SOIs. In these cases, the AAP should maintain its previously developed weights rather than adapt to an erroneous environment. The Dominant Mode Block Update algorithm handles this circumstance very well: the weight update is based on calculations of  $R_0^{-1}R_1$ . Since there is no SOI present during  $R_1$  data collection, and the jammers are assumed stationary, the  $R_1$  data should exhibit the same statistics as the  $R_0$  data in this case. Calculations of  $R_0^{-1}R_1$  should repeatedly approach the identity matrix  $I$ , and the new weight estimate would equal the old. Simulations verify this expected result. In addition, the algorithm could easily determine that no SOI is present and discontinue adaptation before degrading previously formed weights.

### 4.3.2.6 RECEIVE ADAPTATION PERFORMANCE ANALYSIS (continued)

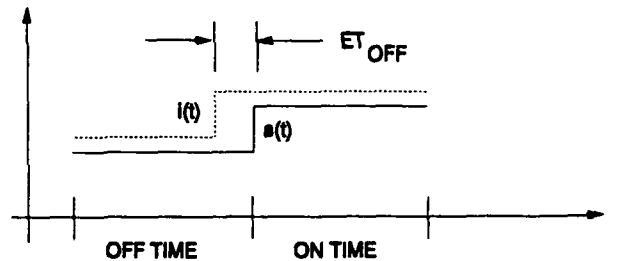
#### Collision Scenarios -

A collision is said to occur when a signal not of interest (SNOI) changes state during a data collection interval. The four most likely collision scenarios are: 1) A SNOI turns off during an off time data collect, 2) a SNOI turns on during an off time data collect, 3) a SNOI turns off during an on time data collect, and 4) a SNOI turns on during an on time data collect.

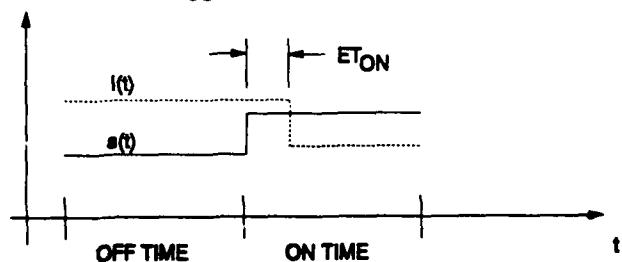
SCENARIO # 1



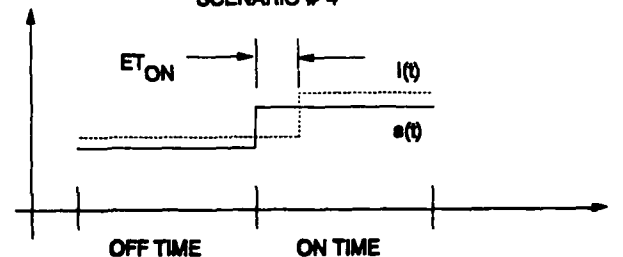
SCENARIO # 2



SCENARIO # 3



SCENARIO # 4



The general equations used in the analysis of these collision scenarios are:

$$i_+(t) = u(t) + a_i i(t)$$

$$A = [ a_s \ a_i ]$$

$$R_0 = R_{uu} + AS_{off}A^H \quad \text{or} \quad R_0 = R_{++} + AS_{off+}A^H$$

$$R_1 = R_{uu} + AS_{on}A^H \quad \text{or} \quad R_1 = R_{++} + AS_{on+}A^H$$

The S matrices depend on which of the collision scenarios are being analyzed. The other terms are defined by:

$R_{uu}$  = autocorrelation matrix of steady state interferers only

$R_{++}$  = autocorrelation matrix of steady state interferers and transient interferer

$a_i$  = aperture of transient interferer

$a_s$  = aperture of the desired signal

$R_{ji}$  = covariance of transient interferer

$R_{ss}$  = covariance of the desired signal

Substituting the first definitions for  $R_0$  and  $R_1$  into the general eigenequation gives

$$\lambda [R_{uu} + AS_{off}A^H]w = [R_{uu} + AS_{on}A^H]w$$

### 4.3.2.6 RECEIVE ADAPTATION PERFORMANCE ANALYSIS (continued)

#### Collision Scenarios (continued) -

The solutions to this eigenequation includes  $m - 2$  solutions with  $A^H w_k = 0$  and  $\lambda_k = 1$ , and two solutions with  $w_m = R_{uu}^{-1} A p_m$  where  $p_m$  satisfies the eigenequation

$$\lambda [I + S_{off}(A^H R_{uu}^{-1} A)] p = [I + S_{on}(A^H R_{uu}^{-1} A)] p$$

The other resulting general eigenequation is

$$\lambda [R_{++} + A S_{off+} A^H] w = [R_{++} + A S_{on+} A^H] w$$

In this case, the solutions of interest are  $w_m = R_{++}^{-1} A p_{m+}$  where  $p_{m+}$  satisfies the eigenequation

$$\lambda [I + S_{off+}(A^H R_{++}^{-1} A)] p_+ = [I + S_{on+}(A^H R_{++}^{-1} A)] p_+$$

**First case** - In this case a SNOI turns off during an off time data collect. The resulting autocorrelation matrices are  $R_0 = R_{uu} + \epsilon a_i a_i^H R_{ii}$  and  $R_1 = R_{uu} + a_s a_s^H R_{ss}$ . Substituting these into the generalized eigenequation gives

$$\lambda (R_{uu} + \epsilon a_i a_i^H R_{ii}) w = (R_{uu} + a_s a_s^H R_{ss}) w.$$

This eigenequation has  $m-2$  solutions with  $\lambda_k = 1$ ,  $a_i^H w_k$  and  $a_s^H w_k = 0$ ; the other two solutions are the solutions of interest:

- 1) The maximum (dominant) eigenvalue solution, which gives  $w_1 \propto R_{uu}^{-1} a_s$  and  $\lambda_1 = 1 + \gamma_{smax}$ .
- 2) The minimum eigenvalue solution, which gives  $w_m \propto R_{uu}^{-1} a_i$  and  $\lambda_m = 1/(1 + \epsilon \gamma_{imax})$ .

These results will hold true for any value of  $\epsilon$  between 0 and 1, even in the extreme case when the interferer turns off at exactly the same time that the SOI turns on. The algorithm should behave robustly in the presence of any collision which actually occurs in the off interval (i.e., where the SNOI energy does not actually interfere with the SOI waveform). This suggests that the algorithm should be compatible with dense FHMA and TDMA communication formats, as long as the signals are not time coincident. This underscores the applicability of the algorithm to multi-node communication networks.

However, the convergence speed of the Dominant Mode algorithm can be affected by these collisions, and the choice of  $u$  becomes more significant in this environment. In particular, the choice of  $u = 1$  can cause the antenna array to beam up on the interferer if the maximum attainable SINR of the SOI is very low. If the magnitude of  $\lambda_m - u$  is greater than the magnitude of  $\lambda_1 - u$ , or equivalently, if  $(\lambda_1 + \lambda_m)/2$  is greater than  $u$ , then the algorithm will capture the minimum mode and reject the SOI. Note the algorithm will not capture the interferer since it is off before the on time data collection interval when the beamformer weights are actually computed and used.

The algorithm will capture the minimum mode only if  $\gamma_s$  satisfies the inequality

$$\gamma_s < \epsilon \gamma_i / (1 + \epsilon \gamma_i) - 2(1 - u).$$

#### 4.3.2.6 RECEIVE ADAPTATION PERFORMANCE ANALYSIS (continued)

##### Collision Scenarios (continued) -

This implies  $\gamma_s < 2u - 1$  and  $\gamma_i > [1/(2u - 1 - \gamma_s) - 1]/\epsilon$ . This condition can be precluded by setting  $u \leq 1/2$ , and is not a threat if  $\gamma_{smax}$  is greater than unity. However, if  $u = 1$  is chosen, then the convergence time may be dominated by  $1 - \lambda_m$  rather than  $\lambda_2 - 1$ .

**Second case -** In this case a SNOI turns on during an off time data collect. The resulting autocorrelation matrices are  $R_0 = R_{++} - (1 - \epsilon)a_i a_i^H R_{ii}$  and  $R_1 = R_{++} + a_s a_s^H R_{ss}$ . Substituting these into the generalized eigenequation gives

$$\lambda(R_{++} - (1 - \epsilon)a_i a_i^H R_{ii})w = (R_{++} + a_s a_s^H R_{ss})w.$$

This eigenequation has two solutions of interest:

- 1) The SOI capture solution, which gives  $w_s \propto R_{++}^{-1} a_s$  and  $\lambda_s = 1 + \gamma_{s+}$ .
- 2) The transient interferer solution, which gives  $w_i \propto R_{++}^{-1} a_i$  and  $\lambda_i = 1/(1 - (1 - \epsilon)\gamma_{i+})$ .

In these equations: 1)  $\gamma_{s+}$  is the maximum attainable SINR over the on time and considers the SOI to be the signal rather than an interferer. 2)  $\gamma_{i+}$  is a function of  $\gamma_i$ , the maximum attainable SOI-free Interference to Noise Ratio (INR), which ignores the SOI and treats the transient interferer as the desired signal. The term  $\gamma_{i+}$  is derived as follows:

$$\begin{aligned} \gamma_{i+} &= a_i^H R_{++}^{-1} a_i R_{ii} \\ &= a_i^H [R_{uu} + a_i a_i^H R_{ii}]^{-1} a_i R_{ii} \\ &= a_i^H R_{uu}^{-1} a_i R_{ii} / (1 + a_i^H R_{uu}^{-1} a_i R_{ii}) \\ &= \gamma_i / (1 + \gamma_i). \end{aligned}$$

Note that while  $\gamma_i$  has a range from 0 to infinity, the range of  $\gamma_{i+}$  is limited between 0 and 1.

For this scenario, it is possible for the dominant mode of the eigenequation to capture the interferer: both eigenvalues can have a magnitude greater than unity, and the eigenvalue associated with the capture of the SOI can be less than the eigenvalue associated with the capture of the interferer. By comparing the associated eigenvalues, the magnitude of  $\lambda_i$  is greater the magnitude of  $\lambda_s$  if  $\gamma_{i+}$  satisfies

$$(1 - 1/(1 + \gamma_{s+})) / (1 - \epsilon) < \gamma_{i+} < (1 + 1/(1 + \gamma_{s+})) / (1 - \epsilon)$$

This yields two conditions:

$$\gamma_{s+} < (1 - \epsilon)\gamma_{i+} / (1 - (1 - \epsilon)\gamma_{i+}) \text{ where } \gamma_{i+} < 1/(1 - \epsilon) \text{ and}$$

$$\gamma_{s+} < (2 - (1 - \epsilon)\gamma_{i+}) / (1 - \epsilon)\gamma_{i+} - 1 \text{ where } 1/(1 - \epsilon) < \gamma_{i+} < 2/(1 - \epsilon).$$

#### 4.3.2.6 RECEIVE ADAPTATION PERFORMANCE ANALYSIS (continued)

##### Collision Scenarios (continued) -

The critical value of  $\gamma_{s+}$  is plotted as a function of  $\gamma_{i+}$  in figure 1.a. The critical value spans the entire range of  $\gamma_{i+}$ , approaching infinity for  $\gamma_{i+} = 1/(1 - \epsilon)$ . However, only a portion of this region is pertinent, since  $\gamma_{i+}$  is bounded by 0 and 1. In particular,  $\gamma_{i+}$  is less than  $1/(1 - \epsilon)$  for every value of  $\epsilon$  ( $0 < \epsilon < 1$ ). Using these relations, a bound on  $\gamma_{s+}$  that is directly dependent on  $\gamma_i$  (the true, maximum attainable INR) can be found:

$$\gamma_{s+} = (\epsilon^{-1} - 1)\epsilon\gamma_i/(1 + \epsilon\gamma_i).$$

This threshold is plotted as a function of  $\gamma_i$  in figure 1.b.

As is evident in figure 1, the Dominant Mode algorithm is guaranteed to capture the SOI if the maximum attainable SOI SINR is greater than  $\epsilon^{-1} - 1$ . Assuming that  $\epsilon$  is uniformly distributed between 0 and 1, then the median value of critical  $\gamma_{s+}$  is given by  $\gamma_i/(2 + \gamma_i)$  which is less than 1 for all  $\gamma_i$ .

The practical significance of this result is that this collision scenario will result in capture of the SOI in over 50 % of all collisions if the maximum attainable SINR of the SOI is greater than 0 dB. The SOI will be captured in over 75 % of these collisions if its maximum attainable SINR is greater than 5 dB.

This collision scenario will directly affect the convergence time of the Dominant Mode algorithm, by decreasing the spread between the two largest eigenvalues. This convergence time will not be significantly affected by choice of  $u$  in the algorithm.

**Third and fourth cases -** The remaining two collision scenarios yield a mixture of the SOI and interference waveforms. In scenario # 3,  $S_{on+}$  and  $S_{off+}$  are given by

$$\underline{S}_{OFF+} = \begin{bmatrix} 0 & 0 \\ 0 & 0 \end{bmatrix} \quad \text{and} \quad \underline{S}_{ON+} = \begin{bmatrix} R_{ss} & 0 \\ 0 & \epsilon R_{uu} \end{bmatrix}$$

which yields the eigenequation

$$\lambda \underline{p} = \begin{bmatrix} p_{ss} R_{ss} & p_{st} R_{ss} \\ \epsilon p_{tu} R_{uu} & \epsilon p_{uu} R_{uu} \end{bmatrix} \underline{p}$$

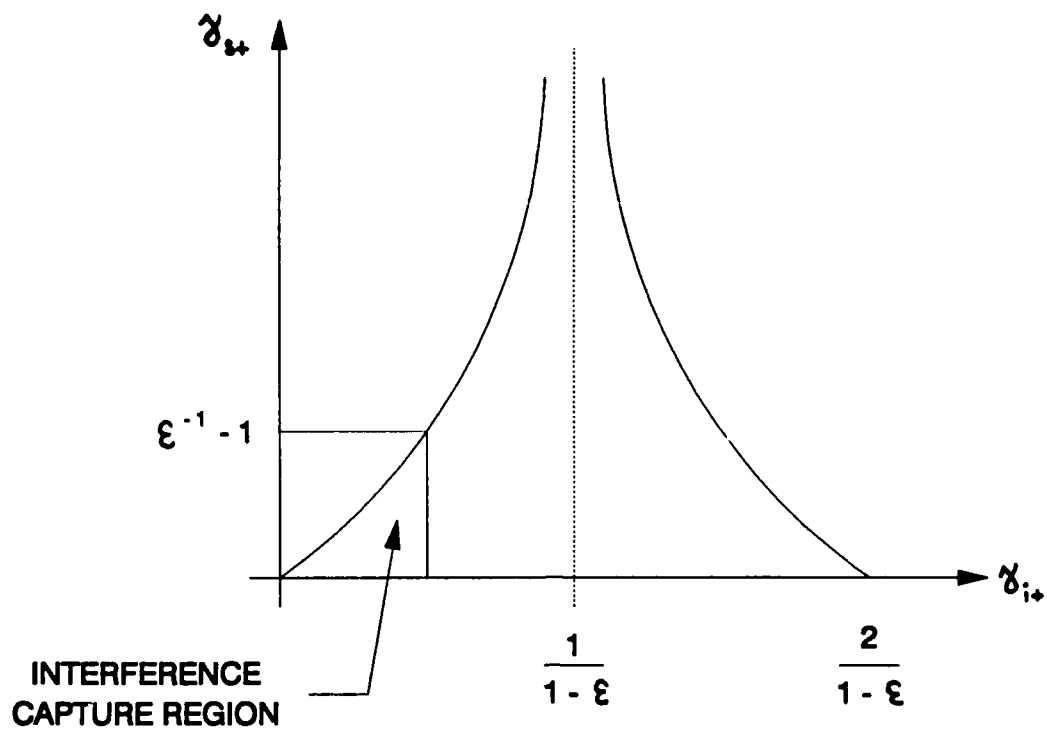


FIGURE 1.A. THRESHOLD VALUE OF  $\gamma_{st}$  VS.  $\gamma_{i+}$ .

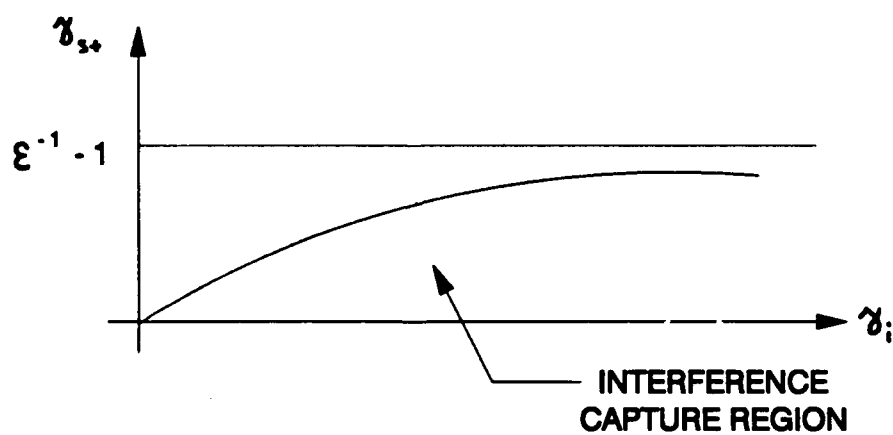


FIGURE 1.B. THRESHOLD VALUE OF  $\gamma_{st}$  VS.  $\gamma_i$ .

FIGURE 1. COLLISION THRESHOLD VALUES

#### 4.3.2.6 RECEIVE ADAPTATION PERFORMANCE ANALYSIS (continued)

In scenario # 4, the corresponding S matrices are given by

$$\underline{S}_{OFF} = \begin{bmatrix} 0 & 0 \\ 0 & 0 \end{bmatrix}; \quad \underline{S}_{ON} = \begin{bmatrix} R_{ss} & 0 \\ 0 & (1 - \epsilon)R_{ii} \end{bmatrix};$$

$$\underline{S}_{OFF+} = \begin{bmatrix} 0 & 0 \\ 0 & -R_{ii} \end{bmatrix}; \quad \text{and} \quad \underline{S}_{ON+} = \begin{bmatrix} R_{ss} & 0 \\ 0 & \epsilon R_{ii} \end{bmatrix}$$

yielding the eigenequations

$$\lambda \underline{P} = \begin{bmatrix} p_{ss} R_{ss} & p_{si} R_{ss} \\ (1 - \epsilon) p_{is} R_{ii} & (1 - \epsilon) p_{ii} R_{ii} \end{bmatrix} \underline{P}$$

$$\lambda \begin{bmatrix} 1 & 0 \\ 0 & 1 - \epsilon p_{ii+} \end{bmatrix} \underline{P}_+ = \begin{bmatrix} p_{ss+} R_{ss} & p_{si+} R_{ss} \\ \epsilon p_{is+} R_{ii} & \epsilon p_{ii+} R_{ii} \end{bmatrix} \underline{P}_+$$

Both of these eigenequations apply, and are appropriate at different times in the collection interval.

It is beyond the scope of this report to analyze these scenarios in any detail. However, it is expected that the dominant mode weight vector will be weighted towards the SOI if  $\epsilon$  is small in scenario # 3 and if  $\epsilon$  is large in scenario # 4. It is also expected that this weighting shall be dependent on the maximum attainable interference SINR. However, this affect should be limited, especially for scenario # 3, since  $\gamma_{i+}$  is limited between 0 and 1 but  $\gamma_s$  is unbounded.

In any case, some measures can be taken to mitigate against these collisions. The last two collision scenarios can all be detected by monitoring the power level of the beamformer output signal. In LPI communications, if the SOI has been captured on previous hops, the previous aperature estimates can also be used to detect capture conditions: if the current aperature estimate is vastly different than the history of aperature estimates, it can be assumed that the algorithm is acquiring the wrong signal, and that timeslot's processing can be discarded.

#### 4.3.2.7 DIRECTIVE / RETRODIRECTIVE COMMUNICATION

The receive mode adaptation simultaneously steers nulls in the directions of jammers and a beam in the direction of the desired signal. This receive antenna pattern, which is customized to the RF signal environment, provides tremendous improvement to the SINR seen by the receiver compared to omni-directional antenna performance. This same information can be used to improve the transmit antenna pattern as well. Two methods of using the receive statistics and weights to direct the transmit energy are considered: retrodirective schemes and directive schemes.

#### 4.3.2.7 DIRECTIVE / RETRODIRECTIVE COMMUNICATION (continued)

Retrodirective transmission schemes apply the complex conjugates of the receive weights to the transmit weighting elements. This is described by  $w_{tx} = w_{rx}^*$  where  $w_{tx}$  is the transmit weight vector and  $w_{rx}$  is the receive weight vector formed by adaptation. If the receive and transmit paths are precisely calibrated, this will result in a transmit antenna pattern which is identical to the receive pattern. The advantage of this approach is that very little power is transmitted in the direction of the jammers since nulls have been formed in those directions. Simultaneously, there is high gain (a beam) in the direction of the last signal received at the current channel frequency.

Directive transmission schemes ignore the jammer locations, and attempt to maximize the power transmitted in the direction of the desired signal. The nulls in the directions of jammers are not maintained, so the jammers will see more transmit power in this case than for retrodirective cases, but more power can be provided in the desired direction and less in all other directions. To achieve directive communications, the transmit weights are set to the complex conjugate of the receive aperture estimates determined during receive adaptation. The pertinent equation is  $w_{tx} = (R_1 w_{rx})^*$ .

The retrodirective transmission weights are very precise since they are based on the high level jammers present during reception. Very deep, accurately directed nulls are provided, and the desired signal direction has relatively high gain. The directive transmission weights are not as precise, at least not with aperture estimates based on a limited number of receive data samples. In this case, the jammer power corrupts data being used to estimate the desired signal's direction of arrival. Inaccuracies in this estimate directly impacts the quality of the directive transmit antenna pattern. This performance can be greatly improved, however, by averaging a large number of aperture estimates taken over a long period of time. There are a variety of ways this averaging can be accomplished; some schemes are outlined below:

- The receive aperture estimates for each frequency hop can be stored. This historical data can be averaged to form the transmit weights for a given frequency.

- The history of receive aperture estimates for each frequency can be averaged, then used to interpolate the aperture estimates for frequencies not previously visited or rarely visited.

- The receive aperture estimates for each frequency hop can be included in the averaging of the aperture estimates for some of the adjacent channels as well as its own frequency channel. This will reduce the number of visits to each frequency required to obtain an accurate transmit beam.

- The output SINR provided by receive adaptation can be calculated by the AAP. This information can be used to weight the aperture estimate calculated during that particular timeslot. For example, if the output SINR is very high, the aperture estimate is more accurate than a low SINR output would provide, so the weight of this estimate should be relatively large. These weighted aperture estimates would then be averaged to determine the transmit weights.

Certainly many other techniques could be suggested, and the techniques listed above could be combined to provide more options.

#### 4.3.2.7 DIRECTIVE / RETRODIRECTIVE COMMUNICATION (continued)

Directive transmission techniques can be combined with receive mode adaptive processing and careful transmit power level control to provide a directive communication link which is very difficult to jam or intercept. This anti-jam (A/J) and low probability of intercept (LPI) link would operate as described below:

- 1) Radio 1 transmits omni-directionally, intending to communicate with Radio 2.
- 2) Radio 2 enables the receive adaptation of its adaptive array processor. This rejects any interference present and assures high gain in the direction of Radio 1. Even if the radios are not in synch, the algorithm can be adjusted such that the signal is acquired.
- 3) After Radio 2 has acquired the signal from Radio 1, and has formed nulls in the directions of jammers, uses this information to determine its transmit weights. These weights are designed to provide high gain in the direction of Radio 1 and little gain elsewhere.
- 4) Radio 1 will employ its AAP to reject interferers and beam up on the signal from Radio 2. It will then be capable of directive transmissions as well.
- 5) At this point the link between Radio 1 and Radio 2 is established. The transmit antenna patterns are optimized to transmit most of their transmit energies in the direction of each other; their receive antenna patterns are optimized to provide the maximum attainable SINR to their demodulators. Each radio could calculate their SINR, and knowing the SINR required for reliable communications they could determine how much margin was available. This information could be transmitted back to the other radio, which would then know how much less power it could transmit and still maintain a reliable link.

With transmissions at minimum power and antenna gains beamed up for the link, and jammers nulled during reception while simultaneously providing gain for the link, a very robust communication link which is difficult for the enemy to detect is provided.

#### 4.3.2.8 DIRECTIVE COMMUNICATION PERFORMANCE ANALYSIS

Evaluation of the directive transmission performance depends on the application; two applications are considered in this study:

##### LPI -

The power radiated from the array is calculated; it is highly dependent on direction. A locus of points around the transmitter are calculated which indicate the geographical area within which the radiated power is sufficient for detection by a reconnaissance receiver. The boundary of this region is identical to the transmit antenna pattern, only depicted on a linear scale rather than logarithmic, and includes a linear scaling factor which reflects the sensitivity of the recon receiver. This locus of points establishes a threshold of transmit power; receivers within this boundary will detect the transmissions, while receivers outside this boundary will not. The area inside this boundary is referred to here as the intercept footprint.

The directive transmissions will result in some intercept footprint which greatly reduces the intercept footprint relative to isotropic transmissions, but which may not be optimal. The optimal pattern would minimize the intercept footprint area while maintaining consistent gain in the direction of the desired link. Thus the figure of merit for LPI communications is the

#### 4.3.2.8 DIRECTIVE COMMUNICATION PERFORMANCE ANALYSIS

##### LPI (continued) -

areas of the intercept footprint. The optimum radiated pattern is derived below, and is used for comparison to the directive patterns generated via receive adaptation in the Simulation section of this report (4.3.4). Isotropic data are also used in the comparisons.

**Derivations** - The terms used in the derivation of the optimal transmit antenna weights and pattern, and in the computation of the intercept footprint areas, are defined below:

$$\begin{aligned}
 d_{rcv} &= \text{distance from xmitter to rcvr} \\
 \theta_{xmt} &= \text{direction from xmitter to rcvr} \\
 \\ 
 d_{recon} &= \text{distance from xmitter to recon system} \\
 \theta_{recon} &= \text{direction from xmitter to recon system} \\
 \\ 
 \gamma_{LPI} &= \text{required rcvr SINR} \\
 \gamma_{det} &= \text{required recon SINR} \\
 \\ 
 NF_{rcv} &= \text{rcvr noise figure} \\
 NF_{recon} &= \text{recon noise figure} \\
 \\ 
 a_{xmt}(\theta) &= \text{xmitter array manifold} \\
 \xi_{xmt} &= \text{xmitter array weightings} \\
 \\ 
 M_{xmt} &= \text{number of xmitter sensors} \\
 M_{rcv} &= \text{number of rcvr sensors}
 \end{aligned}$$

When both the transmitter and receiver are isotropic, the ratio of distances that the reconnaissance and desired receivers are located from the transmitter, both capable of detecting the transmission, is given by

$$\frac{d_{recon}}{d_{rcv}} = \sqrt{\left(\frac{\gamma_{LPI}}{\gamma_{det}}\right)\left(\frac{NF_{rcv}}{NF_{recon}}\right)} \quad \forall \theta_{recon}$$

When the transmitter is isotropic but the desired receiver employs an AAP and has established the optimum antenna pattern, this ratio becomes

$$\frac{d_{recon}}{d_{rcv}} = \sqrt{\frac{1}{M_{rcv}}\left(\frac{\gamma_{LPI}}{\gamma_{det}}\right)\left(\frac{NF_{rcv}}{NF_{recon}}\right)} \quad \forall \theta_{recon}$$

If both the transmitter and receiver employ antenna arrays, and directive transmissions are provided, the distance ratio is

#### 4.3.2.8 DIRECTIVE COMMUNICATION PERFORMANCE ANALYSIS

LPI (continued) -

$$\frac{d_{recon}}{d_{rcv}} = \sqrt{\frac{1}{M_{rcv}} \left( \frac{\gamma_{LPI}}{\gamma_{det}} \right) \left( \frac{NF_{rcv}}{NF_{recon}} \right)} \frac{|g_{xmt}^H a_{xmt}(\theta_{recon})|}{|g_{xmt}^H a_{xmt}(\theta_{xmt})|}$$

The area of the intercept footprint corresponding to the isotropic transmission and adaptive reception is given by

$$A_{iso} = \pi d_{rcv}^2 \times \frac{1}{M_{rcv}} \left( \frac{\gamma_{LPI}}{\gamma_{det}} \right) \left( \frac{NF_{rcv}}{NF_{recon}} \right)$$

where  $M_{rec} = 1$  for non-adaptive reception. The area in the directive transmission case is

$$A(g_{xmt}) = A_{iso} \times \frac{g_{xmt}^H R_{a_{xmt} a_{xmt}} g_{xmt}(\theta_{recon})}{|g_{xmt}^H a_{xmt}(\theta_{xmt})|^2}$$

where

$$R_{a_{xmt} a_{xmt}} = \frac{1}{2\pi} \int_{-\pi}^{\pi} a_{xmt}(\theta) a_{xmt}^H(\theta) d\theta$$

The optimum transmit weights for LPI directive communications would be those weights which minimize the intercept footprint area. The solution to the minimization of  $A(g_{xmt})$  is

$$g_{opt} \propto R_{a_{xmt} a_{xmt}}^{-1} a_{xmt}(\theta_{xmt})$$

The resulting minimum intercept footprint area is then

$$A(g_{opt}) = A_{iso} / a_{xmt}^H(\theta_{xmt}) R_{a_{xmt} a_{xmt}}^{-1} a_{xmt}(\theta_{xmt})$$

A/J -

The concept for A/J applications is very similar to LPI except the reconnaissance receiver is replaced by a jammer, and the location of the jammer relative to the receiver is of importance. The transmit power is assumed to be fixed - the transmitter will transmit at its maximum level during all transmissions, disregarding the likelihood of being detected by a reconnaissance

### 4.3.2.8 DIRECTIVE COMMUNICATION PERFORMANCE ANALYSIS

#### A/J (continued) -

receiver. The directive communication system must use the adaptive antenna arrays at the receiver and transmitter to provide the maximum power into the receiver given the fixed transmit power limitation. Thus, in the A/J case, the figure of merit is the SOI output power of the receiver's AAP (given the fixed transmit power constraint).

The calculations in the A/J case are very similar to the LPI case. As was done for the LPI analysis, the optimum radiated pattern is derived below, and is used for comparison to the directive patterns generated via receive adaptation in the Simulation section of this report (4.3.4). Isotropic data are also used in the comparisons.

**Derivations** - The terms used in the derivation of the optimal transmit antenna weights and pattern, and in the computation of the receiver input power, are defined below:

$d_{rcv}$  = distance between xmitter and rcvr  
 $\theta_{rcv}$  = DOA of xmitter at rcvr

$d_{jam}$  = distance between jammer and rcvr  
 $\theta_{jam}$  = DOA of jammer at rcvr

$\gamma_{a/j}$  = required rcvr SINR  
 $\alpha_{iso}$  = isotropic jammer-free link margin

$P_{xmt}$  = total xmitter ERP  
 $P_{jam}$  = total jammer ERP

$a_{rcv}(\theta)$  = rcvr array manifold  
 $g_{xmt}$  = xmitter array weightings

$M_{xmt}$  = number of xmitter sensors  
 $M_{rcv}$  = number of rcvr sensors

For A/J applications, the distances of interest are the jammer and the desired receiver relative to the transmitter; the analysis uses the ratio of these two distances. When both the transmitter and receiver are isotropic, this distance ratio is given by

$$\left(\frac{d_{jam}}{d_{rcv}}\right)^2 = \frac{\gamma_{a/j}}{1 - \alpha_{iso}^{-1}} \left(\frac{P_{jam}}{P_{xmt}}\right)$$

When the transmitter is isotropic but the desired receiver employs an AAP and has established the optimum antenna pattern, this ratio becomes

## 4.3.2.8 DIRECTIVE COMMUNICATION PERFORMANCE ANALYSIS

A/J (continued) -

$$\left(\frac{d_{jam}}{d_{rcv}}\right)^2 = M_{rcv} \alpha_{iso} \gamma_{aj} \left(\frac{P_{jam}}{P_{xmt}}\right) \max\left\{0, \frac{G_{jam}}{1 - (M_{rcv} \alpha_{iso})^{-1}} - 1\right\},$$

$$G_{jam} = \left| \frac{1}{M_{rcv}} a_{rcv}^H(\theta_{rcv}) a_{rcv}(\theta_{jam}) \right|^2$$

In the fully adaptive case, both the transmitter and the receiver employ antenna arrays, and directive transmissions are provided. The resulting distance ratio is

$$\left(\frac{d_{jam}}{d_{rcv}}\right)^2 = M_{rcv} \alpha_{iso} \gamma_{aj} \left(\frac{P_{jam}}{P_{xmt}}\right) \max\left\{0, \frac{G_{jam}}{1 - (M_{xmt} M_{rcv} \alpha_{iso})^{-1}} - 1\right\}$$

The optimum transmit weights for A/J directive communications would be those weights which maximize the receiver input power. These weights are given by the solution to

$$\max_{g_{xmt}} |g_{xmt}^H a_{xmt}(\theta_{xmt})| \quad \text{such that} \quad \|g_{xmt}\|^2 = P_{xmt}$$

results in the optimal A/J transmit weights

$$g_{xmt} = \frac{a_{xmt}(\theta_{xmt})}{\|a_{xmt}(\theta_{xmt})\|} P_{xmt}^{1/2}$$

### 4.3.3 ARCHITECTURE DEVELOPMENT

#### 4.3.3.1 INTRODUCTION

To implement the algorithm developed in Phase I, the architecture must include specific features; different algorithms will require other features. The intent of the ACM Systems architecture development was to provide all the functions necessary to implement a large variety of algorithms, and simultaneously allow compatibility with an existing Army tactical radio. One of the long term goals of this study is to lead to the hardware development of an AAP unit which could be produced in high volume and deployed with Army radios already in the field. The corresponding constraints on the AAP unit requires the architecture to be small, have low complexity, low cost, and accommodate a range of applications.

To allow adaptation of the weights, a minimum number of RF statistical measurements are required. Depending on the algorithm being used, the statistics may be accumulated in vector form (such as the input to output cross-correlation vector) or in matrix form (such as the input covariance matrix). If the algorithm is minimizing output power when it is known that only interference plus noise is present (no signal), then "off time" data only is required. However, if the algorithm is maximizing the Signal to Interference plus Noise Ratio (SINR), then data must be acquired when the signal is present "on time" and when not present "off time". As discussed in the Algorithm sections, "on time" and "off time" refers to the expected presence of the signal of interest. This section's notation for the correlation vectors and matrices corresponding to off time and on time data collects are defined below:

$$\begin{array}{l}
 \text{Off time cross-correlation vector} = \mathbf{R}_{xy0} = \begin{array}{|c|} \hline E(x_1y) \\ \hline | \\ \hline E(x_my) \\ \hline \end{array} \\
 \text{(measured when signal is} \\
 \text{known not to be present)} \\
 \\
 \text{On time cross-correlation vector} = \mathbf{R}_{xy1} = \begin{array}{|c|} \hline E(x_1y) \\ \hline | \\ \hline E(x_my) \\ \hline \end{array} \\
 \text{(measured when signal is} \\
 \text{expected to be present)} \\
 \\
 \text{Off time covariance matrix} = \mathbf{R}_0 = \begin{array}{|c|} \hline E(x_1x_1) \quad - \quad E(x_1x_m) \\ \hline | \\ \hline E(x_mx_1) \quad - \quad E(x_mx_m) \\ \hline \end{array} \\
 \text{(measured when signal is} \\
 \text{known not to be present)} \\
 \\
 \text{On time covariance matrix} = \mathbf{R}_1 = \begin{array}{|c|} \hline E(x_1x_1) \quad - \quad E(x_1x_m) \\ \hline | \\ \hline E(x_mx_1) \quad - \quad E(x_mx_m) \\ \hline \end{array} \\
 \text{(measured when signal is} \\
 \text{expected to be present)}
 \end{array}$$

In the definitions above,  $E()$  denotes the expected value of the product inside the brackets. The baseline architecture design is capable of measuring all of the statistics identified above; the baseline algorithm assumed for subsequent discussion is the Dominant Mode Block Update.

### 4.3.3 ARCHITECTURE, INTRODUCTION (continued)

The minimum statistical data required for the off time is the collection of covariance data and the calculation of  $R_0^{-1}$ . During the on time, the requirements are more demanding: A block of on time cross-correlation data  $R_{xy1}$  is measured. This is combined with  $R_0^{-1}$  and the last calculated weight estimate  $w(m)$  to calculate an update of the weight estimate  $w(m+1)$ . This procedure is iterated with sequential blocks of on time data, resulting weights which converge to values which provide the maximum attainable output SINR. Several iterations are made during each timeslot; as the weights are updated, the receive antenna gain pattern changes, ultimately steering nulls in the directions of jammers and a beam in the direction of the desired signal.

In a frequency hopped system the on time is entirely defined by the tactical radio the AAP is operating with; there is no flexibility in when on time data may be collected. The off time data, however, may be separated from the on time either spectrally or temporally (by frequency or time). This is illustrated in figure 2. Spectrally separated off time data is collected by sampling the RF statistics in a frequency bin adjacent to the on time frequency, and is done simultaneously with on time processing. Temporally separated off time data is collected at the same frequency as the on time signal, but at a time when the signal is not on. The baseline selected by ACM for temporally separated data collection uses the immediately preceding timeslot, and is therefore called anticipative.

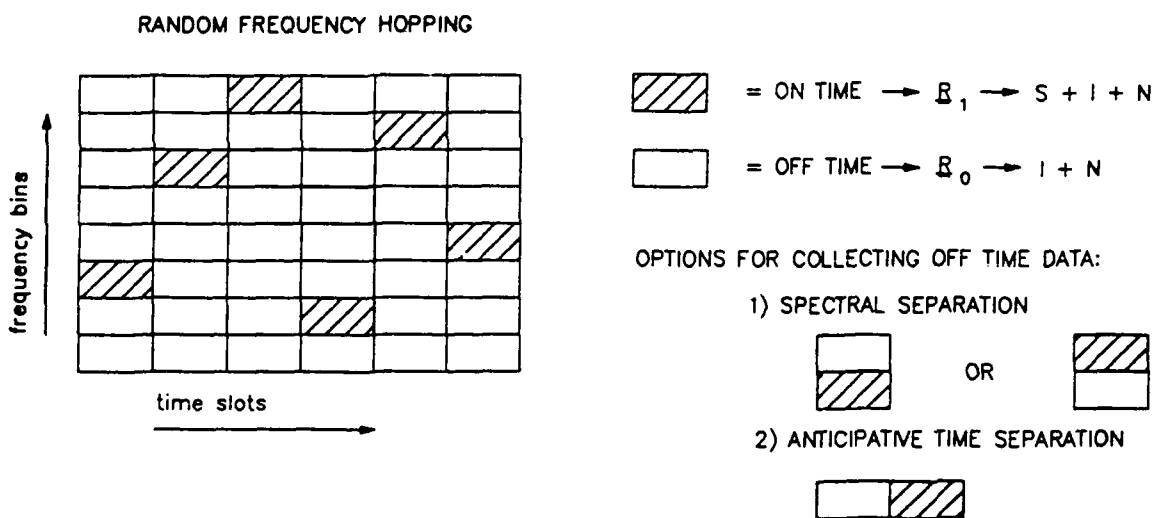


Figure 2. Data Collection Timing.

The spectral and temporal means of off time data collection provide two candidate top level architectures; these are both presented and a baseline is selected and justified. This leads to examination and selection of each feature of the architecture implementation. Topics discussed below includes the key electrical functions (complex weighting elements, statistical measurements, and weight calculation), other functions specific to the chosen architecture (RF assembly, IF chains, frequency synthesizer, interface and control, etc.), the necessity of some calibration and proposed methods to achieve it, a complete baseline receive AAP block diagram, and some comments regarding the transmit architecture required for directive or retrodirective communications.

### 4.3.3.2 DATA COLLECTION AND TOP LEVEL ARCHITECTURES

#### Introduction -

As discussed above, two methods of separating off from on time data are considered - spectral and temporal. A section below is dedicated to each method, and includes block diagram of the top level architecture capable of implementing them. In both cases, the following key function implementations are assumed: The complex weights are realized at IF, the statistical measurements are made at both IF and baseband, and the weight calculations are done digitally.

#### Spectral Separation -

A block diagram showing how on time and off time data can be collected simultaneously using spectral separation is given in figure 3. The basis for this technique are two statistical measurement circuits in each channel operating in parallel. ("Channel" refers to the different antenna elements and their associated circuits). The data provided to the two statistical measurement circuits are from different frequency bands by virtue of the filtering provided by FLTR 0 (off time) and FLTR 1 (on time).

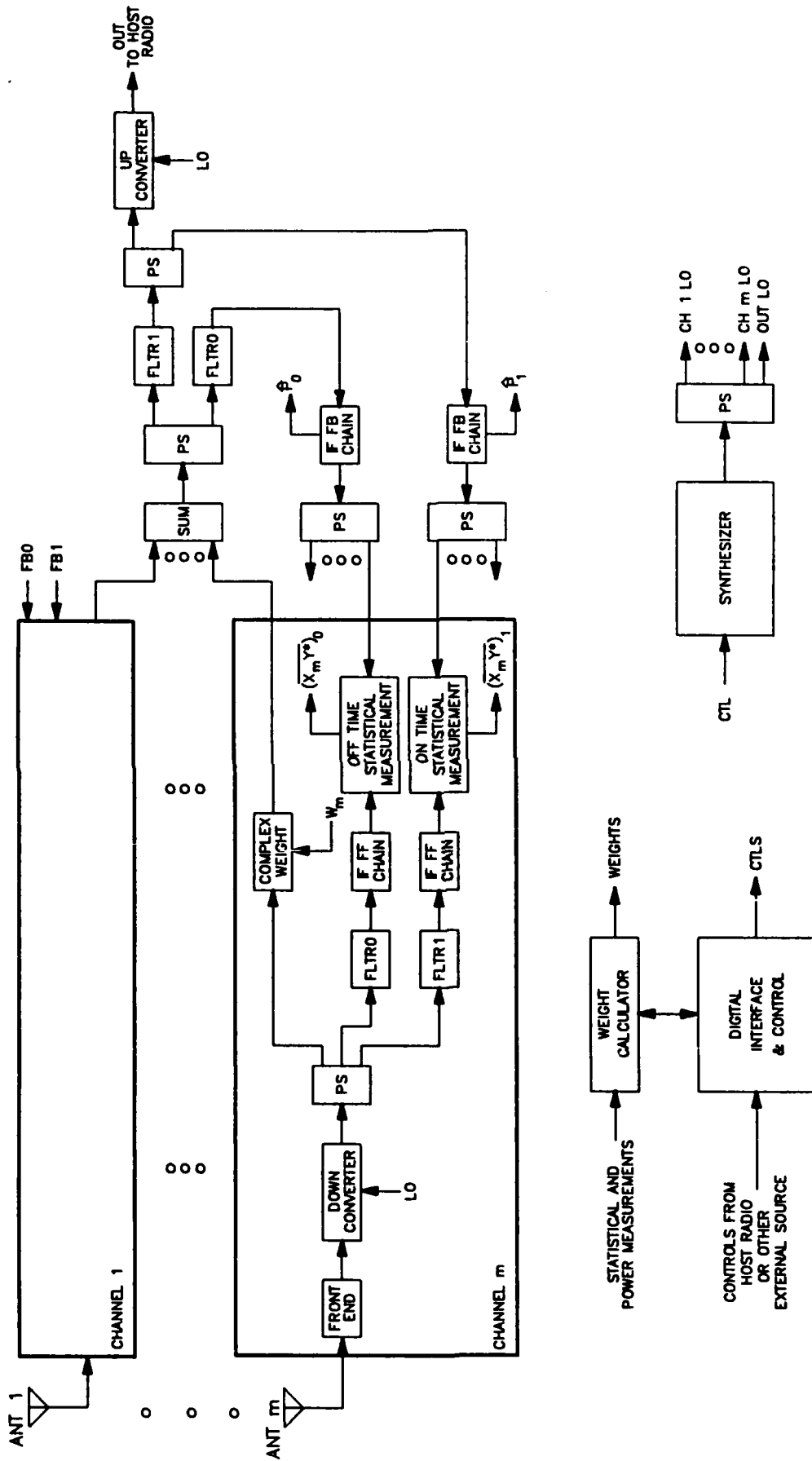
The incoming RF signals are sensed by the antenna elements and processed by the receiver front ends which filter out signals beyond the operating range of the host radio and establish a low noise figure for the AAP system. A Local Oscillator signal (LO) is provided to the downconverters which hops synchronously with the host radio to cause the signal of interest (SOI) to always fall within the fixed IF passband provided by FLTR 1. The same downconverter is used to simultaneously cause an adjacent RF band to fall at an offset IF band which is passed by FLTR 0. The circuits following these two highly selective IF filters all use wideband devices capable of processing both bandpass signals equally well, and are therefore identical. The IF feedforward chains are required to process the IF signals so they are within the most linear region of the statistical measurement circuits' operating range. The statistical measurement circuits provide multiplications, integration, and A/D conversions as required (discussed in later sections), and forward digitized statistical data to the digital circuits used to calculate the complex weights. The calculated weight estimates are applied to the weighting elements of each channel, and the weighted results from each channel are summed to form a composite signal. The on time band is filtered and output to the host radio (after coherent upconversion to RF), and is feedback to the on time statistical measurement circuits for measuring input to output cross-correlation data. In addition, a parallel feedback path is provided for off time data collection. Power monitors are provided in both feedback channels to allow measurement of the output powers in both on and off time bands.

#### Comments regarding this architecture -

- Inverting a complex matrix such as  $R_0$  is time consuming. If the algorithm being used requires  $R_0^{-1}$ , only a few (perhaps just one) updates of the weight estimates may be available in a timeslot. One way around this limitation is to delay applying the off time data until the following timeslot, which is essentially anticipative processing.

- Since the on and off time signals are not processed by the same circuits, errors will be introduced: measurements are made over two frequency bands selected by different filters, the signals are processed by different feedforward and feedback circuits, and the actual measurements are performed by different circuits.

FIGURE 3. BLOCK DIAGRAM, SPECTRAL SEPARATION FOR OFF TIME DATA



### 4.3.3 ARCHITECTURE, DATA COLLECTION (continued)

#### Comments regarding spectral separation (continued) -

o The off time data may not include the same jamming signals as the on time data since they are from different frequency bands. For the same jammers to be present over adjacent frequency bands simultaneously requires an assumption that the jammers are wideband.

o Using data collected from different frequency bands to perform weight estimate calculations may introduce frequency dependent errors. If operating with a radio network having a large message bandwidth (such as EPLRS which uses DSSS), some form of frequency compensation may be required.

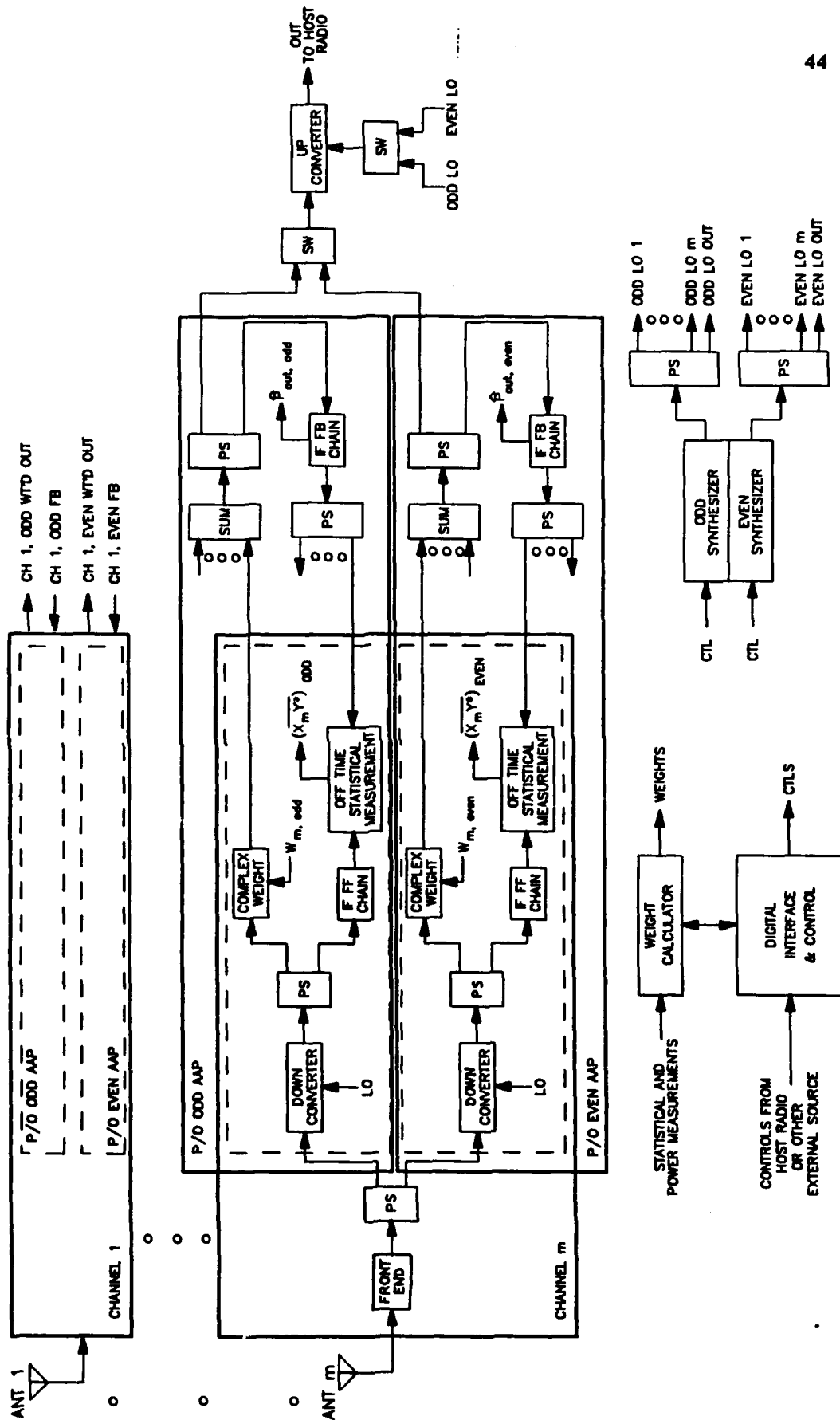
#### Anticipative -

A block diagram showing temporally separated collection of on and off time data is shown in figure 4. Two downconversions are required in this case; one is tuned to the present frequency being received by the host radio, the other is tuned to the next frequency to be received by the host radio. The latter sample provides off time data in advance of the on time data collect (anticipative). Since these frequency conversions are done simultaneously in parallel, two frequency synthesizers are required.

Figure 4 shows that the majority of circuits are duplicated; although they do not include all the circuits required to be stand alone AAPs, they are labeled "ODD AAP" and "EVEN AAP". An example of which circuits are used in what capacity for a given timeslot is described: Assume the synthesizer associated with the odd AAP is tuned to correspond to the host radio's present receive frequency. The even AAP is therefore tuned to the next frequency to be received by the host radio. In this case, the odd AAP is processing on time data, the even AAP is collecting off time data in the frequency band to be received in the next timeslot. The even AAP collects a long sample of off time data, forms the matrix  $R_0$ , performs the calculations necessary to form  $R_0^{-1}$ , and stores this data for use during the on time to follow in the subsequent timeslot. The odd AAP, having its  $R_0^{-1}$  available from the last timeslot, collects a block of on time data (perhaps 16 or 32 bits long) by measuring  $R_{xy1}$ , then calculates the next weight estimates using the equation (or one very similar):  $w(m+1) = R_0^{-1}R_{xy1}$ . Since  $R_{xy1} = R_1w(m)$ , the new weight estimates are updates of the old estimates, but are calculated without requiring forming the entire covariance matrix  $R_1$ . A vector measurement ( $R_{xy1}$ ) is used in place of a matrix measurement ( $R_1$ ) and matrix operation, thereby reducing the processing time for generating each weight update.

All the critical circuits for each AAP (even and odd) are provided separately. Each AAP collects its own off and on time data, using the same circuits operating at the same frequency for each measurement. This eliminates many of the errors introduced in the spectral separation architecture. The weights are applied and updated in the AAP which is processing on time data only; the resulting composite waveform is selected by the output switch, coherently upconverted and passed on to the host radio at its RF. The AAP processing off time data may not use the weighting elements during its off time, but will in the subsequent timeslot (which will be its on time). The weighting elements of the AAP processing off data may be updated in concert with the on time weight updates to provide a real time estimate of the output interference plus noise power; this may be useful to the adaptation algorithm or may be used for a coarse verification of adaptation performance. Other blocks in figure 4 are similar to blocks in figure 3 and are described in the "Spectral Separation" paragraphs above.

FIGURE 4. BLOCK DIAGRAM, ANTICIPATIVE OFF TIME DATA



### 4.3.3 ARCHITECTURE, DATA COLLECTION (continued)

#### Comments regarding the anticipative architecture -

o Simultaneous processing of on and off time data from different RF bands requires duplicate hardware (compared with the spectral separation approach), including a synthesizer, frequency conversions, and complex weights.

o Providing dedicated circuits for each AAP, particularly complex weighting, downconversion and IF processing, and statistical measurements, allows independent adaptation and eliminates errors which result in attempting to share these functions between two AAPs.

o The on and off time data is derived from the identical frequency band, therefore frequency compensation is not required.

o The on time is split into several blocks over which data samples are accumulated, then weight calculations and updates are provided. The off time has the same (or more) time available, but only one set of statistical measurements are required ( $R_0$ ). This allows for longer averaging and time to invert this matrix ( $R_0^{-1}$  is usually required).

o Since the off time statistics, in the form of  $R_0^{-1}$ , are stored and ready for use in the adaptation equation, and since the on time measurements require the vector  $R_{xy1}$  only rather than a matrix, the on time calculations are quick and simple, allowing multiple iterations within the same timeslot.

#### Combination of Approaches -

It is possible to use both spectral and temporal separation simultaneously for collecting off time data. This may be beneficial to the extent that more data bits are collected, thereby providing a better average of the actual environment. However, since the off time allows ample time for averaging a large number of bits on its own, and in light of the added complexity for allowing both methods, it is recognized that a combination of the two approaches is not cost effective.

#### Selection -

It is evident in the preceding discussions that the optimal configuration is an anticipative architecture. This is the baseline selected for further architecture development presented in the rest of this report. The reasons for this choice are briefly summarized below:

- o Long off time allows  $R_0^{-1}$  calculation.
- o Availability of  $R_0^{-1}$ , ease of measuring  $R_{xy1}$ , and simple calculations allow several iterations of the weight estimates within each timeslot.
- o Duplicate circuits add little risk or cost.
- o Same circuits used for all measurements, etc. thereby eliminating errors.
- o On and off time data from same frequency band, thereby eliminating errors.

### 4.3.3.3 COMPLEX WEIGHTING

#### Introduction -

Implementing the complex weights can be accomplished a number of ways. The primary variables are whether they are realized at RF, IF or baseband (analog or digital), and whether the magnitude and phase (polar) components or the real and imaginary (quadrature) components are controlled. These options are illustrated in figure 5; control of the magnitude and phase of the baseband signals is not presented since it is not a reasonable option. Also, the baseband approach shows analog multiplications, although an actual system would probably digitize these signals and perform the calculations digitally.

These options are presented and discussed in the following sections. The baseline approach for this report is then selected and justified.

#### At RF with Quadrature Weighting -

This option is shown in figure 5a; the device which performs this function is the Complex Phasor Modulator (CPM). It consists of a quadrature power divider, two linear voltage variable attenuators (VVA), and a power combiner. The quadrature divider splits the signal into in-phase (I) and quadrature (Q) components. Each of these components are multiplied in proportion to the weights applied to their control ports. These weights are based on correlation data and are calculated in the digital circuits of the AAP. The weighted in-phase and quadrature RF signals are then added together in the power combiner to form a resultant signal which is coherent to the original signal but can have any phase or amplitude relative to the original signal. When combined with the phase and amplitude adjusted resultant RF signals from the other channels the composite signals may be maximized or minimized for a given input signal (steering of a beam for signals of interest or nulls for jammers).

**Comments regarding RF, quadrature implementation -** The critical components of the CPM are the VVAs; parameters of interest for these devices include:

- o Since they are applied at RF, their operating frequency band must exceed the host radio's RF bandwidth. The amplitude and phase adjustments of the resultant signals must be consistent regardless of which RF channel is being adapted, otherwise the weights calculated digitally must be corrected depending on the center frequency being adapted.

- o Since the CPMs follow the front end circuits of the AAP, they must exhibit a large dynamic range to avoid degrading the system's composite dynamic range. If the VVAs cause nonlinearities for moderately high level signals, the amount of gain in the front end must be reduced, potentially degrading the overall noise figure of the system. If the VVAs are very lossy, their output signals may drop to levels below the internal noise of following active devices, thereby directly degrading the dynamic range of the system. The VVAs must accept high level signals and be low loss devices.

- o The weights are calculated digitally then applied to the CPMs in an iterative fashion. The VVAs must respond to the weight updates quickly so they do not delay adaptation. This control voltage to RF output level settling time is often related to the allowable input RF power levels, so a design trade-off between speed and dynamic range may be necessary.

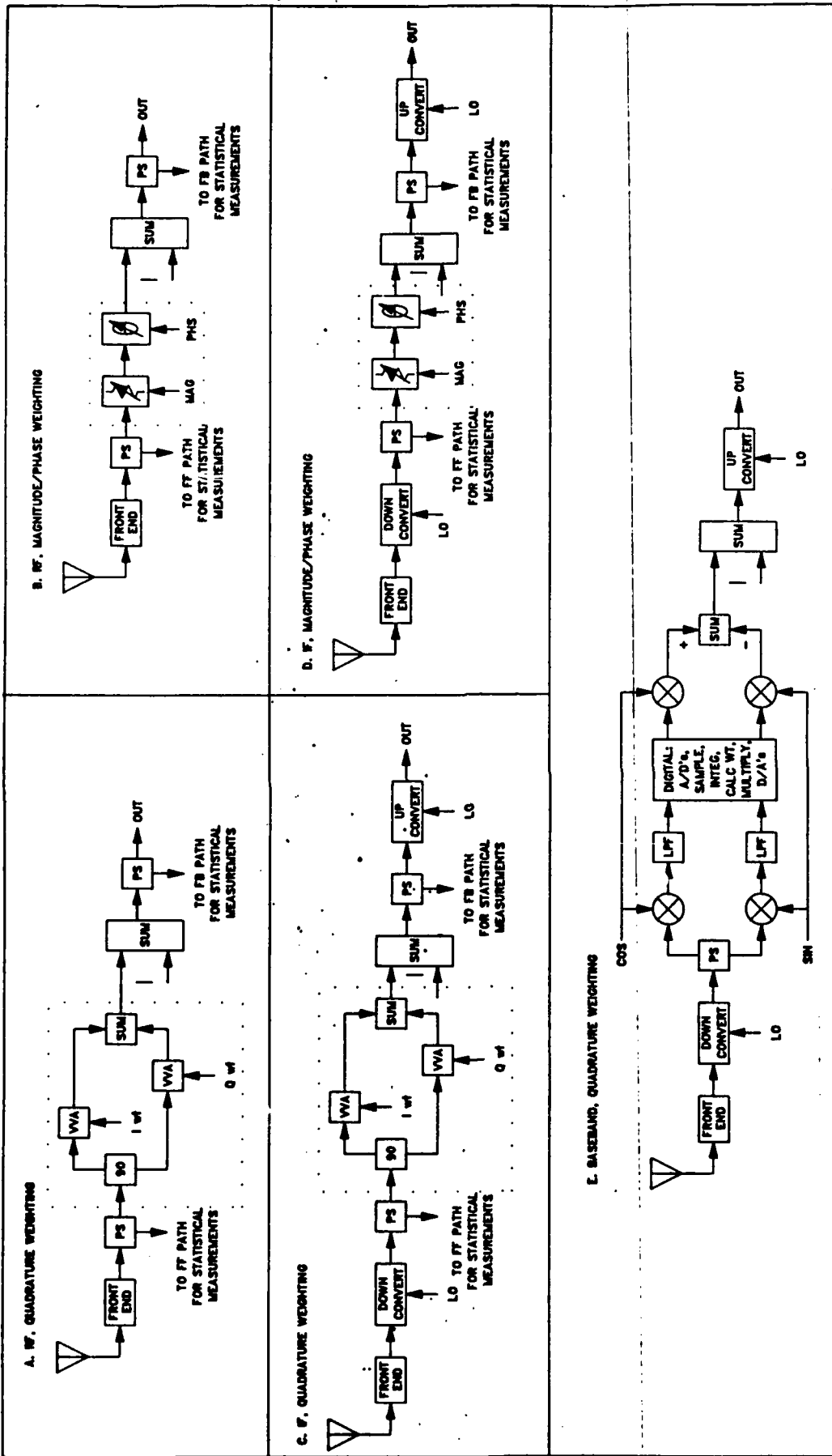


FIGURE 5. COMPLEX WEIGHTING OPTIONS

#### 4.3.3.3 ARCHITECTURE, COMPLEX WEIGHTING (continued)

##### Comments regarding RF, quadrature implementation (continued) -

○ The transfer function of RF gain versus control voltage must be nearly perfectly linear to allow weights calculated digitally to be applied at RF and provide the desired results. This is very important and very difficult to achieve using commercially available devices. One solution to this problem is to provide a custom correction term to each VVA control word. This is discussed further in the calibration section of this report.

○ To achieve 360 degrees of phase shift thru the CPMs, they must be capable of weighting both the I and Q components with either positive or negative weights. This is accomplished by the VVAs if they are bipolar devices. The magnitude of the gain thru the VVA must be the same for a given negative voltage as it is for the same positive voltage, but must introduce a phase shift of 180 degrees.

○ The VVAs must provide a large range of attenuation; to support eight bit digital weight calculations an RF power attenuation range of 48 dB is required.

##### At RF with Polar Weighting -

This option is illustrated in figure 5b; the gain and phase are controlled directly and independently (whereas the quadrature approach requires controlling both I and Q components to accomplish either a gain or phase adjustment). This circuit could be realized a number of ways:

○ The attenuator could be a bipolar VVA identical to the devices described for quadrature weighting, thereby requiring a phase shifter with just 180 degrees of adjustment range.

○ The attenuator could be a unipolar VVA which controls the magnitude only; the companion phase shifter would provide a full 360 degrees of adjustment range.

○ It is unlikely that the attenuator could be a digitally controlled device due to the resolution which would be required. For example, eight bit resolution would require the minimum step size to be less than 0.034 dB of full scale.

○ The phase shifter could be digitally controlled, but the resultant errors due to phase resolution limitations are even more sensitive than those due to amplitude resolution limitations.

**Comments regarding RF, polar implementations - Regardless of the exact implementation of this circuit, the composite attenuator and phase shift function must meet the following requirements:**

○ As in the RF/quadrature case, these devices must operate over a frequency band which exceeds the host radio's RF bandwidth. See discussion above.

### 4.3.3 ARCHITECTURE, COMPLEX WEIGHTING (continued)

#### Comments regarding RF, polar implementations (continued) -

o As in the RF/quadrature case, since these devices follow the front end circuits of the AAP, they must exhibit a large dynamic range to avoid degrading the system's composite dynamic range. See discussion above. In addition, since these devices operate in series, they both must have high dynamic range, with the second device in the chain requiring the higher intercept point of the two.

o As in the RF/quadrature case, these devices must respond to digital control signals quickly and not limit the adaptation time of the AAP. See discussion above.

o Both the magnitude and phase transfer functions versus control voltage must be very precise to assure the weights calculated digitally are achieved at RF. The phase resolution required will be even more difficult to achieve than I and Q magnitude resolution. To achieve the required accuracy and maintain it over temperature, a correction factor customized for each device in every channel would be required.

o As in the RF/quadrature case, the total range of the attenuation must be at least 48 dB to accommodate 8 bit weight resolution. The combination of phase shift range between the VVA and the phase shifter must be at least 360 degrees.

#### At IF with Quadrature Weighting -

This option is illustrated in figure 5c; it is identical to quadrature weighting at RF only it is realized at a lower frequency (IF) and occurs after dehopping so the required bandwidth is less. Most of the circuit description and component performance requirements are identical to those discussed for RF, quadrature weighting above, with the following differences:

o Since the signal at IF is dehopped, the bandwidth requirement for this circuit needs to just exceed the message bandwidth of the host signal. If a 70 MHz IF is selected, and the message bandwidth is 3 MHz (as for EPLRS), the percent bandwidth is only 4.3%. There may be no significant frequency dependent variations in performance over this bandwidth.

o Since this implementation occurs after significant RF and IF signal processing, the AAP system dynamic range will be less sensitive to dynamic range limitations of these circuits.

o Since implemented at a lower frequency, the devices used will be less sensitive to secondary factors such as impedance matching, dielectric variations in the circuit cards, cross coupling of signals, etc. Also, at lower frequencies there will be more commercially available devices to choose from, typically with faster delivery and less expense.

o The number of components in the RF input to RF output signal path is greatly increased in this case. This is undesirable since these more narrowband components are likely to introduce amplitude, phase and delay distortions to the signal. This may adversely effect the host radio system's performance.

### 4.3.3 ARCHITECTURE, COMPLEX WEIGHTING (continued)

#### At IF with Polar Weighting -

This option is illustrated in figure 5d; it is identical to polar weighting at RF except at the lower frequency, smaller bandwidth IF. The advantages and disadvantages of IF versus RF implementations discussed for the quadrature weighting approach also holds true for polar weighting; similarly, the advantages and disadvantages of polar versus quadrature implementations discussed for the RF approaches also holds true at IF. See the discussions presented in the preceding paragraphs.

#### At Baseband with Quadrature Weighting -

This option is illustrated in figure 5e; it is significantly more complex than the other options described above because it requires quadrature downconversion to get to baseband, then must be quadrature upconverted to return to IF. The only advantage to this approach is that the weights can be implemented digitally (if message bandwidth is small enough), thereby eliminating the errors introduced applying precisely calculated digital weights to RF components which are not ideal.

**Comments regarding baseband implementation -** Problems associated with this approach are listed below:

- The amplitude, phase and delay distortions of the desired signal by frequency conversion to and from IF would be much more severe if converted all the down to baseband and back up to RF. In addition to the distortion from more components with more narrow bandwidth, the quadrature conversions would introduce phase errors between in-phase and quadrature components of the signal.

- The benefit of applying the weights digitally introduces a limitation to the bandwidth of the message to be processed. If spread spectrum signals must be processed, depending on the extent of frequency spreading, it may become difficult to perform digitization of the signal at a sufficient rate.

#### Selection -

The quadrature approach is preferable to the polar approach because VVAs are more widely available, exhibit less variations and require less control resolution than phase shifters. There are several manufacturers of integrated circuits that can achieve the basic VVA requirements, particularly if implemented at IF. Phase shifters manufacturers are more specialized; more options are available at microwave frequencies than VHF or UHF. The electronically controlled phase shifters are based on tuning varactor diodes - components which introduce the following problems: high control voltages (exceeding 24 volts) are often required for a wide range of phase shift; the transfer function is nonlinear near the ends of the phase shift range; there is significant drift in phase shift over temperature; the bandwidth of operation is usually limited to ten percent; and variations are expected as a function of frequency, even over this limited range. Similar limitations can be identified for VVAs, but they are not as severe and can be corrected for more easily. Finally, the control resolution of the phase shifter would have to be four times more sensitive than required for the VVAs used in the quadrature approach; that is, the phase shifters would require two more bits of control resolution to achieve the same accuracy (null depth) as the VVAs.

### 4.3.3 ARCHITECTURE, COMPLEX WEIGHTING (continued)

The choice between RF and IF implementations is more difficult to make. Assuming the statistical measurements originate at IF (discussed later), implementing the complex weights at IF would provide more flexibility than the RF approach. All significant AAP functions would be included in modules operating after downconversion from RF - the AAP could be applied to many different radio networks by merely providing the necessary frequency down/up conversions and timing data for specific applications. More options exist at IF than RF for the components to be used in the weighting circuits, but components are readily available for implementations below 500 MHz. The deciding factor, however, will depend on the host radio system the AAP is to be deployed with. The additional delays caused by IF processing may degrade the radio system's time of arrival calculations, a critical parameter in position location systems such as EPLRS. The amplitude and phase distortions introduced by IF processing which are not required in RF processing may degrade the radio system's performance to such a degree that IF weighting is prohibited. Until the specific host radio is selected, and these concerns are proven to be negligible, RF weighting is selected as the baseline since it appears to present the lower risk to the composite (radio / AAP) system performance.

#### 4.3.3.4 STATISTICAL MEASUREMENTS

##### Introduction -

The information required to calculate the weights which result in the forming of nulls in the directions of jammers while simultaneously forming a beam in the direction of a signal of interest is the correlation data between each of the antenna elements of the array. This data is used to form the covariance matrix  $R_{xx}$  discussed previously in other sections. Also of interest is the correlation between each of the antenna element inputs and the AAP output, which may be measured directly as the cross-correlation vector  $R_{xy}$  or calculated knowing the covariance matrix and the weight vector from  $R_{xy} = R_{xx}w$ . The measurement of these correlation statistics is the topic of this section.

The basis of these measurements, the correlation function, requires common mathematical operations to be performed on the signals present at the AAP inputs and output - multiplication, integration, addition and subtraction. These functions are not optional, they are required. At what frequency they are implemented is the option to be selected in this section. The options are RF, IF or baseband, or combinations of these.

##### RF Approach -

The RF option is eliminated immediately because the statistics are least corrupted when made only over the bandwidth of the message. To accomplish this at RF would require a very precisely tuned preselector filter which follows the hops of the host radio system (and is therefore incredibly fast), and has extremely steep stopband roll-off performance. Such devices do not exist. The superhet receiver solves this problem by downconverting the message bandwidth to a fixed IF frequency; this allows highly selective filtering and requires only that the frequency synthesizer be fast enough to follow the hopping radio. This downconversion scheme is employed in the AAP whether the statistics are measured at IF or baseband.

### 4.3.3 ARCHITECTURE, STATISTICAL MEASUREMENTS (continued)

If RF statistical measurements were attempted, all the jammer power present over the entire RF operating band would be included, as well as the internal noise of the AAP within the RF band. The message, however, would be contained entirely within its bandwidth, which is a fraction of the RF bandwidth. Obviously, this results in a very dramatic reduction in the Signal to Interference plus Noise Ratio (SINR). This approach would also require all components to be capable of operation over the RF bandwidth - a much more difficult requirement than operation over the relatively narrow message bandwidth.

#### IF Approach -

This option is selected if the multiplication occurs at IF; the desired output of the multipliers is at baseband, so low pass filters are employed to separate the baseband signals from the signals at twice the input frequency. These low pass signals are then integrated to acquire the desired statistical information. This IF approach is illustrated in the block diagram, figure 6a.

#### Comments regarding IF statistical measurements -

◦ Compared to implementation at baseband, the IF approach requires only half as many multiplications. This is because each IF signal includes in-phase and quadrature components, whereas each baseband signal has its in-phase and quadrature components separated, essentially forming two separate signals. This is evident in the following equations:

▷ At IF -

$$(x_k)(y) = (x_{ki}\cos(\omega_c t) - x_{kq}\sin(\omega_c t))(y_i\cos(\omega_c t) - y_q\sin(\omega_c t))$$

$$\text{After low pass filtering, } (x_k)(y) = ((x_{ki})(y_i) + (x_{kq})(y_q))/2$$

$$\text{Similarly, } (x_k)(y') = ((x_{ki})(y_q) - (x_{kq})(y_i))/2$$

where  $y'$  is the Hilbert transform of  $y$

▷ At baseband -

$$(x_{k+})(y_+) = (x_{ki} + jx_{kq})(y_i + jy_q)$$

$$= (x_{ki}y_i + x_{kq}y_q) + j(x_{kq}y_i - x_{ki}y_q)$$

▷ Comparison of the above calculations reveals the following -

$$\text{After filtering, the IF multiplication } (x_k)(y) = \text{Re}[(x_{k+})(y_+) \text{ at baseband}]/2$$

$$\text{and } (x_k)(y') = -\text{Im}[(x_{k+})(y_+) \text{ at baseband}]/2$$

◦ Both multiply and integrate outputs are used to determine the desired correlation of one antenna element input to the output. This is demonstrated in the following equation:

$$E[x_k y^*] = 2(E[x_k y] - jE[x_k y'])$$

◦ The number of IF multiplications required to calculate the input to output cross-correlation vector  $R_{xy}$  is equal to  $2m$ , where  $m$  is the number of antenna array elements. A four element array would require 8 multipliers, which is a reasonable number.

◦ The number of IF multiplications required to calculate the input covariance matrix  $R_{xx}$  is equal to  $2m^2 + m$ . The same four element array would take 36 multipliers, a quantity which would be difficult to achieve with reasonable size, cost and power dissipation.

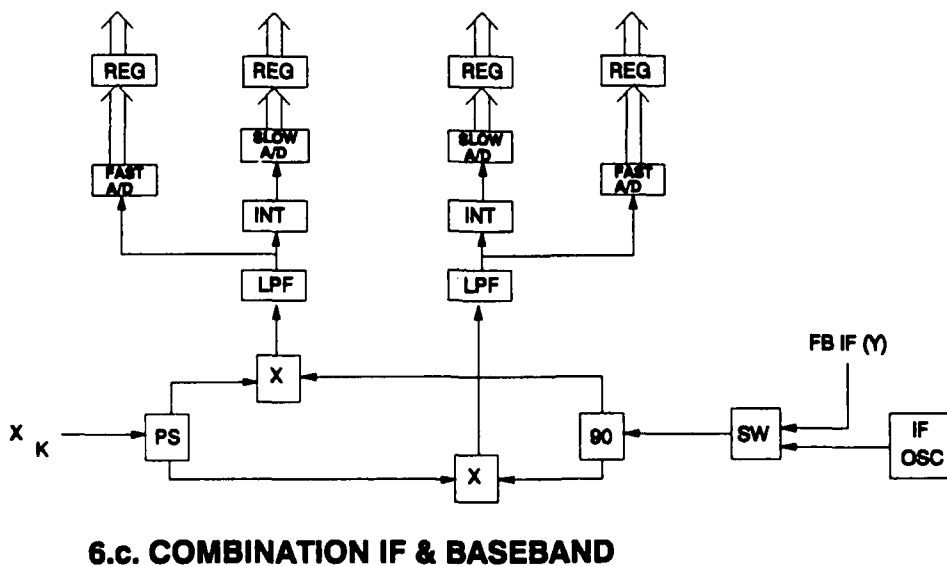
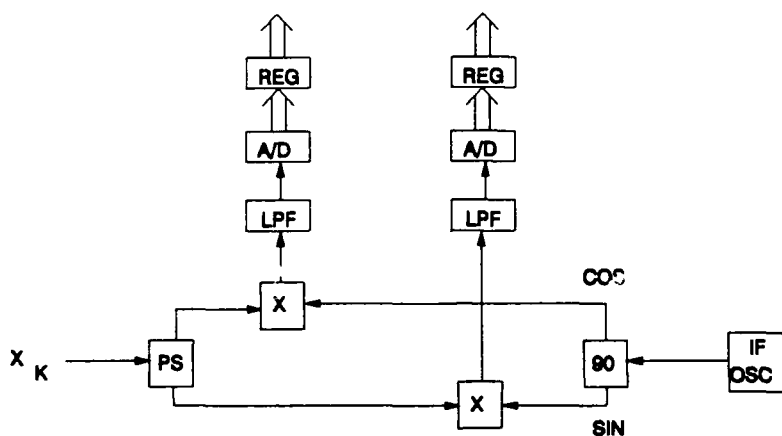
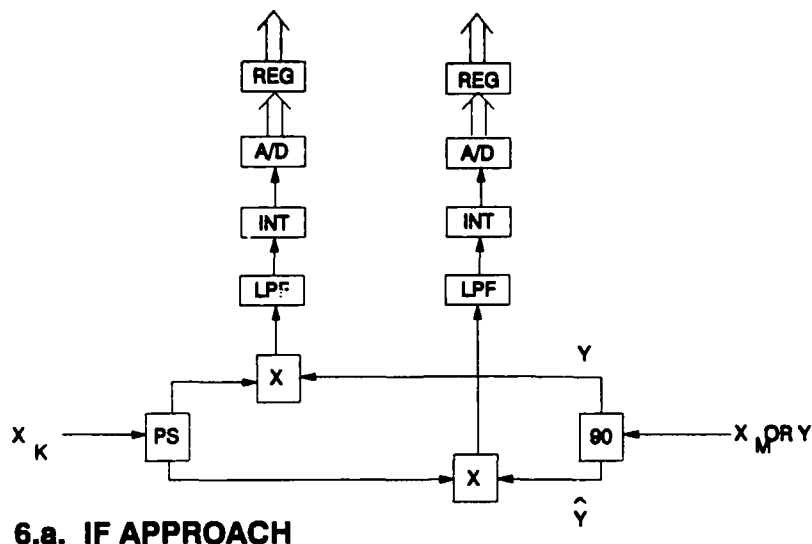


**FIGURE 6. STATISTICAL MEASUREMENT OPTIONS**

### 4.3.3 ARCHITECTURE, STATISTICAL MEASUREMENTS (continued)

#### Comments regarding IF statistical measurements (continued) -

o Based on the number of multiplications required, if only  $R_{xy}$  were needed an IF scheme would be very attractive. Only  $R_{xy}$  is needed for some algorithms, but others (including Dominant Mode Block Update) require  $R_{xx}$ ; to maintain the flexibility to implement a variety of algorithms using the same hardware, limiting statistical measurements to IF is prohibitive.

#### Baseband Approach -

This approach requires quadrature downconversion to baseband, and is illustrated in figure 6b. Once at baseband, the multiplication and integration can be done with analog or digital processing. To be achieved digitally, the baseband signal would need to be sampled at a rate exceeding twice the message bandwidth, then a large set of samples would have to be summed and divided by the number of samples to determine the integrated result. This implies a large number of digital calculations at potentially high clock rates, depending on the bandwidth of the message spectrum after spreading. The analog approach would perform all functions thru integration, then sample the resulting integrated output. This requires a much lower sample rate and relieves the speed requirements of the digital circuitry. The analog calculation circuitry is presented in block diagram form in figure 7.

#### Comments regarding baseband statistical measurements -

o Quadrature downconversion of each antenna element's signal is required. The circuits required to perform this downconversion are identical to the circuits used to perform the IF multiplications discussed above.

o All the information required to calculate the elements of the covariance matrix is available from the baseband data. The baseband data is of the form  $x_k = x_{ki} + x_{kq}$ . If formed digitally, the covariance between channels k and m requires integration of the following calculation:  $x_k x_m^* = (x_{ki} x_{mi} + x_{kq} x_{mq}) + j(x_{kq} x_{mi} - x_{ki} x_{mq})$ .

o Having all the covariance matrix data available allows for the most flexibility in algorithm selection. Few algorithms can be used if only vector measurements are available.

o The speed required of the digital calculations is greatly reduced by performing the multiply and integrate functions in analog circuits. The integration will be performed over a period corresponding to at least 16 data samples; for EPLRS, having a chip rate of about 3 MHz, this requires a digital sampling rate of once every 5.33 microseconds (187.5 KHz). The same EPLRS data, if sampled at baseband before integration, would need to be sampled at least twice during each chip, or at least every 167 nanoseconds. To avoid aliasing, this rate would need to be higher than this; assume every 125 nanoseconds (8 MHz). The sampling rate of EPLRS statistics is therefore 43 times faster if integration is done digitally. For systems which do not use DSSS, the factor of 43 still holds true, but the sample rates would be much slower (and within reason) since the message bandwidth is so much less.

o The precision of the digital calculations is superior to either IF or baseband analog methods. In any case, a calibration sequence will be needed; this is described later in a section dedicated to calibration issues, section 4.3.3.7.

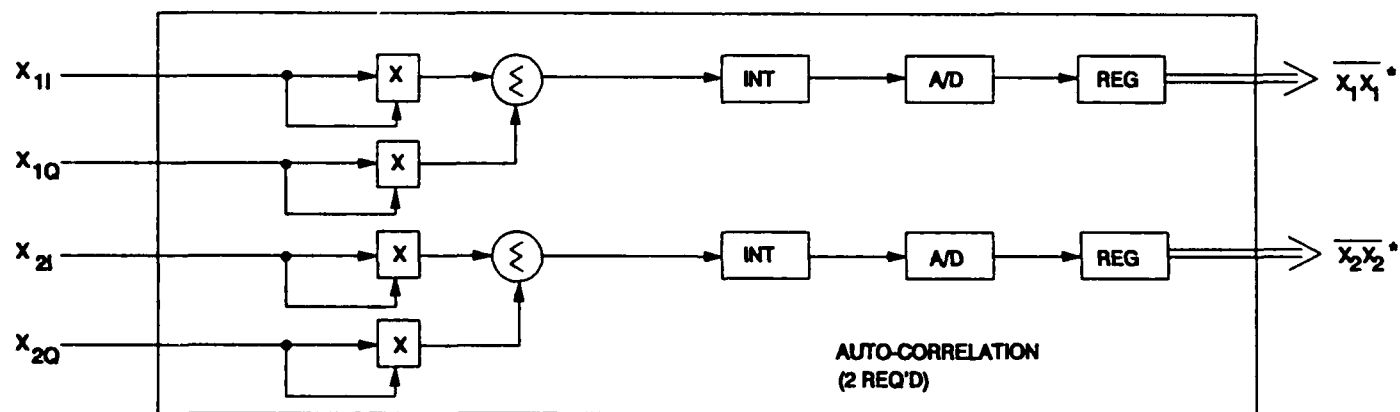
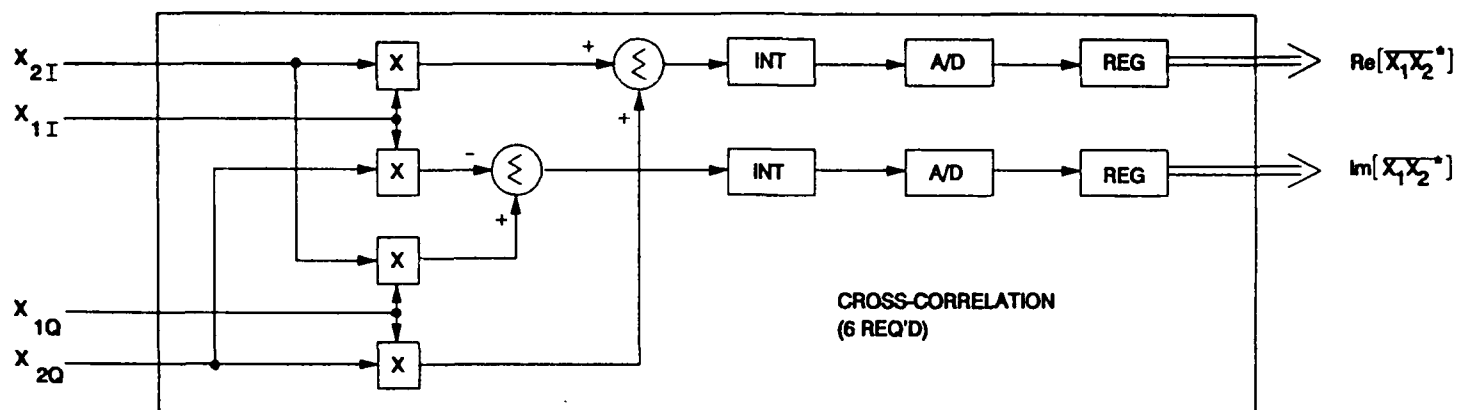


**FIGURE 7. ANALOG CALCULATOR BLOCK DIAGRAM**

### 4.3.3 ARCHITECTURE, STATISTICAL MEASUREMENTS (continued)

#### Combination IF & Baseband -

As discussed above, both the IF and baseband approaches offer advantages for accumulating different sets of data. All the matrix data is available using baseband measurements, but this is slower and more cumbersome than IF vector measurements. Realizing that many algorithms require the inverted covariance matrix for off time data only, and that several iterations of weight estimates are desired during on time processing, it is apparent that both techniques could be employed in an optimal system, providing the added circuit complexity is not prohibitive.

A means of providing fast statistical vector measurements at IF and complete statistical matrix measurements more slowly at baseband, with the addition of only an IF switch, is illustrated in figure 6c. When off time data is to be collected, the IF switch selects the fixed oscillator as the input to the multipliers. The quadrature power splitter provides the cosine and sine terms required for quadrature downconversion to baseband. As described above, this baseband data can be processed with analog or digital circuits for forming the desired statistics. The entire timeslot may be used for calculating the off time statistics, since the weights are not iterated during this period. The last portion of the off timeslot could be used to invert the matrix formed from off time measurements, then the  $R_0^{-1}$  matrix will be ready for use in calculating updates of the weights during on time processing.

The on time data requires only the cross-correlation vector; by using the IF switch to select the output (feedback) IF signal, the multipliers have the input signals required to perform these measurements. In this case, the quadrature power splitters after the IF switch provide the output  $y$  and the Hilbert transform of  $y$  which are required for cross-correlation measurements. The on time data can be collected and integrated in blocks of 16 samples or more, and an update of the weight estimates can be calculated based on each of these blocks. The calculations can be performed quickly in the digital calculator, since  $R_0^{-1}$  is stored in memory and  $R_{xy}$  is updated every 16 chip samples or so. In the Dominant Mode Block Update algorithm, the equation being implemented is  $w(m+1) = R_0^{-1}R_{xy}$

#### Selection -

Based on the discussion above, the obvious baseline choice is to implement the statistical measurements both at IF and baseband since the only added complexity is an IF switch.

### 4.3.3.5 WEIGHT CALCULATIONS

#### Introduction -

To be compatible with multiple algorithms, the architecture must provide for digital calculation of the complex weights. If a specific algorithm is to be implemented, and the hardware can be customized for that particular type of algorithm, then a non-digital approach may be justified. For general applications, such as the type addressed in this study, digital weight calculation is mandatory.

The digital implementation is described below, with indication of its power and flexibility. An example of a non-digital approach, which has been employed and proven successful, is then introduced. The limitations of this technique are discussed and revealed to be too restrictive.

### 4.3.3 ARCHITECTURE, WEIGHT CALCULATIONS (continued)

#### Digital Approach -

Calculating the weights digitally, especially using a microprocessor based design, provides a great deal of flexibility to the AAP system. The inputs to the weight calculations are the digitized correlation measurements and some power level measurements made at IF. Equations are used to manipulate this data and generate estimates of the optimal weights; the equations used and the details of the manipulations are dictated by the algorithm selected. Different calculations, all using the same data, can be performed in a microprocessor based system by installing different firmware programs. Since most algorithms use the same data, but perform different calculations, reprogramming the firmware allows implementing different algorithms. The outputs are the digital representations of the complex weight estimates for each antenna element; these will be converted to analog voltages within the CPM assemblies for application to the VVAs' control ports. Since the correlation data available digitally includes both on and off time data, the AAP will steer nulls in the direction of jammers while simultaneously steering a beam in the direction of the desired signal.

Additional benefits of using digital weight calculations: 1) Including digital circuits between the IF measurements and the VVA controls allows the weights calculated at each timeslot to be stored; this allows adaptation for each timeslot to begin with weights which were optimized at the last visit to that frequency bin. 2) Digital circuits can be implemented on a monolithic chip which requires very little space and dissipates minimal power. These features could be exploited if development proceeds to full scale production activities.

Use of a microprocessor based system for calculating the weights allows flexibility in other aspects of the AAP as well. The same microprocessor could be used for interfacing to external devices and controlling other internal functions besides the complex weights. A block diagram of a digital controller capable of such functions is presented in figure 8; the basic functions of this controller are discussed under the paragraph "Digital Controller", part of the "Baseline AAP Architecture" section (4.3.3.6).

#### Non-digital Approaches -

One example of a non-digital approach is the hybrid analog/digital approach described below: An LMS steepest descent algorithm may be selected which attempts to minimize the output power of the AAP when it was known that no signals of interest were present. The only statistical data required, using the terminology associated with this study, is the off time cross-correlation vector data. This measurement could be performed at IF, resulting in an analog voltage proportional to the degree of correlation between the output error and each input channel. This analog output (rather than being digitized for weight calculations) is used to generate a digital bit stream whose duty cycle is proportional to the voltage level. This bit stream provides the up/down control to a digital counter; the output of the digital counter is the weighting of one component (I or Q) of one of the antenna elements' signals. If the component of a particular complex weight is optimal, the correlation between the output error and that channel's input would be zero, resulting in a fifty percent duty cycle, causing the control word to the weighting element to toggle by its LSB about its optimal weight. Similarly, if there is a portion of the output error which correlates with the input of that channel, the duty cycle would not be fifty percent, so the counter output would either increase or decrease, thereby changing the weight in a way which will reduce the output power.

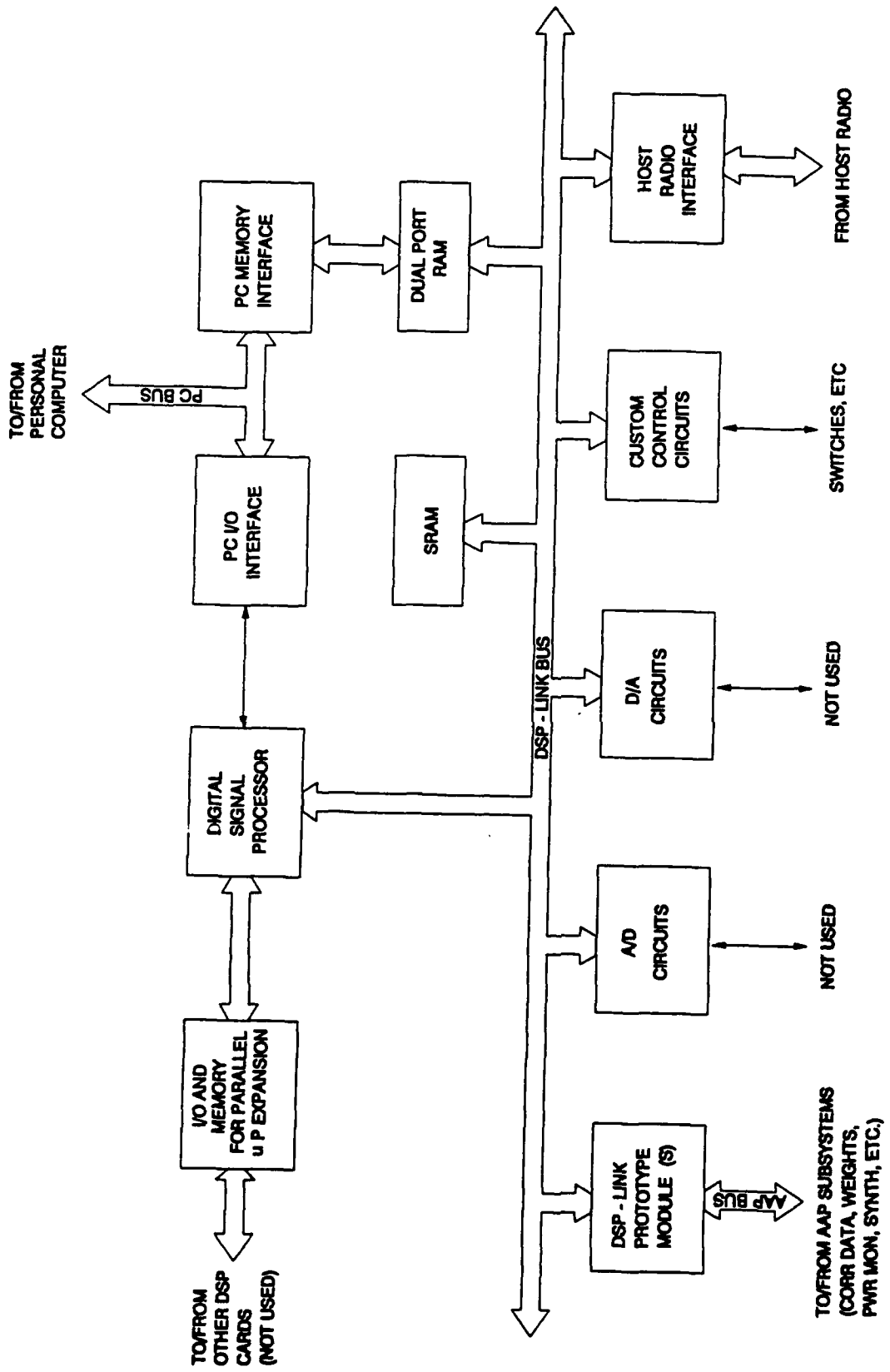


**FIGURE 8. DIGITAL CONTROLLER BLOCK DIAGRAM**

### 4.3.3 ARCHITECTURE, WEIGHT CALCULATIONS (continued)

#### Non-digital Approaches (continued) -

The hybrid analog/digital approach has been used and worked precisely as it was designed. This approach has limitations, however. First, since an algorithm based on the minimization of output power in the presence of interference plus noise only is used, the architecture is optimized for off time cross-correlation data collection only. Any adaptive processing performed using off time data only can steer only nulls; the signal of interest may be arriving at an angle at which the AAP has inadvertently steered a null, resulting in unintentional degradation in output SINR. By allowing for on time data collection and processing as designed and simulated in this study, a beam is always provided in the direction of the desired signal. Secondly, the weight updates are provided by a closed loop integration, without dedicated calculations. Alternative equations for calculating and updating the weights are not provided for. The digital calculations provided by this study's architecture allows much more flexibility in selecting and optimizing adaptation algorithms.

### 4.3.3.6 BASELINE AAP ARCHITECTURE

#### Introduction -

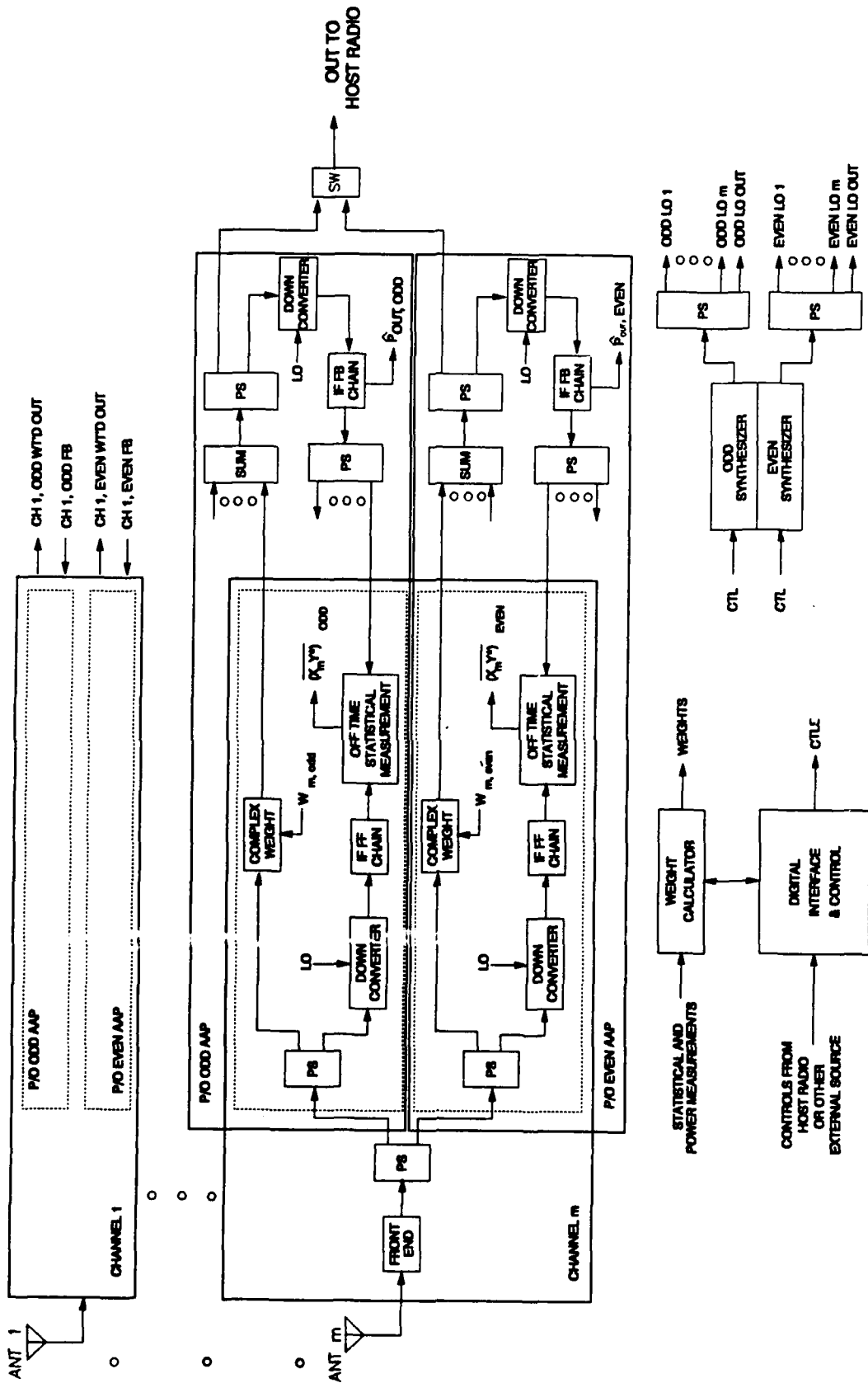
This section begins by compiling all the architectural choices made in the preceding discussions (including RF weighting) to form our first choice baseline architecture. This baseline will be further developed in this section by detailed discussion of each major subassembly, and completed by a discussion of the calibration circuits and sequences required for optimal performance (section 4.3.3.7). Since an IF implementation of the weights is such an attractive option, it is also presented as a baseline, but is identified at this time as our second choice. The discussions regarding further development of the architecture is generally applicable to both baseline choices, and includes design details for the RF Assembly, the IF Chains, the Frequency Synthesizers, the Digital Controller, the DC Power Supplies, and the Antenna Array.

#### Baseline Choice #1 -

Based on the selections made in sections 4.3.3.2 thru 4.3.3.5 above - off time data collected during anticipative timeslots, the complex weights implemented at RF, a combination of IF and baseband statistical measurements, and digital weight calculations - a block diagram of the baseline AAP system can be drawn. This is shown in figure 9.

The input signals come from each element of the antenna array. A receiver front end conditions this signal for the following circuits, establishing the AAP noise figure. The signal is power split to form two identical signals. Both signals will undergo on and off time processing, but during opposite timeslots from one another. The timeslots alternate between odd and even timeslots; allow the path which processes on time data during odd timeslots to be called the odd AAP and the path which processes on time data during even timeslots to be called the even AAP. This implies that the odd AAP processes off time data during even timeslots, and the even AAP processes off time data during odd timeslots. Components are grouped and labeled "odd AAP" and "even AAP" in figure 9 to reflect this convention.

**FIGURE 9. BLOCK DIAGRAM, BASELINE CHOICE # 1**



#### 4.3.3 ARCHITECTURE, BASELINE (continued)

Both the odd and even AAPs split the RF signal again, providing identical signals: one is applied to the CPMs for complex weighting, the other is downconverted to IF for conditioning prior to being applied to the statistical measurement circuits. A chain of IF components provide this signal conditioning.

During odd timeslots, the output of each odd AAP CPM is a phase and amplitude adjusted version of the signal present at its antenna element; a composite signal is formed by combining all those weighted RF signals. When properly adapted, this signal will have the maximum attainable SINR, meaning the jammers have been minimized by steering nulls in their directions while the desired signal has been maximized by steering a beam in its direction. This composite signal is power split to provide an output to the host radio and a feedback signal for further AAP processing. The feedback signal is downconverted and processed for application to the statistical measurement circuits. A chain of IF components very similar to those used for processing the feedforward IF signal is used in the feedback path as well. During odd timeslots, the statistical measurement circuits in the odd AAPs perform the correlation measurements between the inputs and the output directly at IF, resulting in  $R_{xy1}$ .

During odd timeslots, the even AAPs are used only to collect off time data. The complex weights in these paths could be set to maximum attenuation and ignored for this timeslot, or could be used for secondary data collection such as estimates of  $P_{out}$ . The feedforward signal is downconverted and processed by its IF chain, ultimately being applied to the statistical measurement circuits. In this case, the output is not applied to the other inputs of the statistical measurement circuits, but rather a sinusoidal waveform is applied via the feedback IF chain. This allows the IF multipliers to perform a quadrature downconversion, thereby generating the baseband data for each channel. This data contains all the information required to calculate and construct the off time covariance matrix  $R_{\phi}$ . This data is accumulated and stored during off times for use in the adaptation algorithm during the subsequent on time.

During even timeslots, the operation of the odd and even AAPs are reversed from those described in the preceding paragraphs. The odd AAP does off time processing while the even AAP performs on time operations. In order to provide a continuous RF output to the host radio, the outputs of the odd and even AAPs are alternately selected in sequential timeslots. This selection is achieved by the RF switch at the AAP unit output.

In this top level block diagram the digital functions are shown simply as boxes. These functions are described completely in sections 4.3.3.5. and 4.3.3.6.

### 4.3.3 ARCHITECTURE, BASELINE (continued)

#### Baseline Choice # 2 -

This architecture is similar to choice #1 except the complex weighting is realized at IF rather than RF. If the host system does not require the minimum distortions and delays provided by RF weighting, this baseline would be more strongly recommended. IF weighting would enable all functions which are purely AAP related to be based on IF signals. This would allow application of the AAP to communication systems having different operating bands by simply replacing the AAP front ends and synthesizers. These assemblies could be plug in modules and easily interchanged. The block diagram for this architecture is shown in figure 10. Only the architectural differences caused by IF rather than RF weighting will be discussed below.

For IF weighting, the RF signal must be downconverted before application to the CPMs. To accomplish this, the downconverter used in the RF weighting approach is moved in front of the power splitter which provides a feedforward path and an input to the CPMs.

Since the outputs of the odd and even AAPs are at IF, which is compatible with the feedback signal requirements, the downconverters provided in the feedback path of the RF weighting approach are no longer necessary. Instead, to translate the output to the host radio's RF band, an upconverter is required after the output switch which interleaves the even and odd time AAP outputs.

#### RF Assembly -

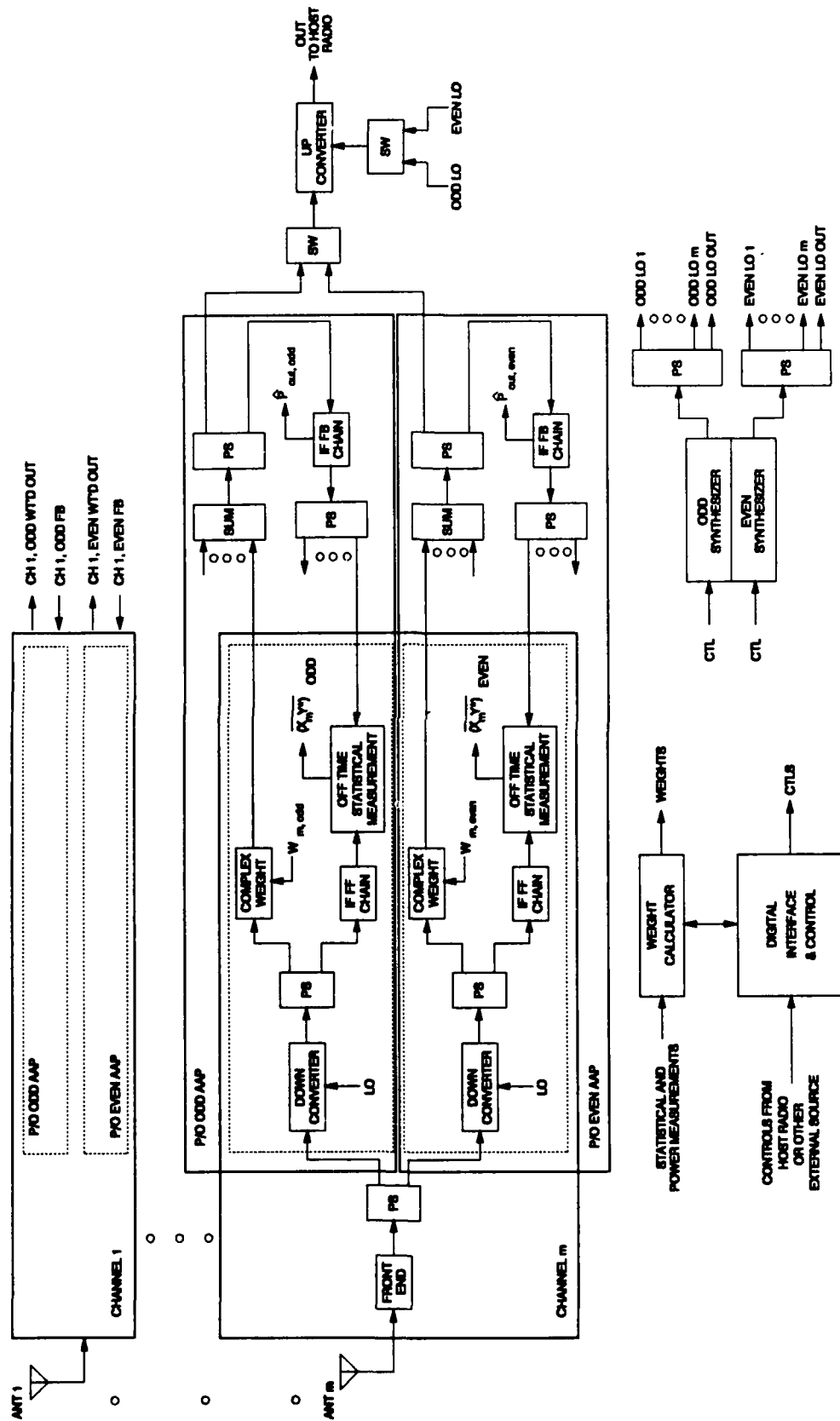
By implementing the weighting at RF, the number of components which process the desired signal are minimized, and are selected to operate over the widest reasonable bandwidth to minimize delay and distortion. A block diagram of the RF Assembly is given in figure 11.

The signals from each antenna element is input to the equivalent of a receiver front end: RF power limiters for protection, bandpass filters for establishing the operating frequency range (for example, matched to EPLRS, approximately 423 to 450 MHz), and low noise amplifiers which impact the dynamic range of the AAP system.

It is important to select components with low insertion losses for each component preceding the RF amplifier, and a low noise amplifier must be used, to minimize the AAP noise figure. As an example, a 20 dB coupler may be used, giving a theoretical "coupling" loss of .044 dB, and an expected total insertion loss of just 0.25 dB. All components except the filter will have an operating frequency range greatly exceeding the EPLRS RF bandwidth, thereby minimizing the accumulated phase and amplitude distortion and insertion delay. The limiter -bandpass filter will limit up to 10 watts of incoming RF signal levels to leakage of less than +13 dBm, while providing steep roll-off via the filter function. The tradeoff between desirable passband performance (low insertion loss, low group delay peaking near 3 dB points, low phase ripple, etc.) and required stopband rejection (particularly image rejection) will be evaluated based on their anticipated impact on system performance. The RF amplifier will be selected based on its overall dynamic range capability; the low end is determined by its noise figure, the high end by its third order intercept point.

The only "custom" component in the RF Front End is the limiter - bandpass filter; all other components will be available as catalog items. Although the limiter - bandpass filter will require a custom design, this is standard procedure for RF filters and can be accomplished in 8 weeks without premium charges.

FIGURE 10. BLOCK DIAGRAM, BASELINE CHOICE # 2



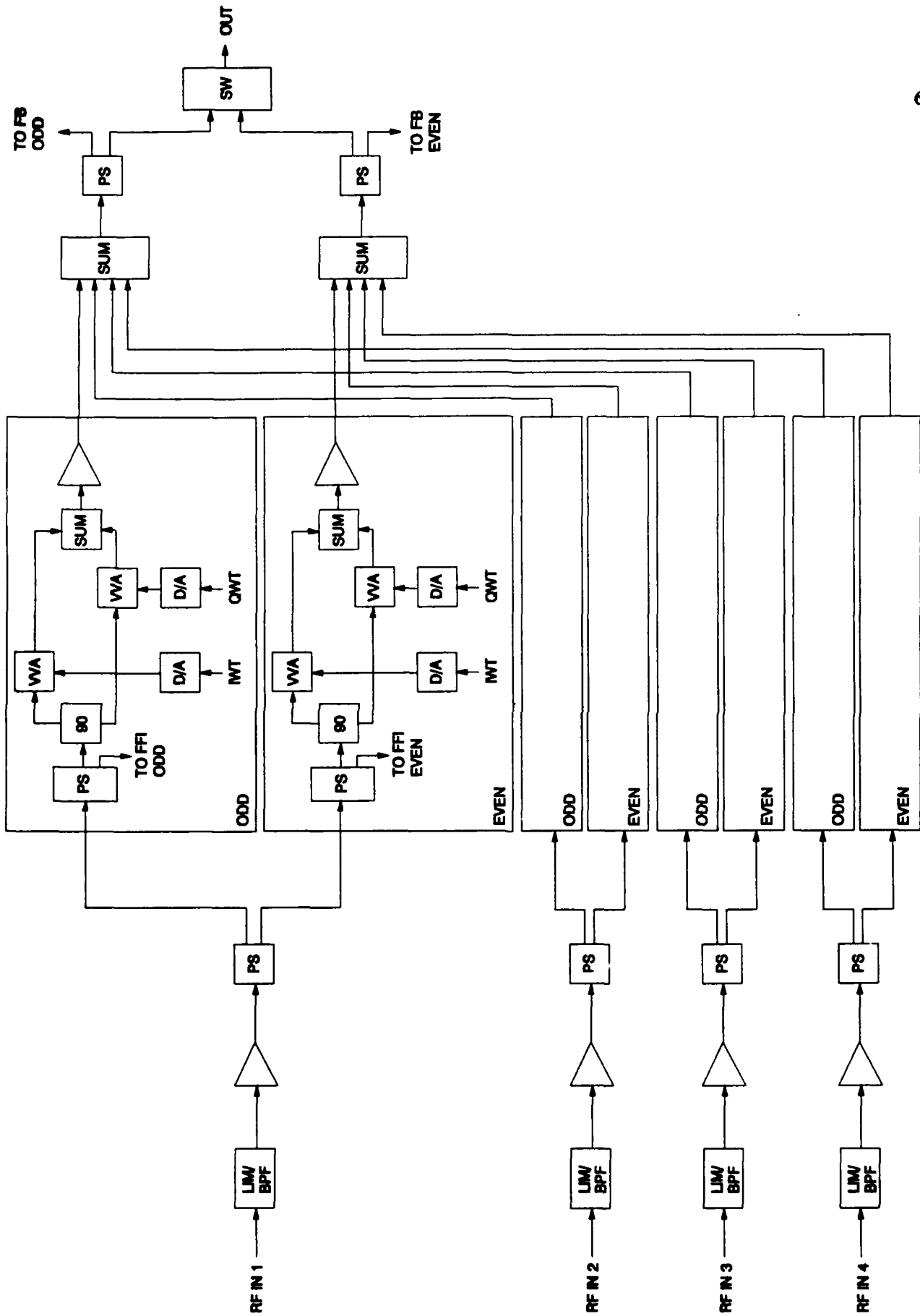


FIGURE 11. RF ASSEMBLY BLOCK DIAGRAM

### 4.3.3 ARCHITECTURE, BASELINE (continued)

#### RF Assembly (continued) -

The primary function included in the RF Assembly is the implementation of complex weighting of each antenna element's output. The baseline approach employs a complex phasor modulator (CPM) which allows the quadrature components of the RF signal to be amplitude weighted independently. The result is a replica of the input signal which may be manipulated to have any desired amplitude and phase relative to the other antenna elements. The CPMs were discussed in detail in section 4.3.3.3; they must include precise error correction capability to assure accurate application of the weights calculated in the digital circuits of the AAP system. Discussion of this calibration technique is included in section 4.3.3.7.

The outputs of the CPMs are combined to form a resultant signal which has the maximum attainable SINR for the given RF environment. This output is power split to provide a feedback signal used in calculating the weights, and an output which is switched between the odd and even AAP circuits to form the final AAP system RF output to the host EPLRS radio.

#### IF Assembly -

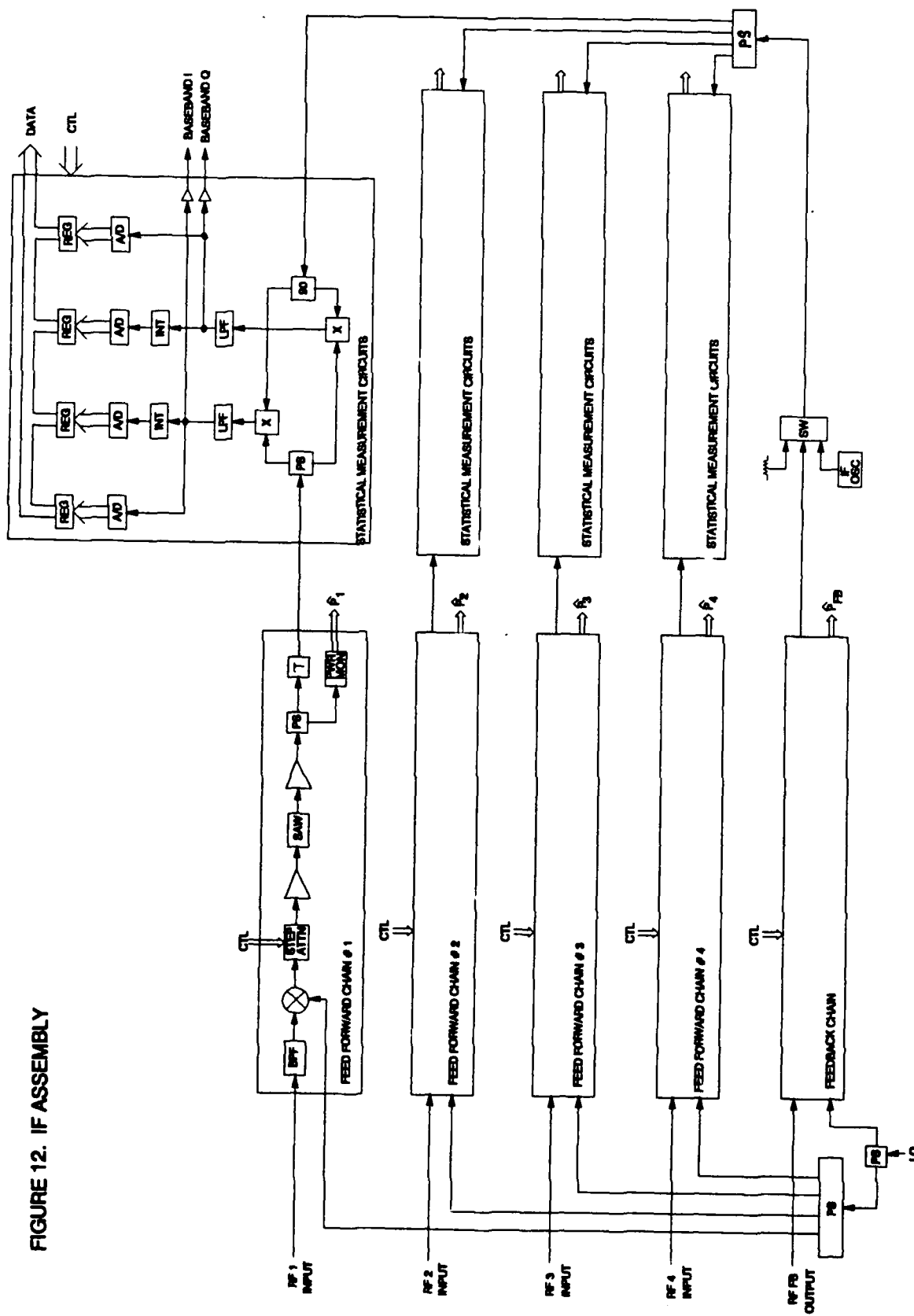
The IF Assembly will include the IF chains (with downconverters) and the statistical measurement circuitry. A block diagram of these functions is provided as figure 11.

**IF Chains -** The inputs to this assembly are at RF frequencies; one of the first functions performed in the feedback and feedforward chains is to downconvert the message band from RF to a convenient IF (such as 70 MHz). This downconversion is accomplished at the mixers of the IF Chains; although the choice of a mixer seems insignificant, its selection is critical to overall AAP system performance. The mixer may generate many undesired, spurious signals which could fall within the 3 MHz IF passband, causing erroneous correlation measurements. Sources of these spurious signals include mixer cross-products and two tone intermodulation products. To minimize these spurs, a termination insensitive mixer could be used. These include additional circuitry which reduces the mixer's dependence upon things such as drive level, IF port termination or RF source impedances, and provides better impedance matches for interfacing components. The mixers must be selected to assure they do not limit the high end of the AAP system dynamic range because of an inadequate third order intercept point. Higher LO drive mixers may be used to relieve this constraint.

The bandpass filter preceding the mixer in the IF chain is to reject the LO leakage from flowing in the opposite direction of the intended signal path and being radiated via the antenna elements. Although this is not a critical component, it may prove necessary to meet FCC regulations for spurious transmissions.

Selection of the LO and IF frequencies must be supported by a spur analysis which will indicate which mixer spurs will fall inside the IF passband. The spurs must be kept to levels which are insignificant compared to the expected SOI levels; this is difficult when jammers exceeding the desired signals by 30 dB or more are present, and are therefore determining the high end of the dynamic range. Careful selection of the operating frequencies and components will optimize this difficult performance requirement. The IF passband and stopband performance will be determined by the SAW filters.

FIGURE 12. IF ASSEMBLY



### 4.3.3 ARCHITECTURE, BASELINE (continued)

#### IF Assembly, IF Chains (continued) -

Surface Acoustic Wave (SAW) filters are used to reject all signals except those within the message bandwidth (as an example, the EPLRS message has a 3 MHz bandwidth). SAW devices are used here because they provide very steep stopband rolloff while providing very linear insertion phase. The only disadvantage to using SAW filters is their insertion loss; losses of about 25 dB are expected. The impact of this high loss can be minimized, however, by careful signal level management to optimize the chain's dynamic range. The amplifiers on either side of the filter help accomplish this, and provide a buffer between the SAW device and other circuit components (SAW devices generally provide poor input and output impedances).

The level of the IF signals are adjusted using digitally controlled step attenuators to fall within the most linear operating range of the key components in the correlator assemblies: the four quadrant multipliers. The step attenuators must have at least 32 dB of range and respond to the digital command in less than one microsecond. Control transient signals leaking through this device to its output must not fall in the IF passband; this can be avoided by proper specification and design of the step attenuator.

The output of the IF chain is coupled off to a power monitor circuit. This circuit will provide a digital output word proportional to the IF chain's output power level. This word may be used by the adaptation algorithm in calculation of the next weight estimate, or just used to adjust the step attenuator. The power monitor circuit could be designed and constructed using catalog ICs to form a successive detection logarithmic IF strip.

The last component in an IF chain is a delay line which must be adjusted at subsystem integration to align the delays of each feedforward path relative to one another to within a fraction of one period at the IF frequency. For example, at 70 MHz one cycle takes about 14.3 nanoseconds. The delays can be adjusted to within less than one nanosecond, or less than 30 degrees. Using .085" diameter semirigid cable, a miniature spool of coax cable could provide ample adjustment range and resolution in a reasonable volume. The coax exhibits about 1 nanosecond of delay per foot.

#### **Statistical Measurement Circuits -**

The key components of these circuits are the four quadrant multipliers. These multipliers operate at IF, and perform one of two functions: 1) For input to output cross-correlation measurements the multipliers are simply that - multipliers. Their output in this case is "x times y"; after low pass filtering and integration this becomes the expected value of x times y, or the cross-correlation between the input and the output. 2) For correlation measurements between the four antenna elements, these multipliers perform quadrature downconversion from IF to baseband. This is realized by switching the feedback signal from the output signal to an internally generated CW signal at the IF frequency. These baseband signals can then be used to calculate all the expected values required to form the covariance matrix, using either analog or digital processing.

Cross-correlation measurements require that the feedback IF (which contains the same narrow band signals as the RF output) be correlated with each feedforward IF (same narrow band signals as each input). To enable this correlation, the feedback IF switch is used to select the signal coming from the IF feedback chain. This signal is power split to provide four identical signals, one for correlation with each of the feedforward signals. Each channel's operation is

### 4.3.3 ARCHITECTURE, BASELINE (continued)

#### IF Assembly, Statistical Measurements (continued) -

identical. The feedback IF is quadrature split to provide I and Q representations. The feedforward IF is power divided to create two identical signals for multiplication with the I and Q feedback representations. The IF multiplication is performed by a linear four quadrant multiplier IC which is available from multiple sources. The dynamic range of these multipliers are limited, however, which is why step attenuators are used in the feedforward and feedback paths to adjust their levels. The step attenuator settings are taken into account in the digital calculators. The outputs of the multipliers are low pass filtered to reject the spectrum centered at twice the IF frequency. These signals are then integrated (which calculates the expected value of input times output, I and Q) and sampled as dictated by the controls provided by the AAP microprocessor. The sampled data is held in registers until retrieved by the microprocessor.

Covariance measurements use the same circuits, but with different functions. The feedback IF switch is used to select a precision oscillator rather than the output IF signal. When quadrature split and multiplied with the feedforward signal the signals out of the lowpass filters are the I and Q baseband components of the message bandwidth. The availability of these baseband signals allow calculation of any covariance terms desired; this allows calculation of the covariance matrix required by the baseline algorithm for off time statistics.

The baseband I and Q signals can be used to calculate covariance terms either digitally or with analog circuits. For digital calculations, both I and Q signals must be sampled at rate greater than twice the message bandwidth. For message bandwidths of 3 MHz (such as EPLRS) this is easily realizable, although it places a burden on the digital calculator circuits. The integration is done digitally by an accumulator which adds the current sample to the previous sum, then after many samples divides the total by the number of samples. As in the IF correlation case, these integrated results are the I and Q components of the expected values.

If analog circuits are used to operate on the baseband data to calculate the covariance statistics, the high speed requirements of the digitization and digital calculations are relieved. The analog approach allows the integration to be done before sampling, resulting in a much slower sample rate. The analog calculator is shown in figure 7. The circuits need only support the message bandwidth and are comprised of linear multipliers, analog summers, and integrators. The integrator timing and digital sampling are controlled by the microprocessor as was the case for IF correlations. The digital samples are held in output registers until retrieved by the microprocessor.

Regardless of which correlation method is used, the accuracy of the measurement is crucial to the AAP system performance. Calibration circuits must be used to provide the required accuracy; the calibration circuits and sequences are described in section 4.3.3.7.

### 4.3.3 ARCHITECTURE, BASELINE (continued)

#### Synthesizer -

The Synthesizer Assembly responds to the commands of the digital controller (based on frequency tuning data from the host radio) to generate a fast hopping Local Oscillator (LO) signal used in the superheterodyne function of each IF chain. The synthesizer must be designed to tune over a range of frequencies compatible with the host radio's operating frequency range in much less time than is allotted for one timeslot. Using EPLRS as an example, the synthesizer must tune over 21 MHz in significantly less than 1.5 milliseconds, preferably less than 60 microseconds. It must settle to within less than 5 KHz of its final frequency in this time. To allow the AAP system to be applied to a variety of Army radio systems, the synthesizer design should support much smaller steps in hop frequencies than the 3 MHz step size of the EPLRS network. A step size of 25 KHz is easily achievable and would be compatible with other Army radios such as Singars. In a single phase locked loop (PLL) design, smaller step size requires longer settling time, a trade-off which can't be made in this system. The solution is to employ a dual PLL synthesizer with the fine step size determined by a very fast direct digital synthesizer capable of DC to 15 MHz operation. The actual range used might only be 13.75 to 15.00 MHz. The coarse tuned PLL has a fixed 1.25 MHz reference, which allows wide loop bandwidths and correspondingly fast settling time. To provide very fast tuning, even over the entire operating band, a coarse tune digital control will pre-steer both the VCOs to nearly the correct frequency, then the PLLs will be enabled to allow accurate and fast settling to the desired frequency. A block diagram of the synthesizer is shown in figure 13.

#### Digital Controller -

As explained in section 4.3.3.5, digital calculation of the weights using a microprocessor based design provides a great deal of flexibility to the AAP system. The algorithm selected for calculating these weights can be changed by reprogramming the microprocessor, assuming the rest of the AAP hardware supports the algorithm as well. The digital controller provides all interface and control functions between the AAP system and external systems such as the host radio and a personal computer. It also interfaces the digital assembly with all other AAP subsystems. Using instructions and information from external sources, it collects the necessary data from the other internal subsystems to perform the algorithm's calculations, then controls the other subsystems for null and beam steering which optimizes the output SINR. The weight calculation requirements of the digital controller were discussed previously (4.3.3.5); this section will address the other digital controller functions.

The same microprocessor used for calculating the weights could be used for interfacing to external devices and controlling other internal functions as well. A block diagram of a digital controller capable of such functions was presented in figure 8; functions other than weight calculations are discussed below.

**Interface and Control -** To perform all the functions required to support adaptation, several sources of information must be input to the digital controller. After manipulating this information, the results must be output to several destinations. To accomplish these tasks, several interface ports should be supported, including:

- o A personal computer (PC) interface could be provided which might be used for loading algorithms, storing and displaying adaptation data, single stepping for debug and trouble shooting, or enabling full speed operation with or without software breakpoints.

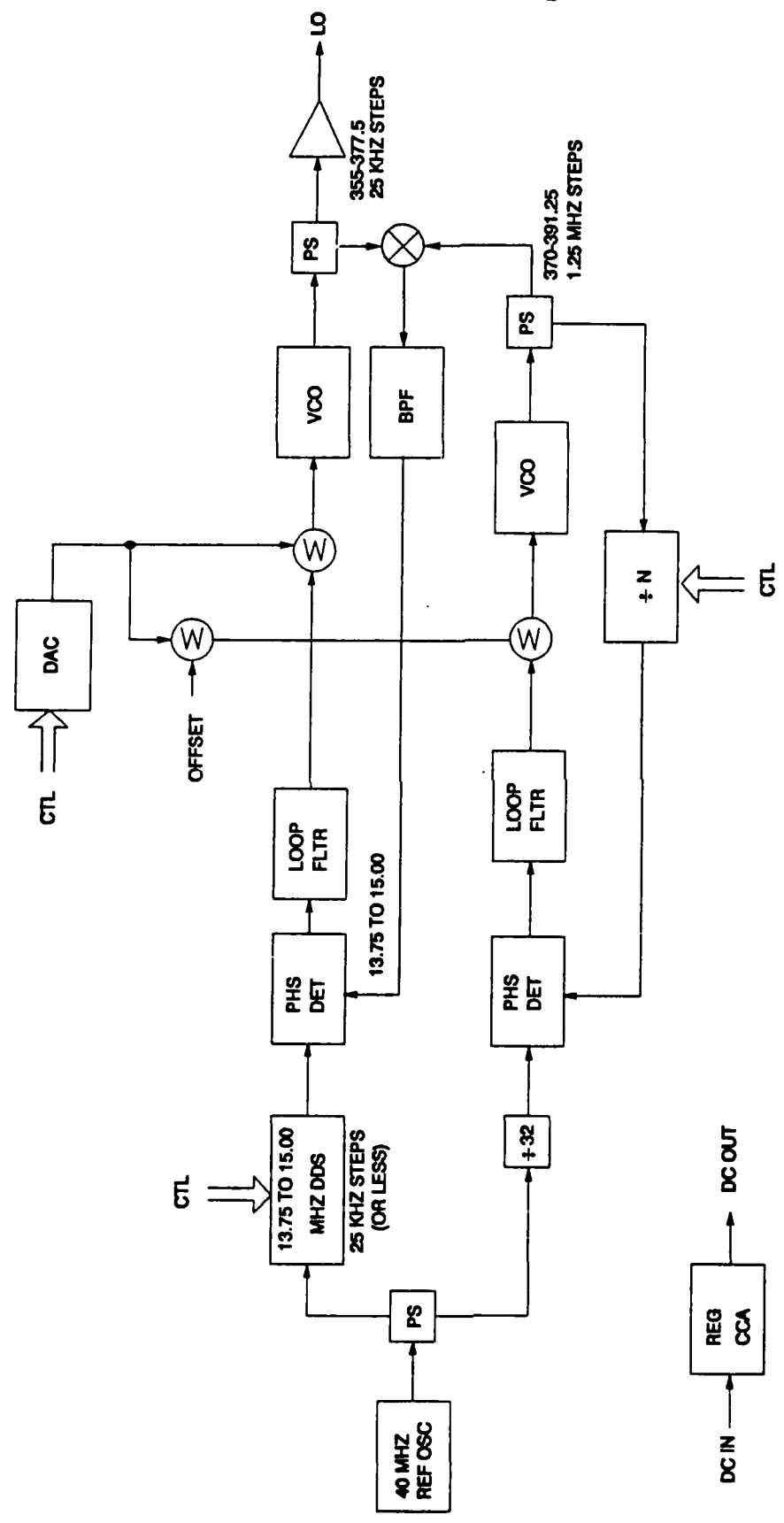


FIGURE 13 SYNTHESIZER BLOCK DIAGRAM

### 4.3.3 ARCHITECTURE, BASELINE (continued)

#### Digital Controller (continued) -

○ An interface compatible with a host radio must be included. This allows transfer of frequency tuning and system timing information from the radio to the AAP.

○ A bus internal to the AAP would allow interfacing to all the other AAP subsystems. Tuning of the synthesizers, retrieval of the correlation data, storing and recalling the weight estimates, sampling the IF power monitors, and controlling step attenuators are examples of the functions provided by this interface.

○ Miscellaneous, special function controls, such as RF switches and calibration components, may require a dedicated port with custom capabilities.

○ If properly designed, the digital controller would allow for future expansion. This could include more I/O ports, and digital to analog and analog to digital converters.

**AAP Functions -** The specific functions required for AAP operation are summarized below.

- Tune the frequency synthesizers per the information provided by the host radio.
- Collect off time statistical data sufficient to form the covariance matrix  $R_0$ .
- Form the off time covariance matrix and perform a matrix inversion, yielding  $R_0^{-1}$ .
- Sample IF power monitor outputs. Based on these power levels, control step attenuators to ensure the signal levels into critical circuits are within their most linear range.
- Establish the timing for adaptation sequences, such as integration time, propagation delay through a chain of RF and IF components, RF or IF path selection of switches, time delay between control signals and output settling, etc.
- Collect blocks of on time statistical data sufficient to form the cross-correlation vector  $R_{xy1}$  several times within one timeslot.
- Calculate new estimates of the weight vector based on the equation  $w(m+1) = R_0^{-1}R_{xy1}$ .
- Update the weight estimates applied to the CPMs as they are calculated.
- Store and recall the weight estimates and other pertinent data at the beginning or end of each timeslot.
- Control the calibration components and sequence as required.
- Perform Built-In-Test functions which provide a level of confidence that the circuits are operating per their design expectations.

An in depth explanation of how these digital controller functions are used to enable the AAP to adapt to its RF environment is provided next.

### 4.3.3 ARCHITECTURE, BASELINE (continued)

#### Digital Controller (continued) -

Generically speaking, the digital controller must perform different operations depending on whether off time or on time processing is being executed. These concepts were introduced in this section under paragraphs describing "Baseline Choice #1". The functions performed by the digital controller are described in terms of the tasks required to generate nulls and a beam at the AAP system output. Although this explanation is given with a particular algorithm in mind, the same sequence or slightly modified sequence could be used for a number of algorithms.

**Off time tasks** - At the beginning of the timeslot, the frequency control data for one advanced timeslot is input from the host radio. The controller immediately tunes the off time synthesizer to this frequency. (The on time AAP for this timeslot was tuned to the correct frequency at the beginning of the last timeslot; each AAP stays at the same frequency for two timeslots). While the synthesizer is settling, the final weights calculated by this AAP in the last timeslot are stored for retrieval at the next visit to that timeslot. The weights are then set to zero for off time operation. Once the synthesizer is settled and the input signals are allowed time to reach the power monitor circuits and accurate power measurements are made, the power monitor outputs are sampled. Based on these measurements, the feedforward step attenuators are set to provide signal levels into the correlator circuits which are within their linear range. The feedback IF oscillator is selected by controlling the feedback switch. After these settings are settled, the power monitor levels are verified. If suitable, the correlators' integrations are enabled for a long integration period (long relative to the on time cross-correlation integration times). While the integration is occurring, the microprocessor is free to accomplish any overhead functions such as monitoring the power monitor outputs to verify a consistent RF environment. After integration, the correlation results are sampled by the digital controller, and used to form the covariance matrix. For a system with four antenna elements, an 8 by 8 covariance matrix is constructed (complex calculations). This matrix is then inverted; the inverted matrix will be used in calculating the new weight estimates during the on time. At the conclusion of the off time timeslot, preparations are made for on time processing.

**On time tasks** - The CPM weights are set to the optimal weights as estimated the last time this AAP was tuned to this frequency by recalling those weights from memory. The input and output powers are then sampled at the power monitors, allowing step attenuator adjustments to be made to place the signal levels into the correlator in its linear range. The feedback switch is controlled to select the IF version of the output, thus allowing cross-correlation measurements rather than baseband conversions. Once the power levels into the correlator circuits are verified, the integrators are enabled for a period of about 128 data bits (assuming EPLRS is the host radio). During this integration period, the microprocessor is free to perform limited overhead functions. At the end of the integration period, the results are sampled and retrieved. These measurements are used as the cross-correlation vector for that block of data. This vector, along with the inverted covariance matrix from off time processing, is used in calculating an update of the weight estimates. The new weight estimates are applied to the CPMs, causing changes in the antenna pattern and output SINR. The entire on time sequence described above is repeated for several blocks of on time data. After the last block of on time data, the weights are stored for initialization at the next visit to that frequency.

### 4.3.3 ARCHITECTURE, BASELINE (continued)

#### DC Power Supply -

The DC voltages required by all the AAP circuits could be generated from a single 110 VAC input within this DC Power Supply Assembly. The designs of the other circuits would be well established so an accurate estimate of the current require at each supply voltage could be formulated. The total current requirements, with considerations for isolating the supplies of some circuits from others, will help determine which AC to DC power converters should be used. Protection features should include input overvoltage, input and output short circuit, reverse voltage and transient suppression. Converters which include most of the regulation and protection circuits required for most of the AAP circuits are available.

Some AAP circuits, such as the synthesizers, the CPMs, and the correlators, are sensitive to noise or transients on their DC supply voltages and will require additional filtering and regulation. These additional circuits may be included in the DC Power Supply Assembly or may be located with the circuits they are supplying. Depending on the power dissipation of the system, the power supplies may need heat sinking and forced air flow to maintain reliable operation. A thermal analysis would need to be conducted to determine those requirements.

#### Antenna Array -

The ability of the AAP to provide spatially distributed nulls in the direction of jammers and a beam in the direction of the signal of interest is based upon the delay experienced by these incoming signals depending on their direction of arrival (DOA). This DOA dependent delay is provided by the antenna array via the physical separation between elements. As a result, the location of each element relative to one another (the array geometry) is critical to the AAP performance. To provide flexibility in the location of individual elements, the array could allow for "floating" antenna mounts. The precise location of each element could be adjusted for a specific test, allowing empirical determination of the array geometry. Subsequent developments could apply this experimental data in selecting permanent, fixed locations.

The design of an antenna array is very dependent on the host radio the AAP is operating with. The elements of the array could be a version of the omni-directional whip antenna used with the host radio. Using the expected antenna gain pattern of these individual elements, the array geometry could be customized based upon computer simulated performance and empirical field test data. Using these constraints, a mechanical engineer would design a support structure for the antenna elements.

### 4.3.3.7 CALIBRATION

#### Introduction -

Circuitry must be included for calibrating or correcting three critical AAP functions:

- o Complex Weights - The weights are calculated digitally, but implemented at radio frequencies. Any errors between the calculated and the applied weights will degrade system performance. An error correction term may be generated at the CPMs which will optimize the match of the applied and calculated weights.

- o Statistical Measurement Circuits - All weight estimates are based on correlator measurements; errors in these measurements will result in inaccurate weight estimates and degraded system performance. The correlation circuits could include self calibration capability, or the correction factors must be measured and taken into account by the digital controller.

- o Amplitude, Phase and Delay Variations - Any amplitude, phase, or delay variations in the RF and IF chains leading to the correlator functions will result in erroneous correlation measurements and degraded system performance. The addition of an RF calibration signal source at the AAP inputs will allow these variations to be measured in the correlator circuits and taken into account by the digital controller for weight calculations.

Each of these calibration or correction techniques are described in the following paragraphs.

Complex Weights - A block diagram for the complete CPM function, including error correction, is shown in figure 14. The calculated I and Q weights are updated by the digital controller then transferred to the VVAs. The algorithm assumes that the exact weight calculated is realized in the CPM; any variation from this ideal degrades the jammer rejection. For example, if the error were just one LSB for both I and Q weights, an eight bit system would yield a 39 dB null against a CW jammer. If this accuracy were degraded to 2 LSBs, the null would degrade to just 31 dB. Since the transfer functions of the VVAs (RF gain versus control voltage) are not perfectly linear, and the bipolar change in phase is not exactly an abrupt 180 degrees, a correction factor is required.

The sources of errors in the VVAs are illustrated as part of figure 14. They include:

- o A highly non-linear saturation region in the  $V_o/V_i$  vs.  $V_{ctl}$  transfer function for high values of control voltages.

- o Any variations from the ideal linear slope in the  $V_o/V_i$  vs.  $V_{ctl}$  transfer function within the linear range of control voltages.

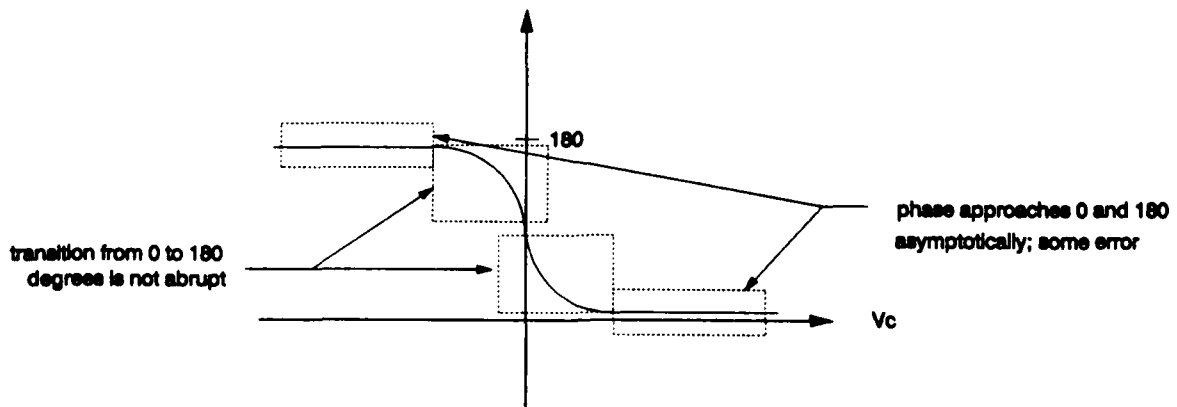
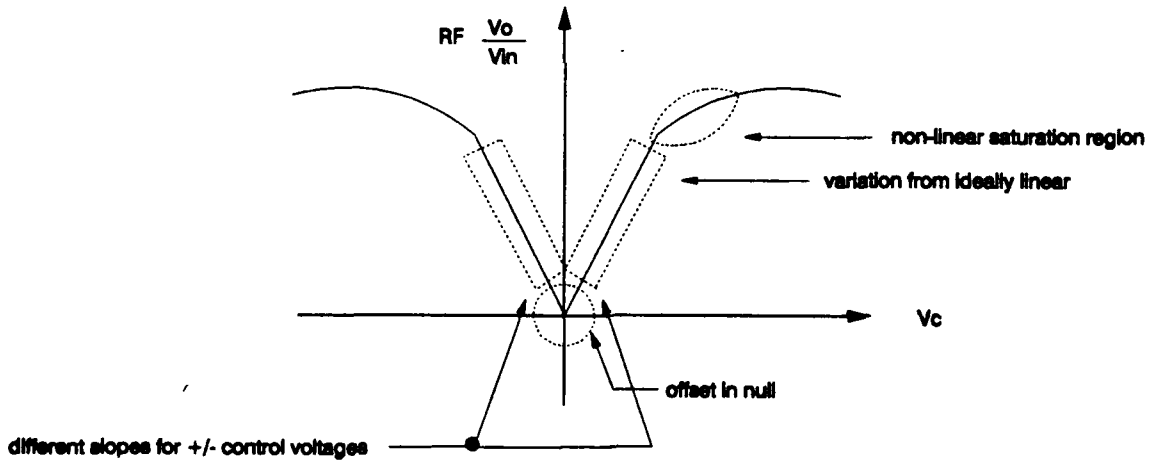
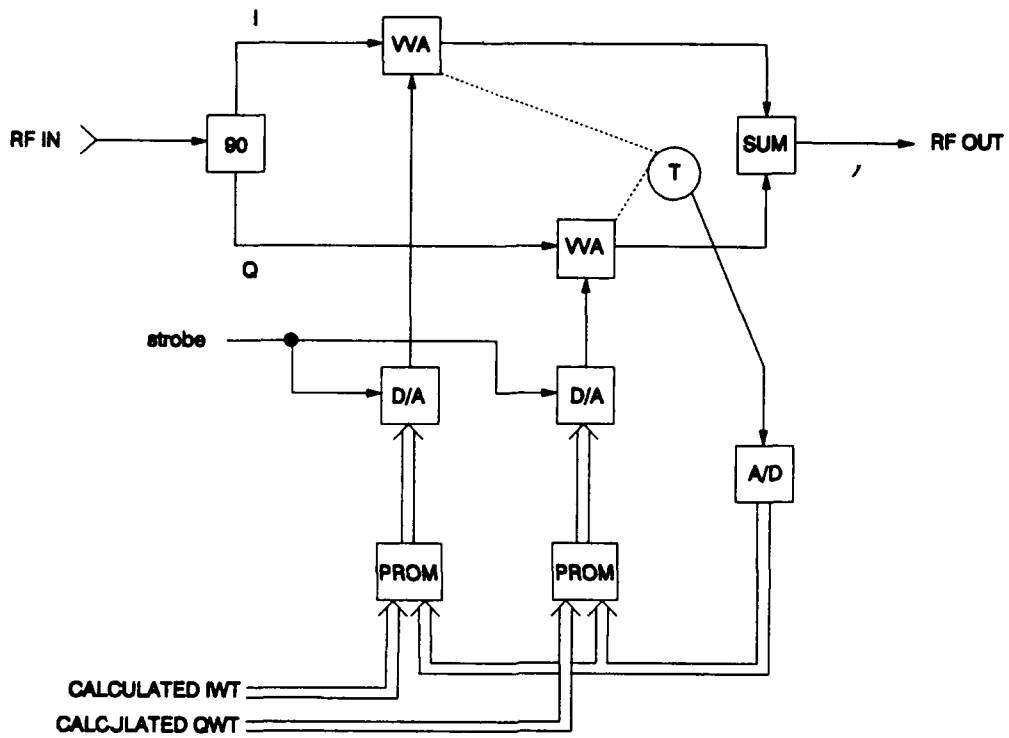
- o Any mismatch in the slopes of the  $V_o/V_i$  vs.  $V_{ctl}$  transfer function for positive and negative control voltages.

- o Any drift in the null offset voltage; the null should occur at precisely zero volts  $V_{ctl}$ .

- o Any phase error resulting from the insertion phase approaching the desired values of 0 and 180 degrees asymptotically. The ideal values of precisely 0 or 180 degrees are never quite achieved.

- o Phase errors resulting from a non-instantaneous transition between 0 and 180 degrees.

**FIGURE 14. CALIBRATION OF COMPLEX WEIGHTS (AT RF OR IF)**



#### 4.3.3.7 CALIBRATION (continued)

##### Complex Weights (continued)

These errors can be corrected for by adding a PROM to each control port of CPM which maps the desired (calculated) weight to the required control word to achieve that weight. To allow for temperature variations at the VVAs, a sensor can be integrated into the CPM assembly which generates a digital word representing its operating temperature. This word can be combined with the calculated control word to address the correction PROM. The entire CPM circuit could be characterized over temperature by an automated test program which would test selected voltages and temperatures, then interpolate to get the data points which fall between measured values.

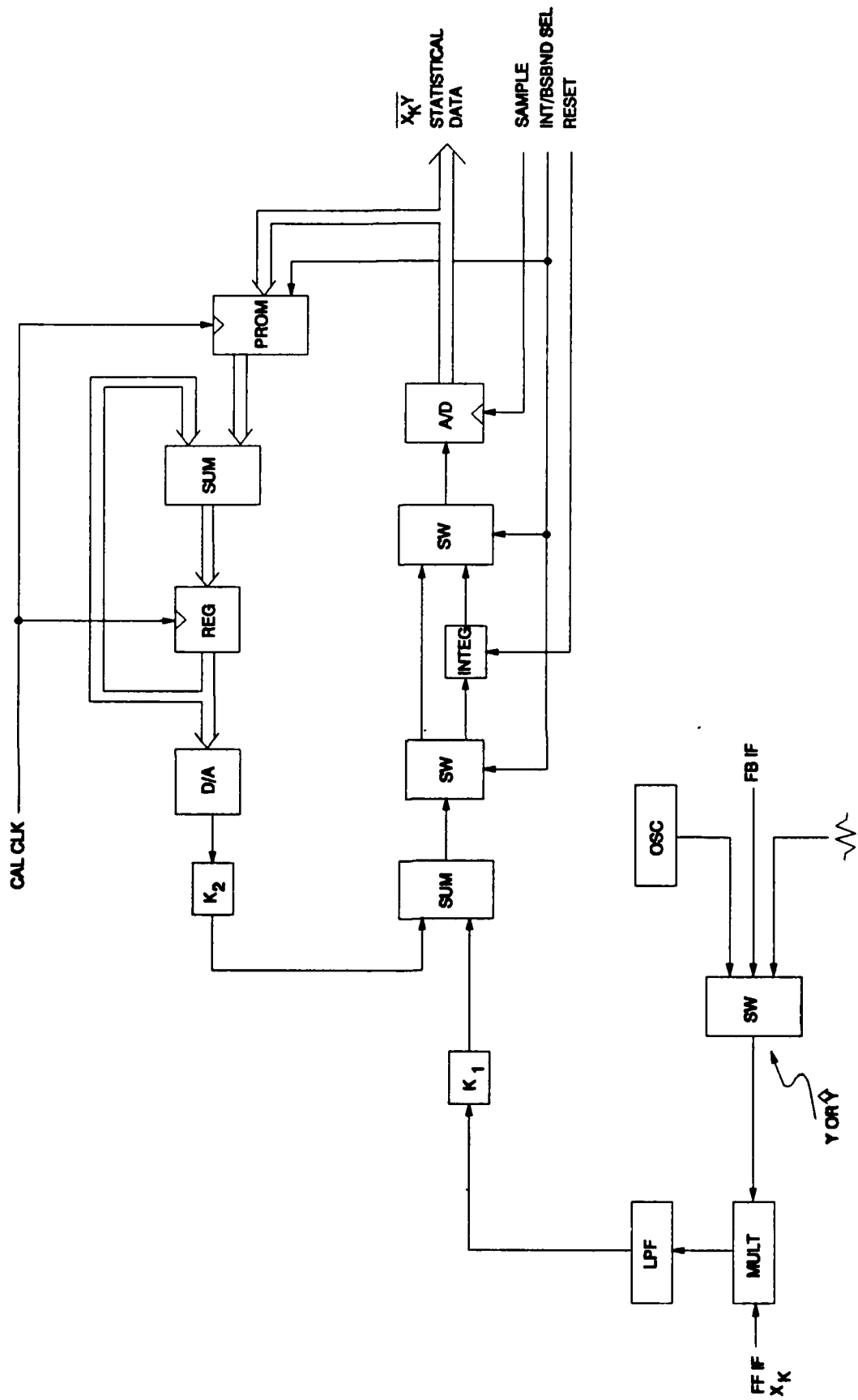
**Statistical Measurements** - The calibration circuits are included in the block diagram for the statistical measurement circuit shown in figure 15. The basic circuit is used to either measure the correlation between two IF signals or to provide quadrature downconversion of an IF signal to baseband. The calibration technique must therefore be capable of measuring and correcting errors in either of these modes. The circuit shown accomplishes this; its operation is explained below.

To calibrate the correlation of two IF signals, the feedback switch selects the termination, thereby setting one of the two IF signals to zero. Regardless of the signal present at the feedforward port of the multiplier, its output should be zero. To assure operation in the multiplier's linear range, however, a test signal should be provided and applied at the feedforward port. The analog switches' positions will be selected to provide integration of the lowpass filter output, as is the case when IF correlation is desired. The integrated output is then converted to a digital word. During normal operation this is the correlator output; for calibration it is a test signal which indicates the amount of error accumulated in all the associated circuitry. This error is input to a PROM, which determines the polarity and amount of correction which must be applied to cancel the detected error. This correction factor is added to the total corrections accumulated by previous samples. The composite correction term is converted to an analog voltage which reduces the total correlation error by summing with the output of the lowpass filter which follows the multiplier.

To calibrate the baseband measurement accuracy, the feedback switch selects the IF oscillator. A quadrature power splitter, not shown in figure 15, provides both  $\cos(\omega_{IF}t)$  and  $\sin(\omega_{IF}t)$  terms for the quadrature downconversion. In this case, the output of the lowpass filter is either the in-phase or quadrature baseband representation of the signal present at the feedforward IF port of the multiplier. When the feedforward signal is disabled (using an IF switch or step attenuator not shown in figure 15), the baseband signal should be zero. If not, the same calibration process discussed above is used to adjust the calibration signal until the composite output is forced to zero. In this case, the analog switches bypass the integration function, just as they do for baseband data collection.

The techniques described above are simple, easy to implement, and inexpensive. Even so, an alternative solution is available: the calibration measurements could be sampled by the digital controller and the errors could be accounted for in its subsequent calculations.

**FIGURE 15. CALIBRATION OF STATISTICAL MEASUREMENTS**



#### 4.3.3.7 CALIBRATION (continued)

**Amplitude, Phase and Delay Variations** - The RF and IF paths leading to the statistical measurement circuits must be precisely calibrated otherwise they may introduce errors in the statistical measurements. The correlation of input signals relative to one another is measured for construction of the off time covariance matrix. The correlation of each input signal to the output signal are measured for construction of the on time cross-correlation vector. These correlation measurements assume they are made using data directly from the antenna elements and directly from the output. Any amplitude, phase or delay errors between the inputs and the statistical measurement circuits, or the output and the statistical measurement circuits, will result in erroneous correlation data. As an example, the measurements and resulting weight estimates are based on the relative separation between each of the antenna elements. If a phase shift or delay is introduced in one feedforward IF chain leading to the correlators which is not introduced in all other feedforward IF chains, the data for that one channel will be in error. Each channel is expected to have different and unpredictable amplitude, phase and delay terms in their overall transfer functions. These must be calibrated to provide the required correlation data accuracy necessary to support null and beam steering.

Since the data required to construct the correlation matrix is collected as baseband data while the cross-correlation vector data is collected as IF correlation measurements, two separate calibrations are required for these two procedures. The measurements required to perform these calibrations are available; there are a number of sequences which could provide the necessary calibration accuracy. Example calibration procedures for baseband data collection and for IF correlation measurements are presented. These procedures may not be optimal (due to Phase I SBIR time and budget constraints), but are representative of the types of measurements and procedures which are available with the proposed architecture.

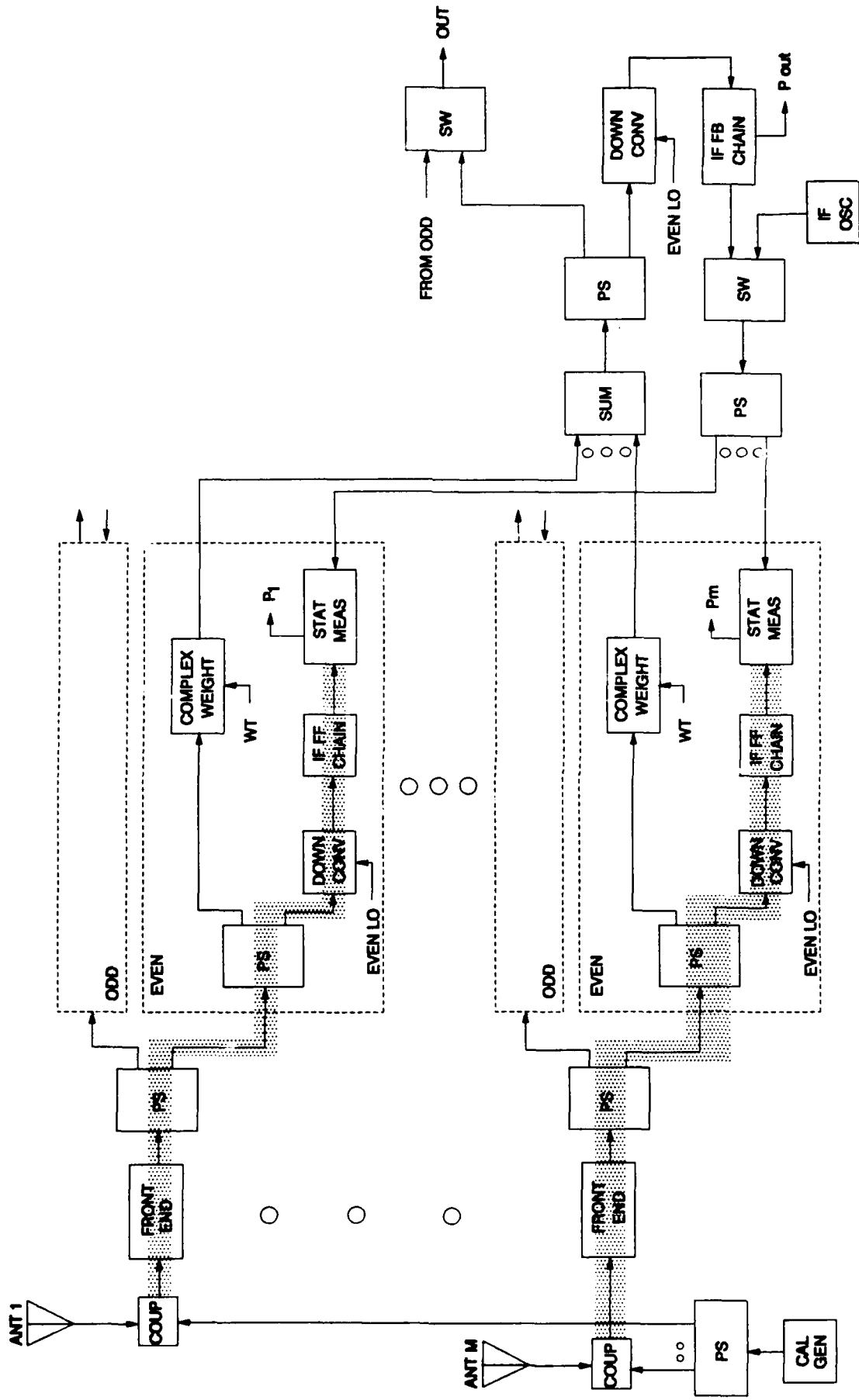
**Calibrating baseband data measurements** - Figure 16 shows a simplified block diagram of the AAP in which the RF and IF paths which are being calibrated are highlighted. An RF generator has been added which is coupled into each of the antenna elements' signal paths. All the CAL signals into each channel's front end are assumed to be amplitude and phase matched to one another. The components in the paths from the antenna input to the feedforward port of the statistical measurement circuits introduce amplitude and phase/delay variations between channels. One procedure for measuring these variations, determining correction factors, and applying these corrections to measured data is outlined below.

1. Enable the IF Oscillator in the feedback path, tune the input RF Cal Generator to the desired frequency and enable its output, and tune the LO for proper downconversion. All of these signals are derived from the same source and are therefore coherent.

2. Use the statistical measurement circuits to measure the phases and amplitudes of each feedforward signal relative to the reference signal from the feedback path. The outputs of the quadrature downconverter provides this information in rectangular coordinates. The digital controller can sample this data and convert it to polar coordinates. For example, the data for channel k would have the form  $R_k \Delta \theta_k$ .

3. Choose one channel to be the reference channel; all other channels will be calibrated to match the amplitude and phase of that reference channel. Assuming channel one is the reference channel, the correction factors are  $C_{1k} \Delta \theta_{1k} = R_1 / R_k \Delta(\theta^1 - \theta^k)$ .

**FIGURE 16. CALIBRATION OF BASEBAND DATA COLLECTION**



#### 4.3.3.7 CALIBRATION (continued)

##### Amplitude, Phase and Delay Variations (continued)

4. Measure the actual data (this occurs after the cal sequence determines the correction factors). Process this data to form the elements of the covariance matrix  $R_0$ , which are the expected values of  $(x_k x_l)$ . Note that the correction factors associated with each component of the expected values are deterministic, and therefore can be moved outside the expected value operation. This allows the correction factors to be applied to the elements of the covariance matrix after integration rather than directly to each sample of baseband data. The number of calculations (and therefore time delay) is greatly reduced for the formation of  $R_0$ . The covariance matrix elements are in rectangular coordinate format, so they must be converted to polar coordinates. Assume this data is  $M_{kl} \Delta \Psi_{kl}$ .

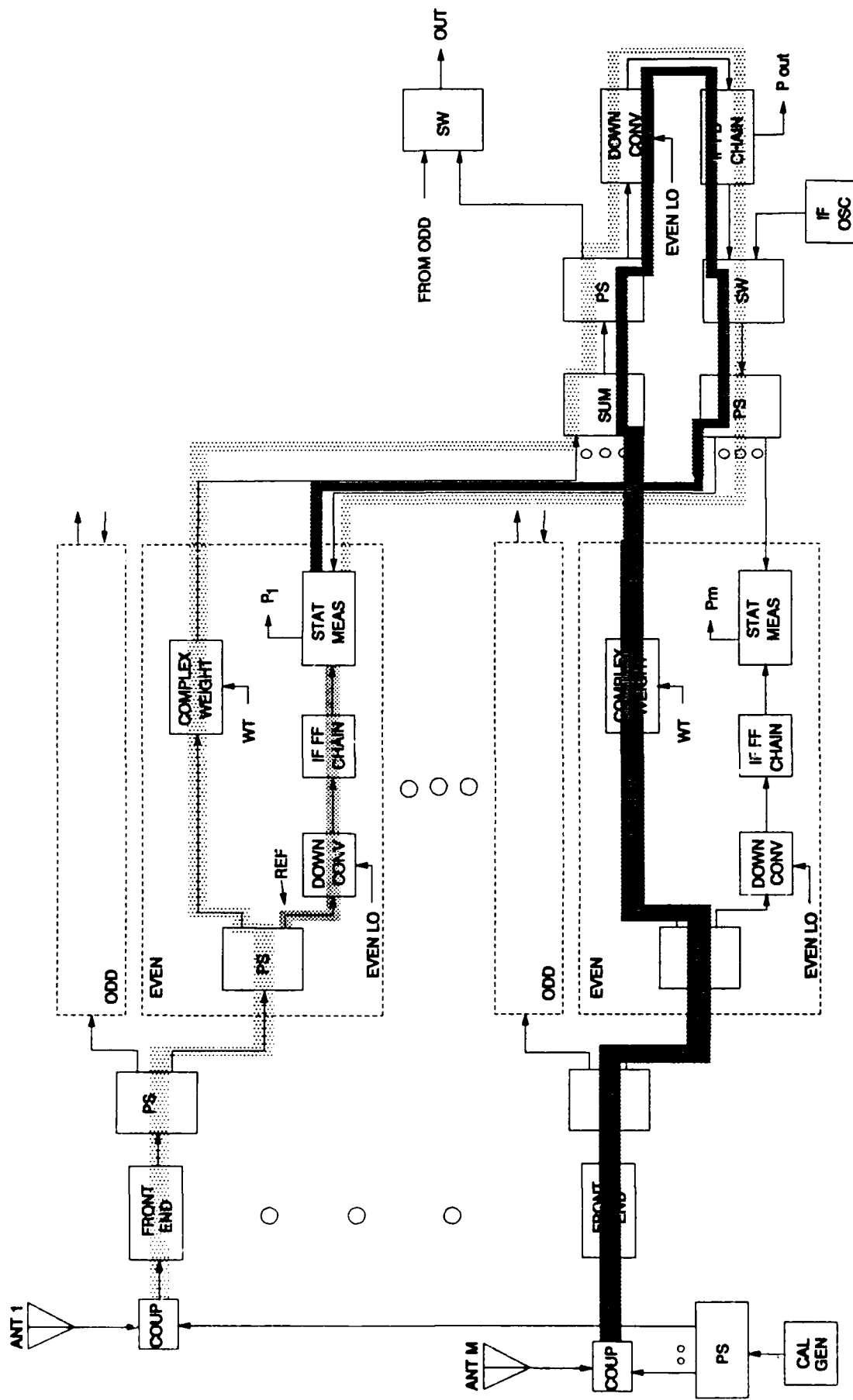
5. For each element of the covariance matrix, the correction factor is provided by the calibration sequence:  $C_{kl} \Delta \theta_{kl} = (C_{1k} \Delta \theta_{1k})(C_{1l} \Delta \theta_{1l}) = C_{1k} C_{1l} \Delta(\theta_{1k} + \theta_{1l})$ . This multiplication factor is applied to the measured data  $M_{kl} \Delta \Psi_{kl}$  to provide the calibrated covariance data to be used by the algorithm for adaptation calculations. This data is used to construct a calibrated  $R_0$ .

**Calibrating IF correlation measurements** - This procedure involves calibrating two sets of paths and applying the calibration factors in different ways to achieve the desired results. The goal of this IF correlation calibration procedure is to calibrate out amplitude and phase/delay errors in the cross-correlation data associated with on time processing. This correlation data is used in vector form (designated  $R_{xy}$ ) by the adaptation algorithm; the elements of this vector are  $E[x_k y^*]$  where  $E[\ ]$  denotes an expected value. Calibrating these measurements can be accomplished by a two step process: Step 1 calibrates all the direct signal paths from the input to the output. As explained below, this effectively provides a calibrated output term  $y = \sum w_k x_k$  for the adaptation algorithm. Step 2 calibrates the inputs ( $x_k$ ) to one another; when steps 1 and 2 are combined, each product  $x_k y^*$  is calibrated.

The first step in this process calibrates the paths shown in figure 17; it recognizes that the theoretical output of the AAP is a summation of all the weighted inputs ( $y = \sum w_k x_k$ ) and that one calibration of the output only is not sufficient unless the paths from input ( $x$ ) to output ( $y$ ) are identical. Since this entire procedure is necessary because those paths are not identical, a means of calibrating each  $w_k x_k$  term is required. The first step of this two step calibration is designed to apply a different correction factor to each complex weight (the  $w_k$  terms). Calibration data is accumulated by measuring the amplitude and phase/delay variations between the direct signal paths from the inputs to the output. After the power combiner which sums the weighted RF signals from each channel, the path to the feedback port of the statistical measurement circuits is common to all channels. Therefore, measurements made at the IF correlators indicate the variations between the RF paths only. A reference signal for measuring each channel's amplitude and phase is provided by the feedforward signal from one of the channels. The channel associated with the correlator circuit selected is the reference channel for these measurements; as done above, a correction factor will be determined for all other channels to result in a set of data which is fully calibrated with one another. An example procedure for accomplishing this calibration is listed below.

1. Turn on and enable the RF calibration generator and the LO. Select the FB IF signal rather than the IF oscillator signal using the feedback switch. The RF calibration signal present in all channels will be downconverted and applied to the statistical measurement circuits' IF feedforward ports, but only channel one's circuits will be used in this step of the calibration procedure. Therefore, the FF IF signal for channel one is the reference to which the feedback signals will be calibrated.

FIGURE 17. CALIBRATION OF IF DATA STEP 1



#### 4.3.3.7 CALIBRATION (continued)

##### Amplitude, Phase and Delay Variations (continued)

2. Enable the real component of the complex weight for channel one only. To accomplish this, set  $w_1 = 1 + j0$ , all other  $w_k = 0 + j0$ .

3. Measure the amplitude and phase/delay of the feedback signal (from channel one only) relative to the reference FF IF signal using channel one's IF correlator. The outputs of the correlator circuits are in rectangular coordinates; convert this data to polar coordinates. This calibration data is  $R_1 \Delta \theta_1$ .

4. Repeat step numbers 2 and 3 for each of the channels, yielding all the cal data  $R_k \Delta \theta_k$ .

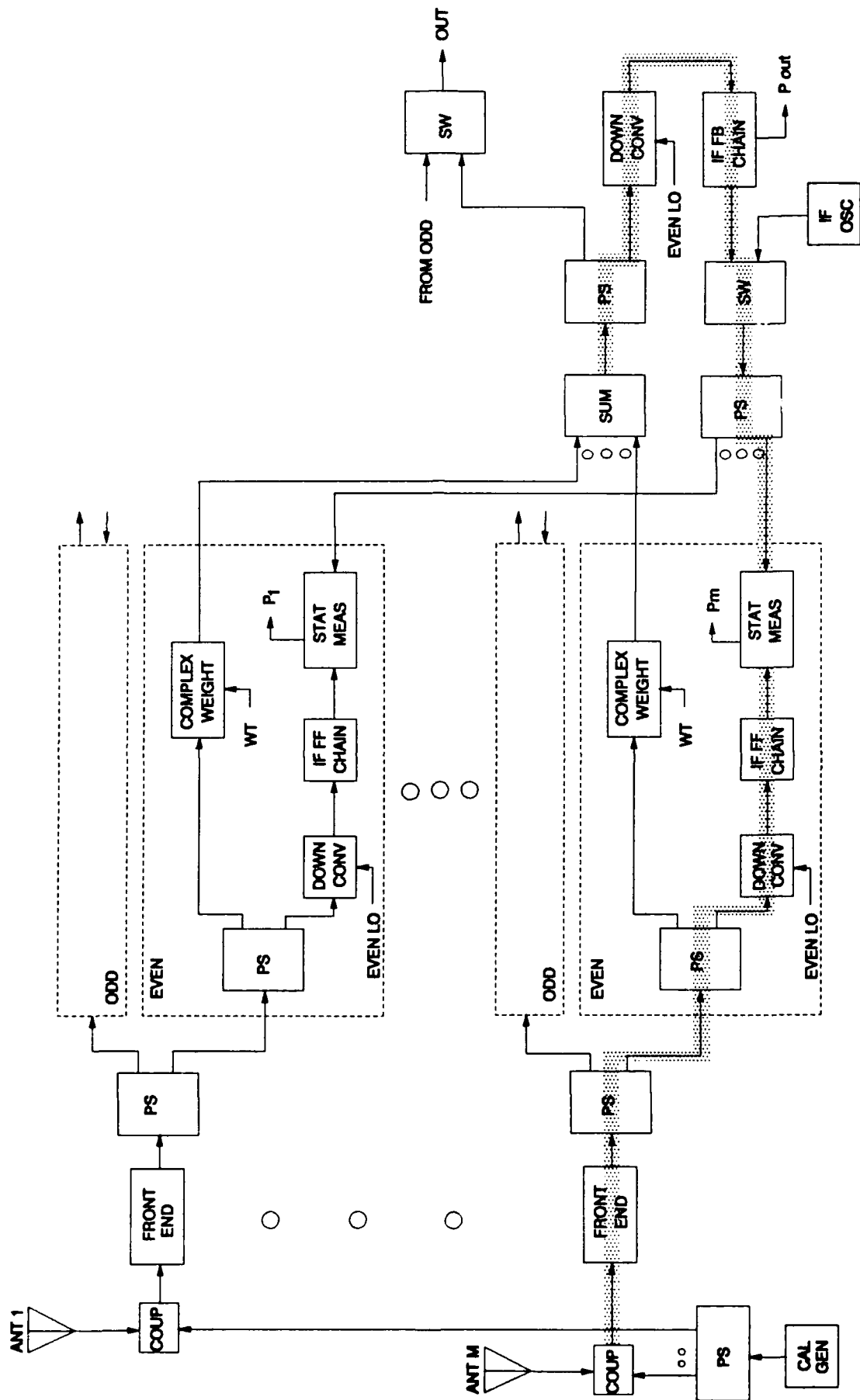
5. Once the summation occurs, the only way each term in the summation can be corrected for (without added circuitry) is by applying the correction factors to the weights rather than to the data. Since channel one is selected as a reference, a correction factor similar to the one calculated in the baseband data calibration procedure is required to calibrate the other channels to channel one's amplitude and phase reference. As in the baseband case, these calibration factors may be written as  $C_{1k} \Delta \theta_{1k} = R_1 / R_k \Delta(\theta_1 - \theta_k)$ .

6. The weight estimates are calculated by the adaptation algorithm; the correction factors described above multiply the weight estimates before application to the RF weighting elements. This assures that  $y = \sum w_k x_k$ , without distributed amplitude and phase/delay errors corrupting each term of the summation.

The second step of the IF correlation calibration involves calibrating the feedforward paths in all the channel's relative to one another. These paths are highlighted in figure 18. This effectively provides calibration of all the inputs  $x_k$ . This procedure is almost identical to the baseband data collection calibration procedure except: 1) The feedback signal used as a reference is not the FB oscillator, but is the signal which originates in the RF cal generator and is allowed to pass through one complex weight. 2) Some of the statistical measurement circuits used for IF correlation measurements are different than those used for baseband data generation and manipulation. 3) Only one term needs corrected ( $x_k$ ) rather than two terms of a product ( $x_k x_1$ ). Following the same procedure as outlined in those paragraphs: calibration measurements are made, correction factors to calibrate channels 2 thru 4 to channel 1 are calculated, real data measurements are made, then the correction factors are applied to the measured data. Again, since the corrections are deterministic, they can be applied after integration.

Combining the two steps described above completes the IF correlation calibration process. The correction factors for the weights are determined per step 1. The input data correction factors are determined per step 2. The calibration data collection cycle is then complete, external signal reception is enabled, and adaptation processing begins. The IF cross-correlation measurements are made, block by block. The correction factor for the input path variations are applied to these cross-correlation measurements. The adaptation algorithm calculates weight estimates based on this corrected data, then the correction factors from step 1 (which corrects for input to output variations) are applied to the weights to determine the desired weights to be applied to the CPMs.

FIGURE 18. CALIBRATION OF IF CORRELATION DATA, STEP 2



#### 4.3.3.8 COMPLETE BASELINE AAP RECEIVE ARCHITECTURE

The baseline AAP receive architecture has been developed through out section 4.3.3. Options for critical components and subsystems have been presented, and choices for the baseline were selected and justified. The resulting AAP receive architecture is shown as a fairly detailed block diagram in figure 19.

Although all the features of this architecture were discussed in detail in previous sections, the following comments are provided as concluding remarks which summarize the AAP receive architecture.

- o The antenna array, shown in the block diagram to include four elements, receives the RF signals present and provides the time delay between sensors which is exploited by the AAP to form nulls in the direction of jammers and a beam in the direction of the desired signal.

- o Several components are included at the inputs of the AAP which are used exclusively for internal calibration. These include the input switches, the CAL Generator, the input four way power splitter, and the input couplers.

- o A front end network is provided for each channel which is shared by the odd and even processors. These networks determine the RF operating band and establish the AAP unit noise figure.

- o For anticipative processing, most of the adaptive processing components must be repeated. Since four channels are included in the baseline, eight identical processor modules are required. These modules include downconversions of the input signal, the IF chains which condition the feedforward signals for correlation measurements, power monitors of the input signals, statistical measurement circuits (IF correlator / baseband downconverter with associated analog or digital processing), and the complex weighting devices.

- o The LO signals must frequency hop with the host radio. Since the odd processor is operating in advance of the even processor, two sets of LO signals are required, hence two synthesizer modules are shown.

- o The feedforward paths include filtering to limit correlation estimates to the message bandwidth, thereby maximizing the SIR. Also included are a delay adjustment, step attenuator for amplitude adjustment, and gain to overcome losses in other components.

- o The statistical measurement circuits shown include the calibration circuits required to assure the accuracy of the IF correlation and baseband data.

- o The complex weighting circuits include the error correction circuits which map the calculated weight values to the transfer functions of the CPMs used to implement them. Temperature dependent variations are also accounted for and correction is provided.

- o A feedback path is provided which is very similar to the feedforward path. This chain includes downconversion, filtering to the message bandwidth, a delay adjustment, a step attenuator for amplitude adjustment, and a power monitor. The feedback path also includes an IF switch which determines the input to the statistical measurement circuits. One of three inputs may be selected: 1) The feedback signal from the output, used for cross-correlation vector measurements. 2) The IF oscillator, which is used in the collection of off time baseband data. 3) A 50 ohm termination, used in calibrating the statistical measurement circuits.

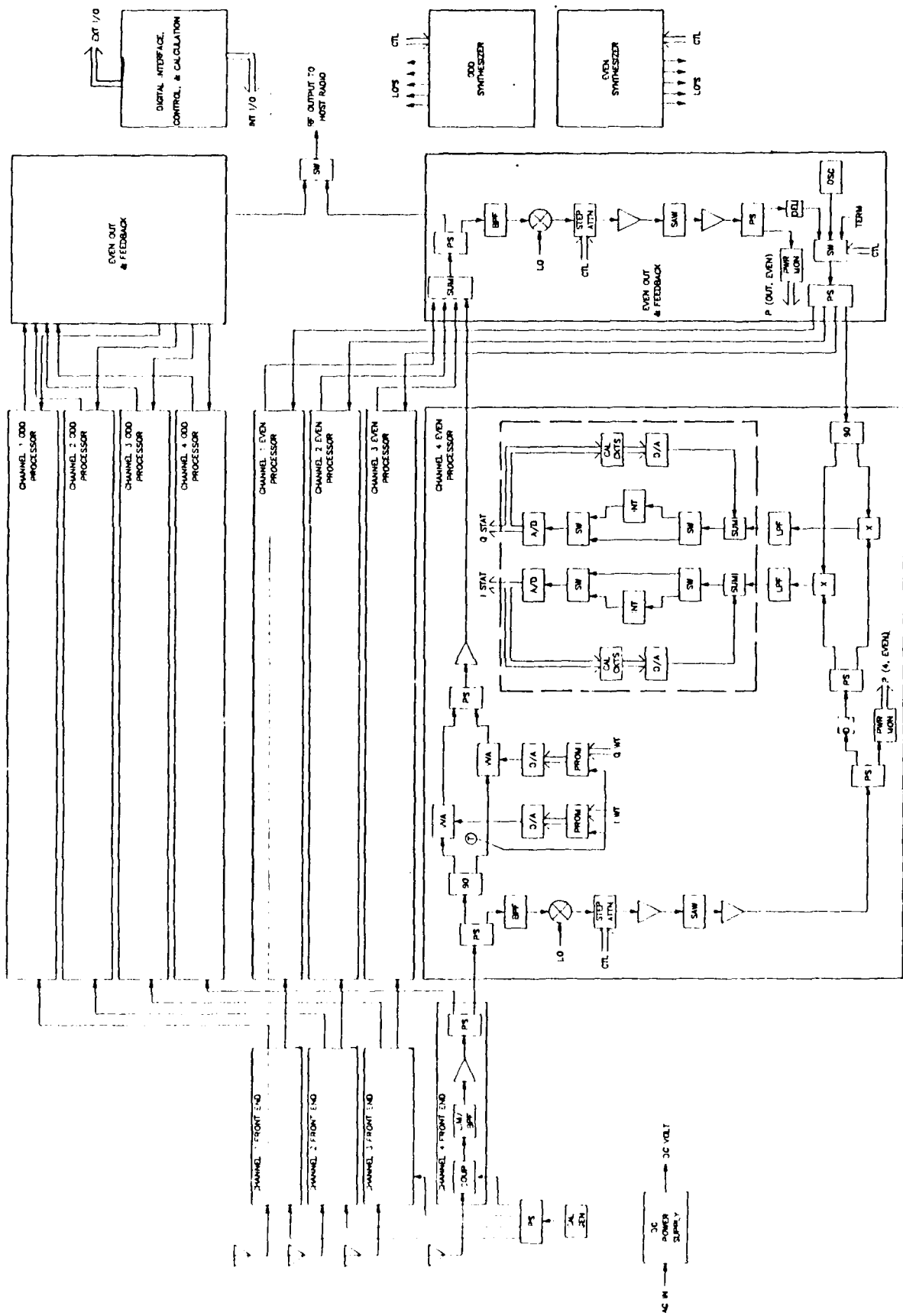


FIGURE 19. COMPLETE BASELINE RECEIVE AAP BLOCK DIAGRAM

#### 4.3.3.8 COMPLETE BASELINE AAP RECEIVE ARCHITECTURE (continued)

○ The even and odd processors include identical circuits and work in parallel. The output is formed by alternatively selecting the processor whose output includes the signal of interest (the processor working with on time data). This selection is done by the RF output switch.

○ The digital controller interfaces with external devices (such as the host radio), samples data from internal subassemblies, controls the internal subassemblies, and performs the calculations required for adaptation. One digital controller can serve both the even and odd processors.

#### 4.3.3.9 TRANSMIT ARCHITECTURE

The concept of using the information acquired via receive adaptation to direct the transmit energy of the host radio has been demonstrated in this and other studies. The simulated system performance improvements are encouraging and deserve additional investigation. While the simulations (which assume ideal components) are encouraging, the directive and retrodirective transmission techniques will be difficult to implement with real components. A top level block diagram of a directive/retrodirective AAP which illustrates some of the issues requiring further investigation is shown in figure 20. Examples of these issues are listed below.

○ Even though the host radio offers a range of transmit power levels, the lowest level is too high - the transmit weighting elements will have limited dynamic range. The transmit power from the host radio needs to be decreased either within the host radio (undesirable since this requires modifying an established design or customizing some units for AAP operation) or within the AAP. This may cause thermal problems in the AAP or degradation in the quality of the transmitted signal.

○ A calibration procedure which maps the transmit weights calculated by the digital controller to the actual weights provided by the RF devices used. This problem is similar to the receive AAP's; the same type of correction circuits associated with the CPMs may be used for the transmit path as well as the receive path.

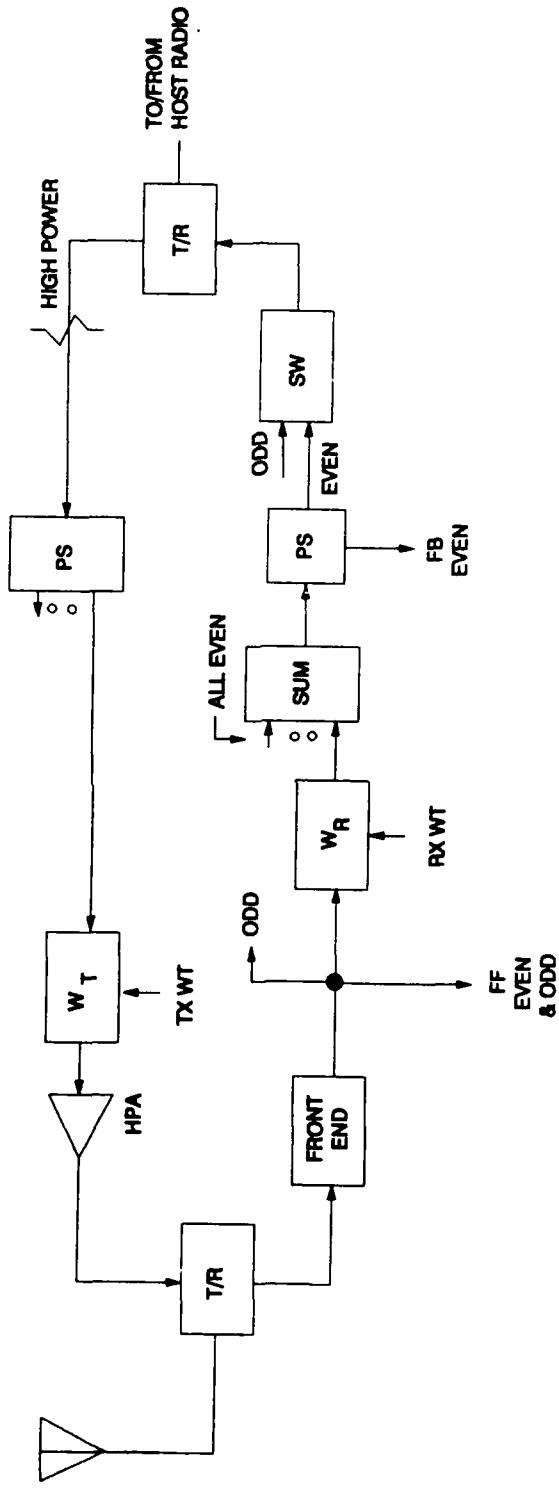
○ A method of calibrating the transmit weights to the receive weights is required.

○ The host radio's transmit signal is power divided into four signals; each of these signals are processed in parallel. The output processing includes the power divider, an attenuator to decrease the levels into the weighting devices, the weighting devices themselves, RF amplifiers and filters (probably, although not shown) and the high power amplifier. All of these transmit paths must be calibrated relative to one another. This is similar to the amplitude and phase/delay calibration procedures identified in the receive AAP discussions.

○ One high power amplifier is required for each channel of the AAP. Although the transmit power required of each amplifier will be less than the power available from the host amplifier (since the AAP outputs are summed together), the inefficiencies of the amps will result in considerably higher DC power dissipations and may cause thermal problems.

An effort was made by ACM Systems to address these issues and develop an architecture capable of supporting directive and retrodirective transmissions, but time and money limitations required a premature conclusion of this effort.

**FIGURE 20. TRANSMIT CONSIDERATIONS**



#### 4.3.4 COMPUTER MODELING AND SIMULATIONS

Note: The notation for matrices and vectors in the following section differs slightly from that of the other sections in this report. For instance  $\underline{M}$  represents a matrix, and  $\underline{v}$  represents a vector.

##### 4.3.4.1 INTRODUCTION

Extensive simulations were performed to demonstrate the effectiveness of blind adaptive antenna array algorithms and architectures on frequency hopped signals in a corrupt environment. This signal environment consists of directional jammers, and a directional, frequency hopped (FH) signal of interest (SOI). The data is modeled as the output of an adaptive array processor (AAP) front end with receiver noise, and with adjustable gain, phase, and delay variations between individual elements. The vector signals generated are essentially down converted, de-hopped, and sampled.

Two algorithms, Dominant Mode Maximin (Block Update) and Maximin [20, 21, 22], were implemented. Each algorithm exploits the FH characteristic of the SOI to reject the jammers and beam up on the SOI. The Dominant Mode is a Maximin-type algorithm which takes an eigen-equation approach, whereas Maximin is a gradient method. This study examines the application of the Dominant Mode algorithm to Army tactical radio systems for the first time.

In order to evaluate the simulations, a variety of outputs were produced. These include weight vectors, aperture vector (steering vector) estimates, and output signal to interference and noise ratios (SINR). The weight vectors were used to generate receive antenna patterns which give a visual measure of the effectiveness of the adaptive array processor. In a similar fashion, the aperture vector estimates were used to generate transmit patterns and power footprints.

##### 4.3.4.2 SIMULATION DESCRIPTION

###### Environment and AAP Front End -

The data used in the simulations was generated with the EPLRS system in mind. Due to the rapid convergence of the Dominant Mode algorithm, the amount of data needed to perform the simulations could be reduced. We chose 256 chips per hop for processing, whereas the EPLRS system has about 2400 chips per hop. This is equivalent to saying that adaptation was discontinued after 256 chip periods. We have also ignored for now the guard time which contains no SOI. That is, processing occurred inside a window during which an SOI should be present (rather than including the period during which it is known no SOI will be present).

The hop increment of the EPLRS system is 3 MHz; the data is spread over frequency using direct sequence spread spectrum (DSSS) techniques with a 3 Mbit/sec chip rate. The EPLRS signal is frequency hopped over eight channels, or bins. In the simulations, the center frequencies of these bins are  $(426 + 3n)$  MHz, where  $n=0,1,2,\dots,7$  is the bin number (see Table 1). The 27 MHz RF bandwidth represents a percent bandwidth of 6.2 percent.

**Table 1** Bin center frequencies and their corresponding bin numbers.

Bin frequency	426	429	432	435	438	441	444	447
Bin number	0	1	2	3	4	5	6	7

#### 4.3.4.2 SIMULATION DESCRIPTION (continued)

For generality, the SOI generated for each simulation was a pseudo-random (PN) constant modulus (CM) sequence ( $s(t)=e^{-j\theta(t)}$ ) with uniformly distributed phase ( $\theta(t)=u[-\pi,\pi]$ ). A timing error (SOI offset advance) was provided as an option, but not investigated as part of this study.

The jammer signals were modeled optionally as either PN CM noise ( $v_{CM}(t)=e^{-j\theta(t)}$ ) with uniformly distributed phase, or complex white gaussian (CWG) noise ( $v_{CWG}(t)=CWGN(\mu=0,\sigma=1)$ ) with zero mean and unit variance. The receiver noise was strictly CWG ( $u(t)=CWGN(\mu=0,\sigma=1)$ ).

It should be noted that these sequences are independent of each other, independent from hop to hop, and independent between on and off times. The receiver noise is independent from element to element. And, fresh sequences were generated for each simulation.

Two sets of data were generated for each hop (timeslot): off time data and on time data. The off time data contains jammers and receiver noise only, as where the on time data contains jammers, receiver noise, and the SOI. In these simulations, the off time data was modeled as though it was collected from the frequency bin of the on time data one timeslot prior to the actual hop to that frequency bin. That is, anticipative off time data collection is being simulated. Thus, the off time data will have the same noise and directional jammers present as the on time data. Remember, though, the jammers and noise are independent between on and off times, but have the same statistics.

The data provided to the algorithm is essentially down converted, de-hopped, and sampled. It is modeled as vector output of an antenna array front end. This modeling is accomplished by creating aperture vectors for the SOI and for each jammer present in the current frequency bin. The aperture vectors provide for the option of gain, phase, and delay variations between antenna elements. In this study, however, time did not permit investigation of these variations. The dynamic range of the system is also taken into account when adding the receiver noise and applying the automatic gain control (AGC).

Table 2 lists the SOI parameters; Table 3 lists the various selectable system parameters with their default values; and Table 4 lists the jammer parameters.

TABLE 2 SOI Parameters

Parameter	Description	Defaults
$\theta_s$	SOI direction of arrival (DOA)	0°
$\tau_s$	SOI timing advance ( $0 \leq \tau_s \leq N_h$ )	0

## 4.3.4.2 SIMULATION DESCRIPTION (continued)

TABLE 3 System Parameters

Parameter	Description	Defaults
M	number of sensors	4
$(d_m)$	sensor locations (units of center frequency wavelength, $\lambda_c$ )	At vertices of a unit square.
DR	dynamic range (dB)	40
$(g_m, \tau_m, \phi_m)$	voltage gain, delay, and phase offset, respectively, of the $m^{\text{th}}$ sensor's RF chain, assumed to be independent of frequency. Delay is normalized to the period of the center frequency.	(1,0,0)
$f_c$	center of frequency band (MHz)	436.5
$M_h$	number of hop bins	8
$N_h$	number of chips per hop	256

TABLE 4 Jammer Parameters

Parameter	Description	Defaults
$L_{SNOI}$	total number of jammers	2
$(\theta_j)$	jammer DOA's	{ 40°, 110° }
$(k_j^-, k_j^+)$	jammer frequency range (bin #'s)	40° - { 3, 7 } 110° - { 0, 4 }
$(CM_j)$	constant modulus (CM) flag T => CM jammer F => CWG jammer	40° - F 110° - F
$(SJR_j)$	in-bin signal to jammer ratios (dB)	40° - -20 110° - -20

#### 4.3.4.2 SIMULATION DESCRIPTION (continued)

The following comprehensively describes the generation of the simulated antenna array front end output. First, the antenna array apertures and attenuators are initialized from the parameters specified in the tables above. The jammer levels are incorporated into their respective aperture vectors for simplicity. The apertures and attenuators are then rescaled by taking into account the dynamic range of the receiver array and applying the AGC.

(In the following,  $k$  = frequency bin number,  $m$  = sensor number.)

1. Set initial (unnormalized) receive antenna gains:

$$\alpha_{km}^{RCV} = g_m e^{-j(2\pi(\frac{f_k}{f_c})\tau_m + \phi_m)}$$

2. Set initial SOI receive apertures:

$$a_{km}^{SOI} = e^{-j2\pi(\frac{f_k}{f_c})d_m^T u(\theta_s)}, \quad u(\theta_s) = \begin{pmatrix} \cos \theta_s \\ \sin \theta_s \end{pmatrix}$$

3. Set SNOI (signal not of interest => jammer) variables:

$L_k$  = No. SNOI's at frequency bin  $k$

$\theta_{kl}$  = SNOI DOA's of jammer  $l$  at bin  $k$

$CM_{kl}$  = SNOI CM/CWG flag

4. Set initial SNOI attenuations and receive apertures:

$$\alpha_{kl}^{SNOI} = 10^{-SJR_l/20}$$

$$a_{klm}^{SNOI} = \alpha_{kl}^{SNOI} e^{-j2\pi(\frac{f_k}{f_c})d_m^T u(\theta_{kl})}$$

## 4.3.4.2 SIMULATION DESCRIPTION (continued)

5. Set the rescaling gain factors (AGC normalization):

$$\hat{\alpha}_m^{RCV} = \frac{\sqrt{M_h 10^{DR(dB)/10}}}{\sqrt{\sum_{k=0}^{M_h-1} |\alpha_{km}^{RCV}|^2 \left[ \frac{1}{M_h} + \sum_{l=1}^{L_k} |\alpha_{kl}^{SNOI}|^2 \right]}}$$

6. Rescale (normalize) all apertures and receiver gains:

$$\alpha_{km}^{RCV} \leftarrow \hat{\alpha}_m^{RCV} \times \alpha_{km}^{RCV}$$

$$a_{km}^{SOI} \leftarrow \alpha_{km}^{RCV} \times a_{km}^{SOI}$$

$$a_{klm}^{SNOI} \leftarrow \alpha_{km}^{RCV} \times a_{klm}^{SNOI}$$

7. Calculate maximum-attainable SINR for each frequency bin:

$$SINR(k) = (a_k^{SOI})^H \underline{R} a_k a_k^{SOI}$$

$$\underline{R} a_k a_k = \underline{I} + \sum_{l=1}^{L_k} a_{kl}^{SNOI} (a_{kl}^{SNOI})^H$$

where the sensor subscript,  $m$ , has been incorporated into the vector notation of the apertures. And, the composite interference and noise is  $\underline{q}(n)$ .

Once the apertures and attenuators are computed, the various signals are generated and combined accordingly:

Over the  $i^{\text{th}}$  hop:

1. Determine  $k$ , the  $i^{\text{th}}$  hop frequency bin (pseudo random number generator).
2. Set the composite interference field,  $\underline{q}(n)$ , for  $n=-N_h$  to  $N_h-1$  ( $n=-N_h$  to  $-1$  is the anticipatory portion) by combining jammers,  $\underline{v}_j(n)$ , and receiver noise,  $\underline{v}_r(n)$ :

## 4.3.4.2 SIMULATION DESCRIPTION (continued)

$$q(n) = \underline{u}(n) + \sum_{l=1}^{L_k} \underline{a}_l^{SOI} v_l(n)$$

$$\underline{u}(n) \sim \text{I.I.D. CWGN}(0, \underline{I})$$

$$v_l(n) \sim \begin{cases} e^{j\theta_l(n)}, & \theta_l \sim \text{I.I.D. } u[-\pi, \pi), & CM_l = T \\ z_l(n), & z_l \sim \text{I.I.D. CWGN}(0, 1), & CM_l = F \end{cases}$$

where I.I.D. = Independent, Identically Distributed.

3. Add SOI:

$$\underline{x}(n) = \begin{cases} \underline{a}_k^{SOI} s(n+\tau_s) + q(n), & -\tau_s \leq n \leq -\tau_s + N_h - 1 \\ q(n), & -N_h \leq n < -\tau_s, \quad -\tau_s + N_h - 1 < n \leq N_h - 1 \end{cases}$$

$$s(n) \sim e^{j\theta(n)}, \quad \theta \sim \text{I.I.D. } u[-\pi, \pi)$$

( $\underline{x}(n)$  is referred to as the augmented hop data).

Algorithms -

Processing can be done with the off time data (no SOI present) as well as the on time data. Two algorithms were incorporated into the processor model, but adequate simulations of their effectiveness was not possible due to time limitations on the SBIR. The two algorithms are: steepest descent null steering and inverse power method null steering. Both techniques minimize the output power in the absence of the SOI; only SNOIs are present - consequently, minimizing output power during the off time steers nulls without regard for SOI DOAs. The inverse power method null steering algorithm accomplishes this by adapting the weights to the minimum eigenvector of the off time auto-correlation matrix. These preprocessing techniques could be explored in subsequent studies since they should decrease initial adaptation times.

The weights are initialized isotropic at the start of simulation (prior to off-time processing).

The two on time algorithms explored in this study are Dominant Mode Block Update and Maximin. The computer simulations of the Dominant Mode Block Update algorithm is described in the following text. The simulation of the Maximin algorithm was attempted, but the results obtained were inconsistent; to avoid wasting time on established results, this effort was abandoned. The reader is referred to [20, 21, 22] for descriptions of the Maximin implementation and its simulations.

#### 4.3.4.2 SIMULATION DESCRIPTION (continued)

##### Dominant Mode Block Update -

The flow chart in Figure 21(a-c) depicts in detail the implementation of the Dominant Mode Block Update algorithm. Table 5 lists the selectable parameters used in the flow chart. Table 6 gives a brief description of the variables appearing in the flow chart.

The Dominant Mode Block Update algorithm relies on the power method to adapt the weights to the maximum eigenvector as shown in the flow chart. In the implementation of the algorithm, however, the on time autocorrelation matrices are not exactly the same from block to block. This method is still valid, though, since the matrices will exhibit the same statistics. As the collect times approach infinity, the block to block variation is eliminated. This is actually a 'stochastic power method' being implemented. The optimal set of weights from block to block (after convergence) will, for the most part, be unchanging except for an overall gain and phase factor. The adapted weights are therefore saved, according to the current frequency bin, from hop to hop in order to significantly reduce adaptation time in subsequent visits to the same frequency bin.

There are a couple of architecture dependent variations which were investigated as part of this study. The first uses  $\underline{R}_{XY1}$  instead of  $\underline{R}_1 \underline{w}$  in the adaptation. This was simulated by bypassing the smoothing applied to  $\underline{R}_1$  from block to block. That is, since  $\underline{R}_{XY1} = \hat{\underline{R}}_1(m) \underline{w}$ , then  $\underline{R}_{XY1} = \underline{R}_1 \underline{w}$  by setting  $\underline{R}_1 = \hat{\underline{R}}_1(m)$  each hop. This variation is motivated by the fact that computation and storage of  $\underline{R}_{XY1}$  is much less intensive than computation and storage of  $\underline{R}_1$ . This variation did not significantly alter the performance of the processor, and has consequently been considered a viable hardware reducing option.

The second variation attempted a similar operation to construct the off time statistics,  $\underline{R}_0$ . The simulation consisted of building  $\underline{R}_0$  one column (vector) at a time by processing the off time data in blocks. Notice, the first column of  $\underline{R}_0$  (denoted  $[\underline{R}_0]_0$ ) is equal to  $\underline{R}_{XY0}$  if  $\underline{w} = \underline{e}_0 = [1 \ 0 \ 0 \ \dots \ 0]^T$ , since  $\underline{R}_{XY0} = \underline{R}_0 \underline{w}$ . In general, then,  $[\underline{R}_0]_j = \underline{R}_0 \underline{e}_j$ . The variation considered consists of obtaining the first column from the first off time data block by setting  $\underline{w} = \underline{e}_0$ ; the second column from the second block  $\underline{w} = \underline{e}_1$ ; and so on. Thus,  $\underline{R}_0$  would not have to be computed directly, reducing hardware components (and thus, simplifying the architecture).

This approach was not successful, though. The resulting matrix had lost some of its most important properties: hermitian and positive definite. An attempt to restore these properties (specifically the hermitian property) did not redeem this approach. These results can be explained, though, by realizing that  $\underline{R}_0$  is not the same from block to block. The statistics from block to block are similar, but, only if a large enough number of samples were used would the matrices begin to be equal. The relation between this convergence and the number of samples used per block is approximately  $(1/\sqrt{n})$ . Thus, the various columns will not combine to give a functional estimate of the off time statistics,  $\underline{R}_0$  due to our finite collect interval.

## 4.3.4.2 SIMULATION DESCRIPTION (continued)

TABLE 5 User Specified Processing Parameters

Parameter	Description	Defaults
$N_0$	off time collect interval	256
$N_1$	on time block collect interval	32
$\mu$	factor for accelerated convergence	0

TABLE 6 Algorithm Variables

Variable	Description
$k$	the frequency bin of the current hop / timeslot
$M_1$	number of on time blocks to process ( $N_h / N_1$ )
$\underline{x}(n)$	the augmented hop data generated above
$\underline{X}_0(n)$	off time data
$\underline{X}_1(n)$	on time data
$\underline{R}_0$	estimated off time auto correlation matrix
$\hat{\underline{R}}_1(m)$	estimated on time auto correlation matrix over block m
$\underline{R}_1$	smoothed $\hat{\underline{R}}_1(i)$ over $i=0, \dots, m$
$\underline{w}_k$	stored weight vector for $k^{\text{th}}$ frequency bin
$\underline{a}_k$	stored aperture estimates for $k^{\text{th}}$ bin
$\gamma_k$	stored SINR estimates for $k^{\text{th}}$ bin
$y(n)$	output
$\eta_k$	number of visits to bin k

Figure 21(a) Dominant Mode Block Update Implementation Flow Chart

For an arbitrary hop / timeslot:

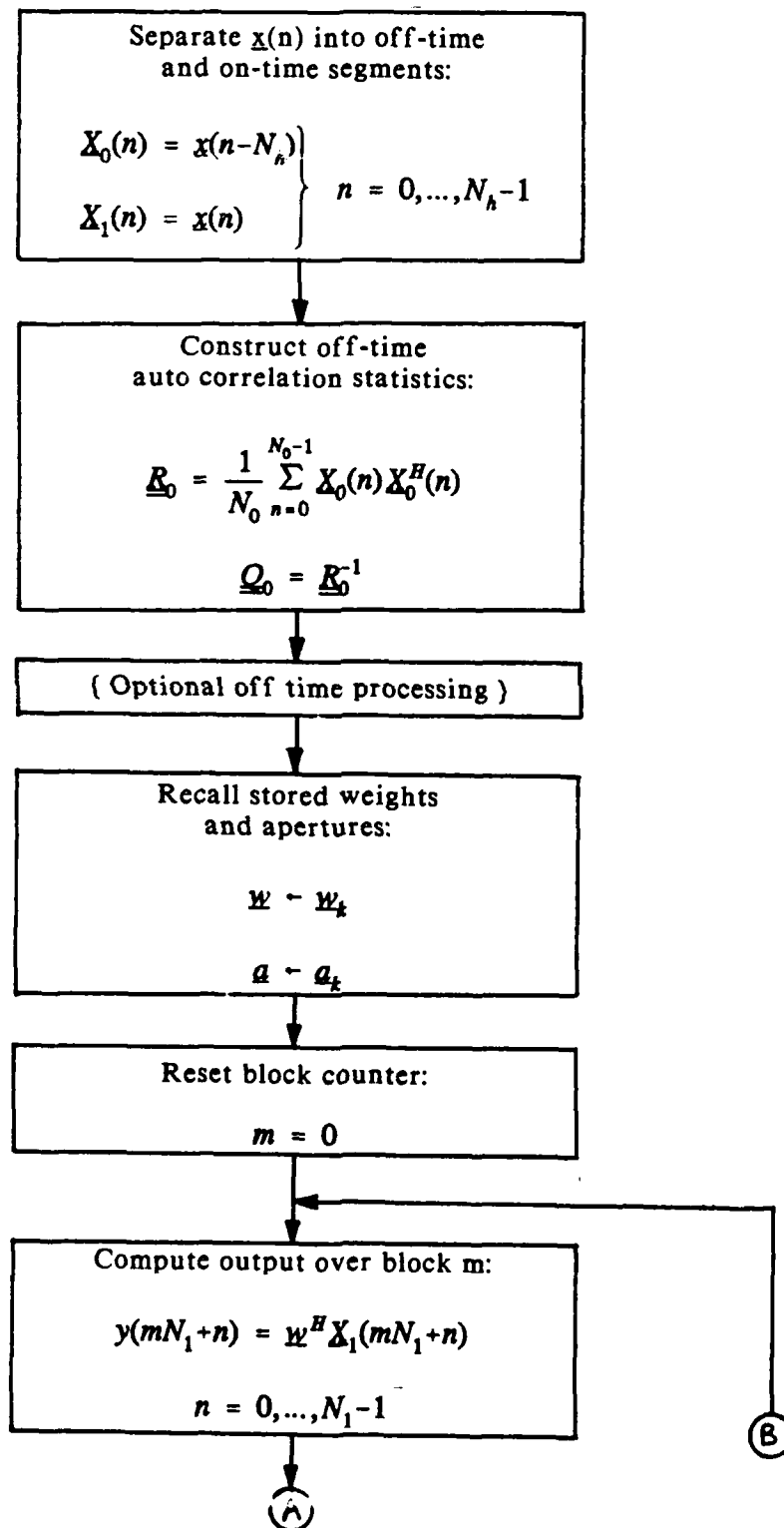


Figure 21(b) Dominant Mode Block Update Implementation Flow Chart

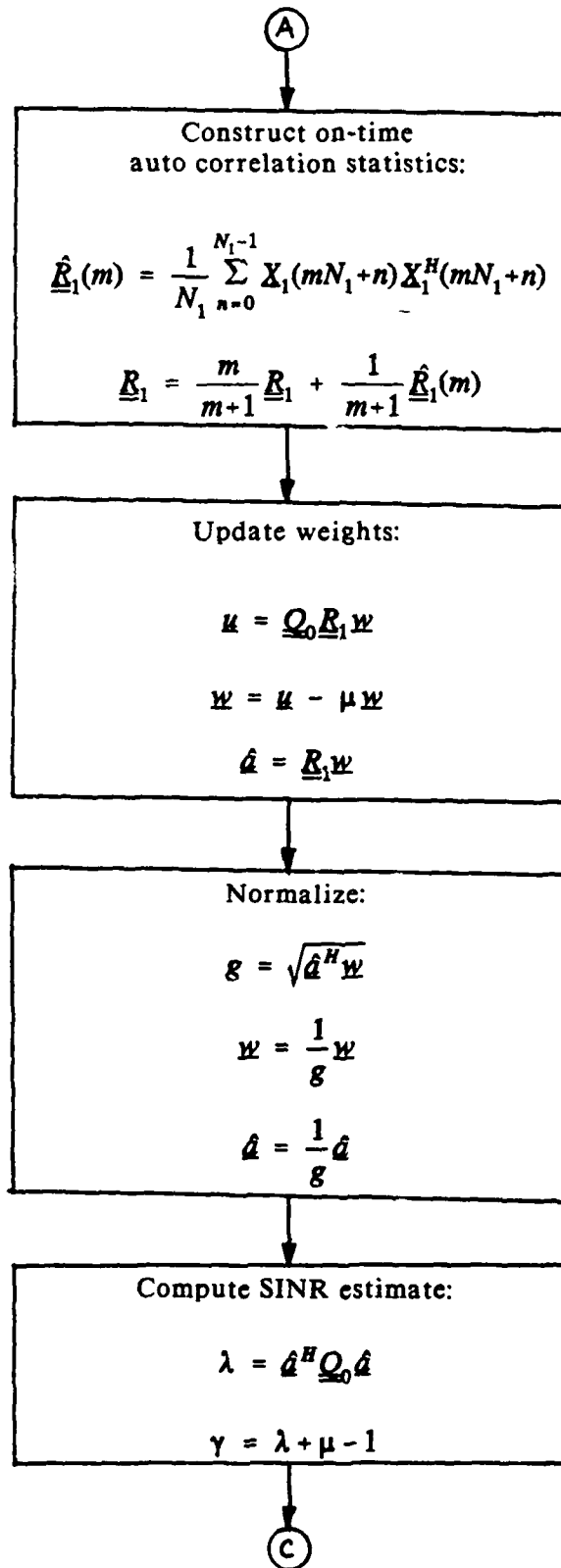
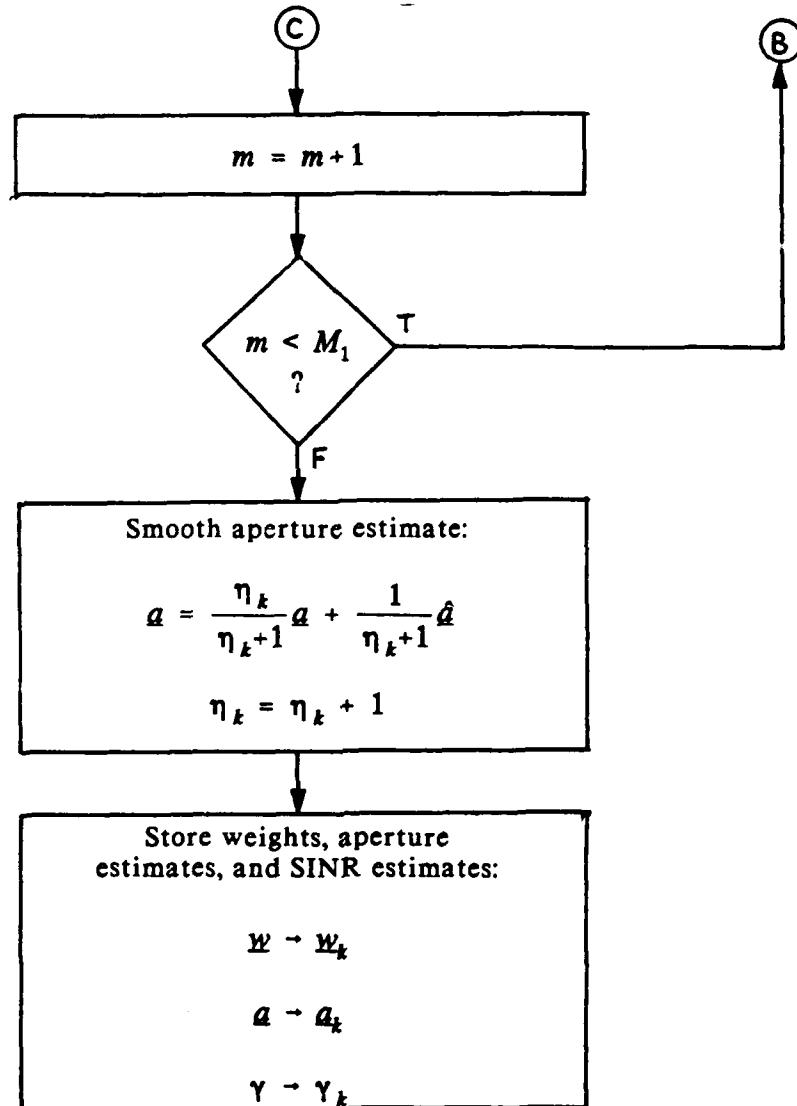


Figure 21(c) Dominant Mode Block Update Implementation Flow Chart



#### 4.3.4.3 SIMULATION RESULTS

In order to evaluate the simulations, a variety of outputs were produced. These include weight vectors, aperture vector (steering vector) estimates, and output signal to interference plus noise ratios (SINR). The weight vectors were used to generate receive antenna patterns which give a visual measure of the effectiveness of the adaptive array processor. The equation used to generate these patterns is:

$$P_k(\theta) = \frac{\mathbf{w}_k^H \mathbf{a}_k^{SOI}(\theta)}{\mathbf{w}_k^H \mathbf{a}_k^{SOI}(\theta_s)}$$

where  $\theta_s$  is the direction of arrival of the SOI. In a similar fashion, the aperture vector estimates were used to generate transmit patterns and radiated power footprints. Recall the calculation of the maximum attainable SINR:

$$SINR_{MAX}(k) = (\mathbf{a}_k^{SOI})^H \mathbf{R}_k^{-1} \mathbf{a}_k^{SOI}$$

$$\mathbf{R}_k = \mathbf{I} + \sum_{i=1}^{L_k} \mathbf{a}_k^{SNOI} (\mathbf{a}_k^{SNOI})^H$$

The output (true) SINR referred to in the following discussion is estimated as:

$$SINR_{OUT}(k) = \frac{|\mathbf{w}_k^H \mathbf{a}_k^{SOI}|^2}{\mathbf{w}_k^H \mathbf{R}_k \mathbf{w}_k}$$

The results of several simulated jammer and array scenarios follows. All of the simulations used the Dominant Mode Block Update algorithm.

##### Receive Adaptation Baseline -

The baseline test cases simulate a 7 element antenna array, with one element in the center and the remaining equally spaced around a circle of diameter  $\lambda_c \sqrt{2}$  (see Figure 28, 7 elements - centered). The scenario for the 5 jammers present in the environment is shown in Figure 22. Parameters not specified are assigned the defaults listed in the tables in section 4.3.4.2.

Figure 23 shows the SINR convergence within individual time slots for the first 12 hops of a pseudo random hop sequence. The sequence of frequency bins appears at the bottom of the figure. The corresponding SINR data (for first visits only) appears in Table 7. One can see the algorithm adapts within the first 3 data blocks for each initial visit to a bin. The jagged line running across the top is the maximum attainable SINR. The maximum attainable SINR varies slightly from bin to bin due to the jammer scenario of the various bins. Upon revisiting a bin,

**Figure 22 Baseline Jammer Scenario**

Jammer	Bin / Frequency (MHz)								
	0	1	2	3	4	5	6	7	
	426	429	432	435	438	441	444	447	
J1: DOA = 30° SJR = -30dB									
J2: DOA = 110° SJR = -30dB									
J3: DOA = 180° SJR = -20dB									
J4: DOA = 235° SJR = -20dB									
J5: DOA = 270° SJR = -20dB									

Jammer Modulations:



Constant Modulus White Noise

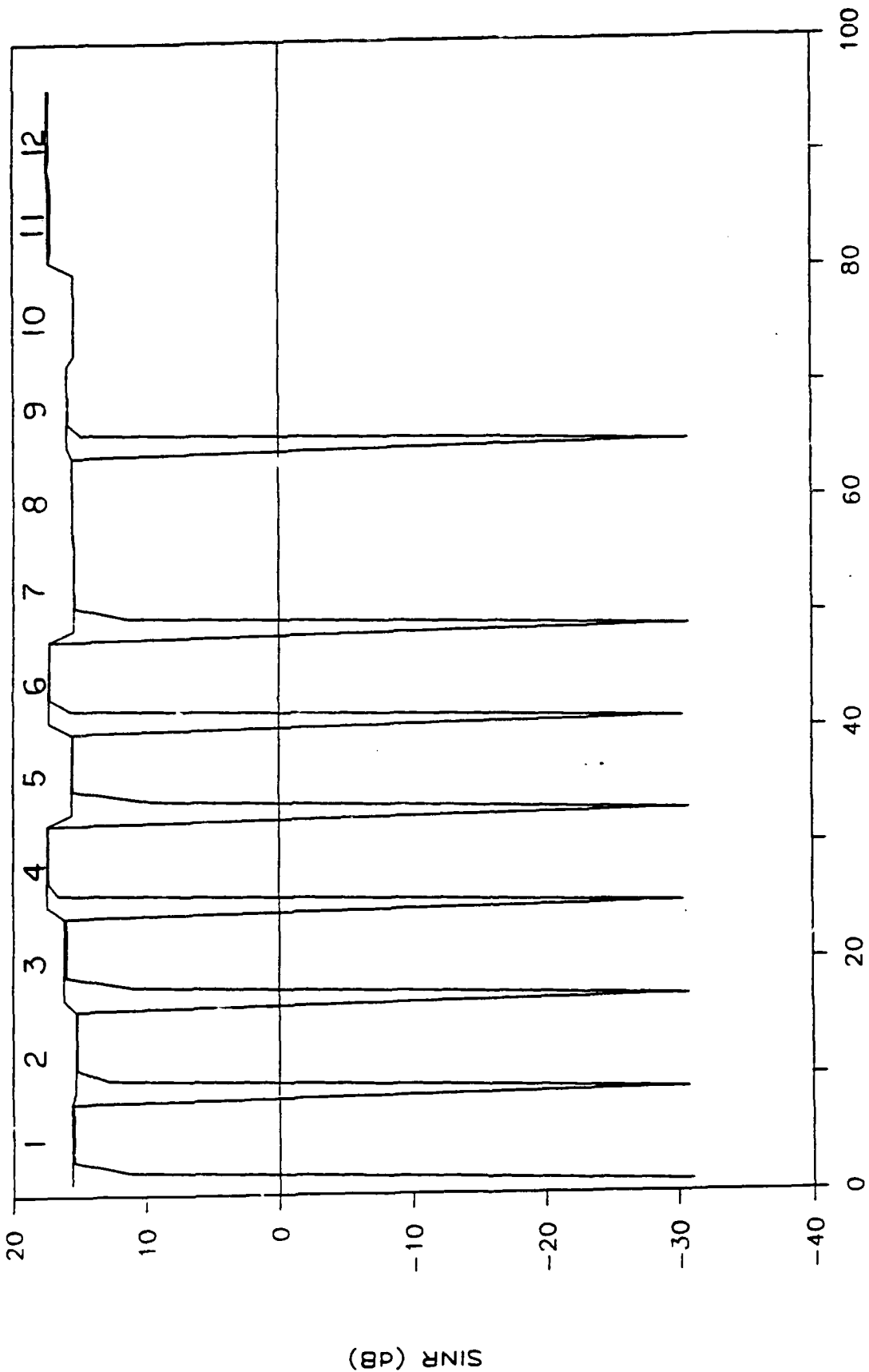


Complex White Gaussian Noise

# SINR VS. TIME

## FIRST 12 TIME SLOTS

Figure 23



DATA BLOCK # (8 PER TIMESLOT)

Time Slot	1	2	3	4	5	6	7	8	9	10	11	12
Freq Bin	5	1	4	0	6	7	2	6	3	2	7	0

**Table 7** Output SINR for initial visit to each frequency bin.

Bin 0		Bin 1		Bin 2		Bin 3	
Blk	SINR (dB)						
0	-30.4	0	-30.8	0	-30.8	0	-30.8
1	16.5	1	12.7	1	11.4	1	14.8
2	17.2	2	15.1	2	15.3	2	15.8
3	17.3	3	15.1	3	15.3	3	15.8
4	17.3	4	15.1	4	15.3	4	15.8
5	17.3	5	15.1	5	15.3	5	15.8
6	17.3	6	15.1	6	15.3	6	15.8
7	17.3	7	15.1	7	15.3	7	15.9
MAX	17.4	MAX	15.2	MAX	15.4	MAX	15.9

Bin 4		Bin 5		Bin 6		Bin 7	
Blk	SINR (dB)						
0	-30.8	0	-31.1	0	-30.8	0	-30.4
1	10.8	1	11.0	1	9.5	1	15.6
2	15.9	2	15.3	2	15.4	2	17.1
3	15.9	3	15.3	3	15.4	3	17.2
4	15.9	4	15.4	4	15.4	4	17.2
5	15.9	5	15.4	5	15.4	5	17.2
6	15.9	6	15.4	6	15.4	6	17.2
7	15.9	7	15.4	7	15.4	7	17.2
MAX	16.1	MAX	15.5	MAX	15.5	MAX	17.3

**Table 8** Output SINR for various jammer levels.

SJR = -10		SJR = -20		SJR = -30		SJR = -40	
Blk	SINR (dB)						
0	-10.0	0	-20.0	0	-30.0	0	-40.0
1	37.5	1	27.2	1	13.9	1	-0.1
2	37.5	2	27.5	2	17.5	2	6.9
3	37.5	3	27.5	3	17.5	3	7.5
4	37.5	4	27.5	4	17.5	4	7.5
5	37.5	5	27.5	5	17.5	5	7.5
6	37.5	6	27.5	6	17.5	6	7.5
7	37.5	7	27.5	7	17.5	7	7.5
MAX	37.5	MAX	27.6	MAX	17.6	MAX	7.6

#### 4.3.4.3 SIMULATION RESULTS (continued)

##### Receive Adaptation Baseline (continued) -

the weights are already adapted to give the maximum attainable SINR (refer to time slots 8, 10, 11 and 12). This is so because the weights are stored and recalled for each frequency bin. The convergence to the optimal weight vector (ie., the maximizing of the SINR) is extremely rapid -- within 96 chips (32 chips per block, 3 blocks).

The antenna patterns for the adapted weight vectors from selected frequency bins appear in Figure 24. The grid lines are spaced 10dB apart. Notice, in each case the nulls are quite sharp and are at least 50dB below the beam in the direction of the SOI.

In order to simulate a communications network such as the EPLRS TDMA, simulations were run where the SOI moved on subsequent visits to various frequency bins. Figure 25 shows the antenna patterns for the first and second visits to frequency bins 1 and 3, with the SOI moving in each case to one of the inadvertent nulls of the first visit. In each case, the weights adapted to produce a beam in the direction of the SOI, while maintaining the nulls in the direction of the jammers. The weights re-converged in less than 3 blocks in all cases tested.

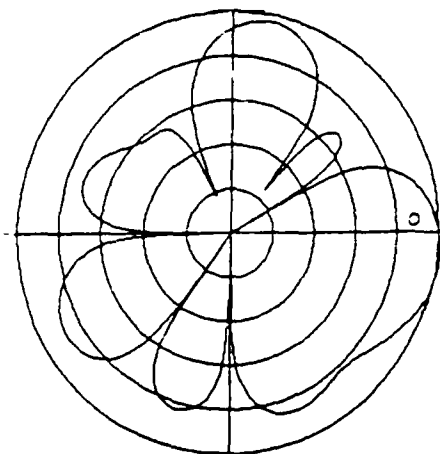
Another situation encountered in network communications is the absence of an SOI. Investigation of the Dominant Mode algorithm reveals that in the absence of an SOI, the off time and on time statistics should be the same ( $R_0 \sim R_1$ ). This implies that the weights should not change since  $w(k+1) = R_0^{-1}R_1w(k) - Iw(k) = w(k)$ . Thus, if the weights were already adapted to the optimal for a particular SOI, and then the SOI disappeared in a subsequent visit to the bin, the weights should not change. In reality, however, the weights will drift because the off time and on time matrices are not identical due to the finite collect time. Figure 26 shows the drift in the antenna patterns during the absence of an SOI in 5 consecutive visits to frequency bin 3. The "SINR" shown in each case is the value obtained from the equation for  $SINR_{OUT}$  above with the same SOI aperture vector as if an SOI were present. As shown in Figure 27, this "SINR" also drifts from the maximum attainable SINR over time. In actual operation, this drift could be stifled by the processor once the loss of the SOI is detected. A way of detecting this is by a significant drop in the value of the dominant mode eigenvalue which is calculated by the Dominant Mode algorithm.

##### Architecture Dependent Simulations -

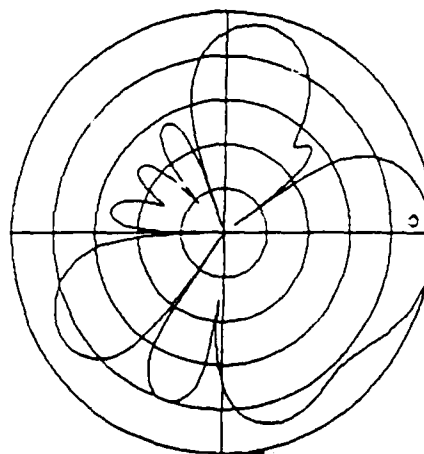
All of the simulations model the off time data as one long block of anticipative data integrated over the entire timeslot. The Dominant Mode Block Update algorithm utilizes the power method with matrices based on smaller blocks of on time data which change from block to block but are statistically similar. This results in a stochastic power method implementation. All of the simulations demonstrate the algorithm to be robust, supporting the validity of this application. Notice, as the collect time (within a block) gets larger (more chips collected) the on time statistical matrices become more constant from block to block. The Dominant Mode algorithm increases the collect time in subsequent blocks within a timeslot by weighted averaging of the previous blocks. This is the smoothing of the on time auto correlation matrix,  $R_1$ , in the algorithm flow chart (Figure 21).

The architecture actually utilizes  $R_{xy1}$  instead of  $R_1w$  for adaptation. This was simulated by suppressing the smoothing mentioned above. This subtle variation did not significantly impact the algorithm's performance. Thus, the architecture only needs to compute the cross correlation between the input and output for the on time statistics.

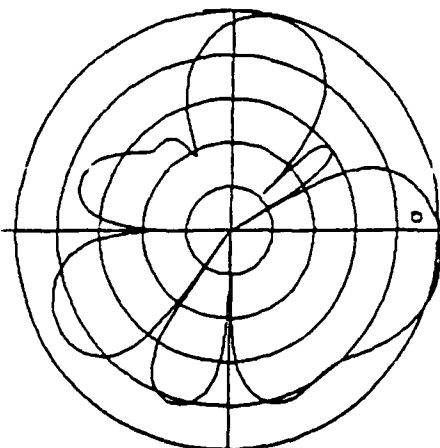
**Figure 24**      **Receive Antenna Patterns for Baseline Simulation**



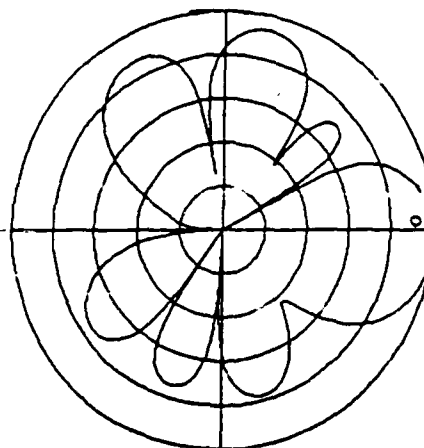
A.    441 MHz (bin 5)  
 J1: 30°, CWG, 30dB  
 J3: 180°, CWG, 20dB  
 J4: 235°, CWG, 20dB  
 J5: 270°, CM, 20dB



B.    429 MHz (bin 1)  
 J2: 110°, CM, 30dB  
 J3: 180°, CWG, 20dB  
 J4: 235°, CWG, 20dB

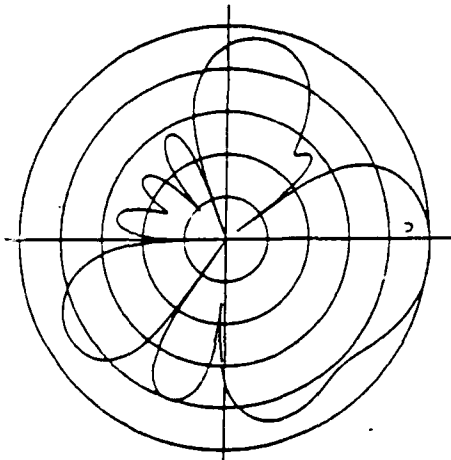


C.    444 MHz (bin 6)  
 J1: 30°, CWG, 30dB  
 J4: 235°, CWG, 20dB  
 J5: 270°, CM, 20dB

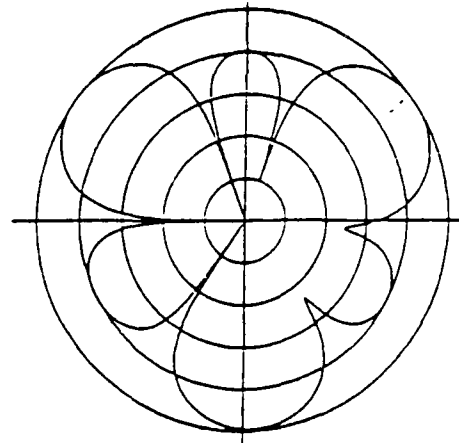


D.    435 MHz (bin 3)  
 J1: 30°, CWG, 30dB  
 J3: 180°, CWG, 20dB  
 J4: 235°, CWG, 20dB

**Figure 25**      **Receive Antenna Patterns for Changing SOI DOA**

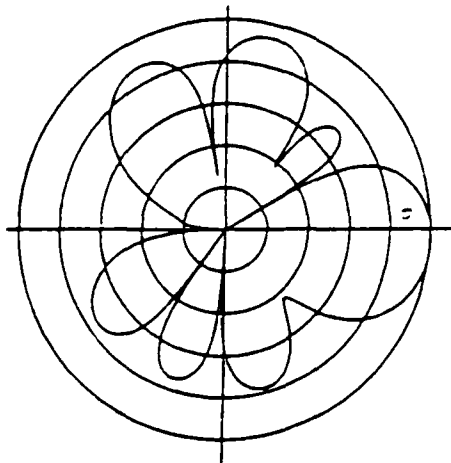


**A. First visit**  
(SOI DOA = 0°)

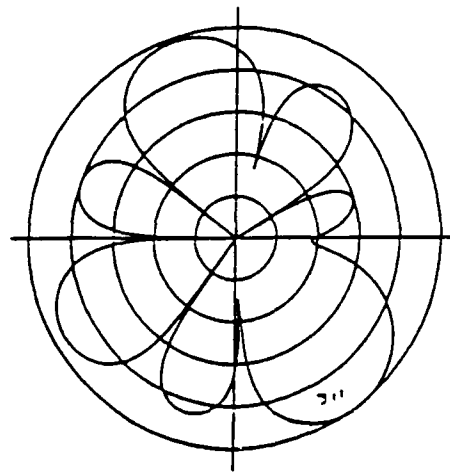


**B. Second visit**  
(SOI DOA = 36°)

429 MHz (bin 1)  
 J2: 110°, CM, 30dB  
 J3: 180°, CWG, 20dB  
 J4: 235°, CWG, 20dB



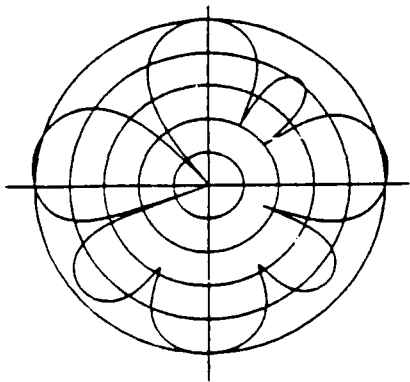
**C. First visit**  
(SOI DOA = 0°)



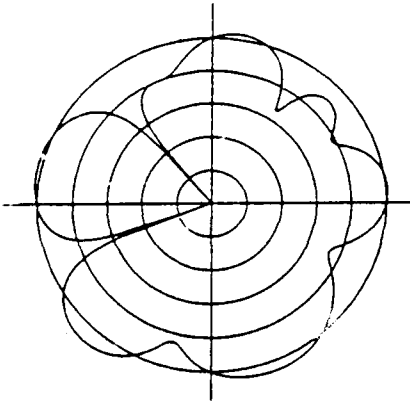
**D. Second visit**  
(SOI DOA = 311°)

435 MHz (bin 3)  
 J1: 30°, CWG, 30dB  
 J3: 180°, CWG, 20dB  
 J4: 235°, CWG, 20dB

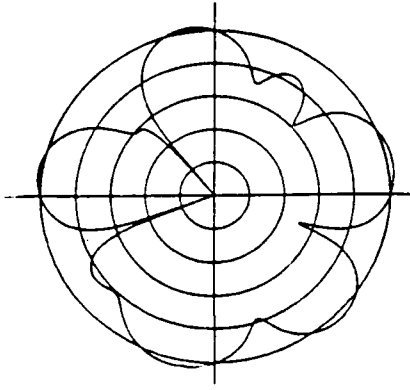
**Figure 26** Antenna Pattern Drift in Absence of SOI (frequency bin 3)



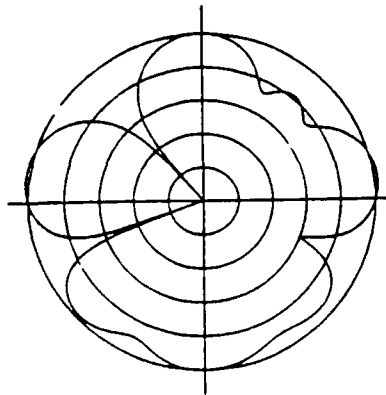
**A. Hop 0 (SOI ON)**  
SINR = 26.8 dB



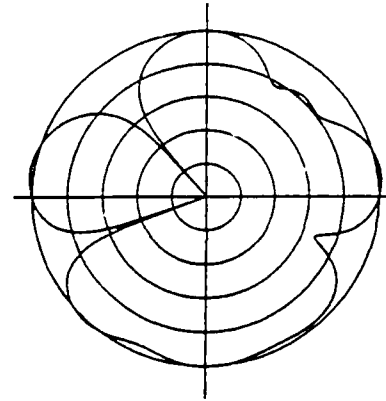
**B. Hop 1 (SOI OFF)**  
"SINR" = 19.4 dB



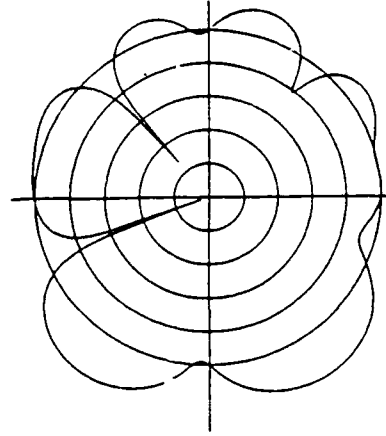
**C. Hop 2 (SOI OFF)**  
"SINR" = 17.6 dB



**D. Hop 3 (SOI OFF)**  
"SINR" = 23.8 dB

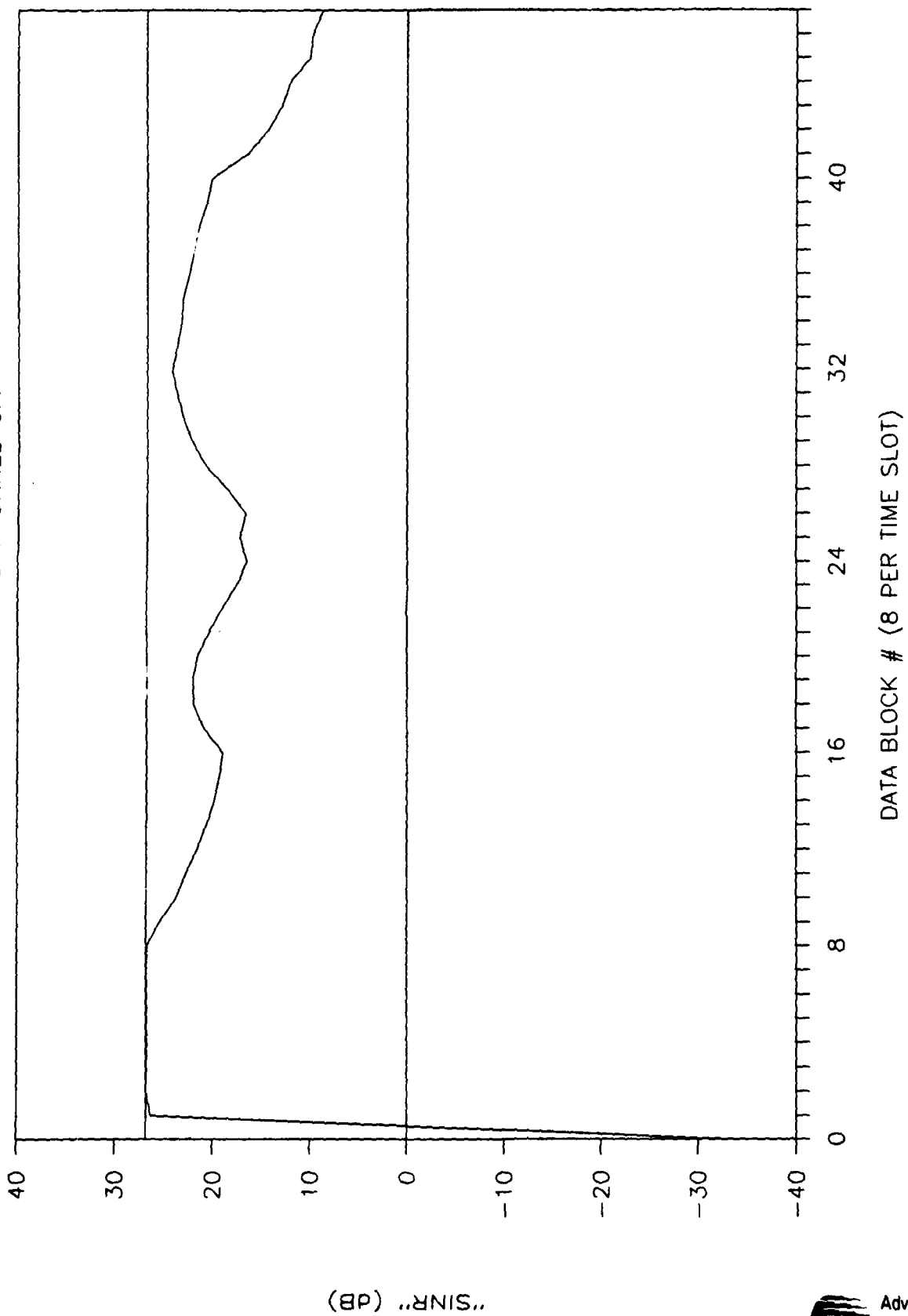


**E. Hop 4 (SOI OFF)**  
"SINR" = 20.7 dB



**F. Hop 5 (SOI OFF)**  
"SINR" = 8.8 dB

**Figure 27**  
"SINR" vs. TIME  
FOR ADAPTATION WITH SOI TURNED OFF



#### 4.3.4.3 SIMULATION RESULTS (continued)

##### Architecture Dependent Simulations -

This technique is not directly applicable to the off time statistics, since the entire off time auto correlation matrix is needed for the Dominant Mode algorithm. A variation of this method was attempted, though. The simulation consisted of building  $\underline{R}_0$  one column at a time by processing the off time data in blocks. Notice, the first column of  $\underline{R}_0$  (denoted  $[\underline{R}_0]_0$ ) is equal to  $\underline{R}_{\underline{X}\underline{Y}0}$  if  $\underline{w} = \underline{e}_0 = [1 \ 0 \ 0 \ \dots \ 0]^T$ , since  $\underline{R}_{\underline{X}\underline{Y}0} = \underline{R}_0 \underline{w}$ . In general, then,  $[\underline{R}_0]_j = \underline{R}_0 \underline{e}_j$ . The variation considered consists of obtaining the first column from the first off time data block by setting  $\underline{w} = \underline{e}_0$ ; the second column from the second block  $\underline{w} = \underline{e}_1$ ; and so on. Thus,  $\underline{R}_0$  would not have to be computed directly, reducing hardware components (and thus, simplifying the architecture). This approach proved invalid over the finite collect time.

In trying to achieve success with this innovative approach, we noticed the resulting matrix had lost some of its most important properties: hermitian and positive definite. An attempt to restore these properties (specifically the hermitian property) did not redeem this approach. These results can be explained by realizing that  $\underline{R}_0$  is not the same from block to block. The statistics from block to block are similar, but, only if a large enough number of samples are used would the matrices begin to be constant. The relation between this convergence and the number of samples used per block is approximately  $(1/\sqrt{n})$ . Thus, with a finite number of samples collected the various columns will not combine to give a functional estimate of the off time statistics,  $\underline{R}_0$ .

An important result is the overall effectiveness of storing and recalling weights from hop to hop. The storage table consists of a weight vector for each frequency bin. This provides for immediate SOI recovery in subsequent visits to a particular frequency bin, as long as the RF environment has not changed significantly. Additionally, storing and recalling weights for separate frequency bins provides very effective frequency compensation. This result was illustrated in Figure 23, where the SINR of a revisited bin begins with nearly the maximum attainable value because of convergence during the previous visit.

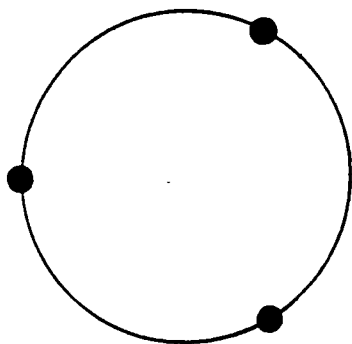
##### Antenna Geometry and Spacing -

The effects of the antenna array geometry and spacing were investigated in this simulation. This includes: varying number of elements; varying geometry of arrays; and varying the spacing of the elements. We examined the performance with 3, 4, 5, and 7 elements. For the 4 and 7 element arrays, the effect of changing the geometry was studied. Specifically, one geometry consisted of having one element in the center, with all remaining elements on the circumference of a circle; the other placed all elements on the circumference. In this simulation, all of the array diameters are  $\sqrt{2}\lambda_c$ . See Figure 28 for the array geometries. The effect of varying the spacing of the elements was performed for the 4 element array, with all of the elements on the circumference of a circle. The diameters compared are:  $\lambda_c$ ,  $\sqrt{2}\lambda_c$ ,  $2\lambda_c$ , and  $2\sqrt{2}\lambda_c$ .

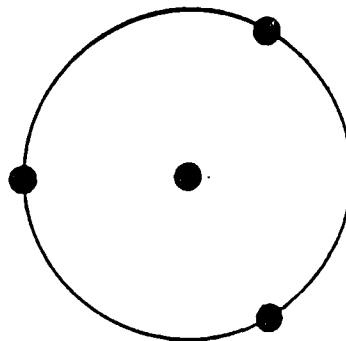
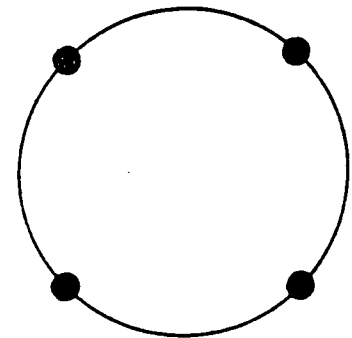
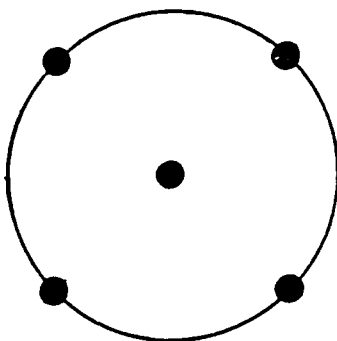
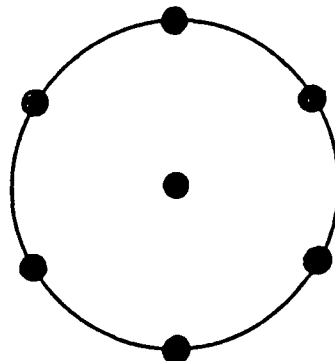
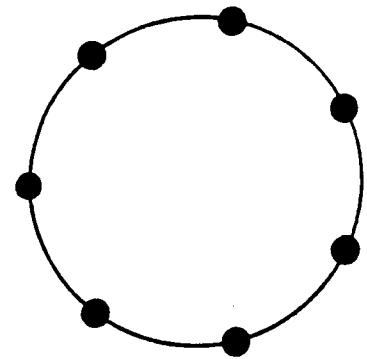
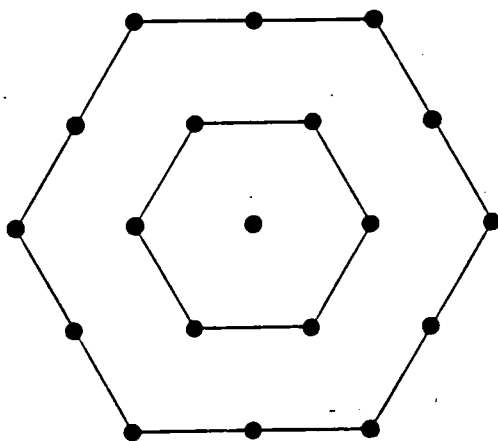
The jammer scenario for each of these simulations is the same. Each simulation was forced to take place in frequency bin 3. Only one timeslot was visited (8 blocks). There were two jammers present in frequency bin 3 for these simulations:  $40^\circ$  and  $110^\circ$ , SJR = -20dB for both.

Figure 28

## Antenna Array Geometries



3 elements

4 elements  
centered4 elements  
non-centered5 elements  
centered7 elements  
centered7 elements  
non-centered19 elements  
hexagonal

#### 4.3.4.3 SIMULATION RESULTS (continued)

##### Antenna Geometry and Spacing (continued) -

Figure 29 shows the antenna patterns for the various number of elements and geometries. Notice the improvement of the antenna patterns as the number of elements increases. There is not a significant improvement, though, between the non-centered 4 element case and the centered 5 element case, nor between the 3 element case and the centered 4 element case. The non-centered 4 element case outperformed the centered 4 element case in this scenario. The centered 7 element case, on the other hand, appears to be a more favorable pattern than the non-centered 7 element case. These results are highly dependent on angles of arrival of the SOI and SNOIs, however, and are not conclusive. The model exists for future exploration.

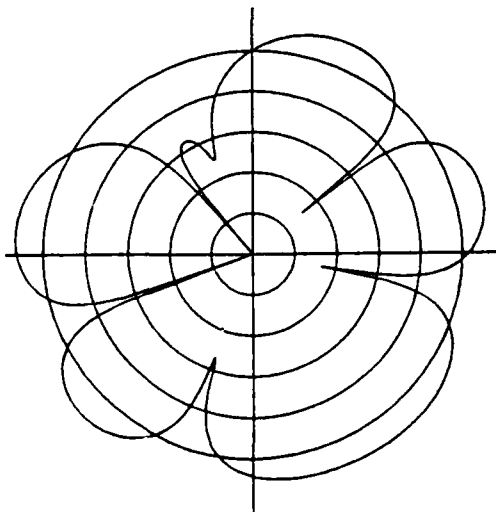
Figure 30 shows the antenna patterns for the various array diameters. The most favorable pattern appears to be the one corresponding to a diameter of  $\sqrt{2}\lambda_c$ . Notice, as expected, the number of inadvertent nulls increases as the diameter increases.

##### Varving Jammer Levels -

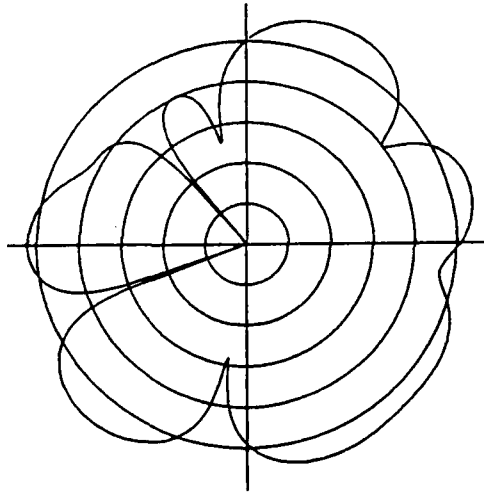
The effect of varying the jammer levels was also studied. The antenna geometry chosen for this simulation was the 4 element, non-centered array, with diameter  $\sqrt{2}\lambda_c$ . Jammer levels (SJR) of -10dB, -20dB, -30dB, and -40dB were studied for a single jammer present in frequency bin 3 with a direction of arrival of 40°. Only one timeslot was processed (8 blocks). Output SINR at the start of each block is listed for each jammer level in Table 8. Maximum attainable SINR is included at the end of each list for comparison. A plot showing the convergence time of the output SINR's, normalized to the corresponding maximum attainable SINR in each case, appears in Figure 31. Notice the weaker jammers are nulled out slightly more quickly than the higher level jammers. In each case, though, the weights still converge within 3 block updates. Actually, the weights adapted within 2 block updates for the weaker jammer levels -- that is, all but SJR = -40dB.

One test performed on the SJR = -40dB case provided quicker adaptation -- within 2 blocks. This simulation set the factor for accelerated convergence,  $\mu$ , equal to 1.0.

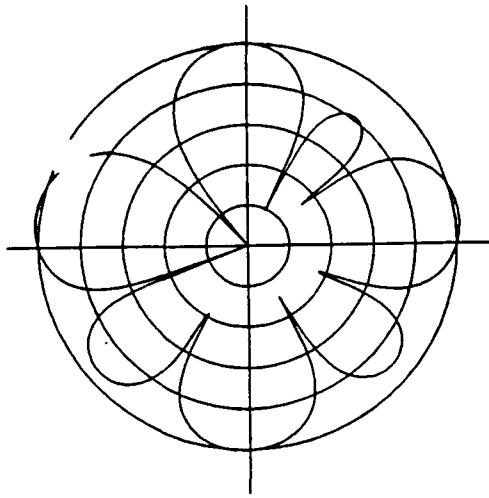
**Figure 29** RECEIVE ANTENNA PATTERNS vs. NUMBER OF ELEMENTS  
 (DIAMETER OF ANTENNA ARRAYS =  $\lambda_c * \sqrt{2}$ )



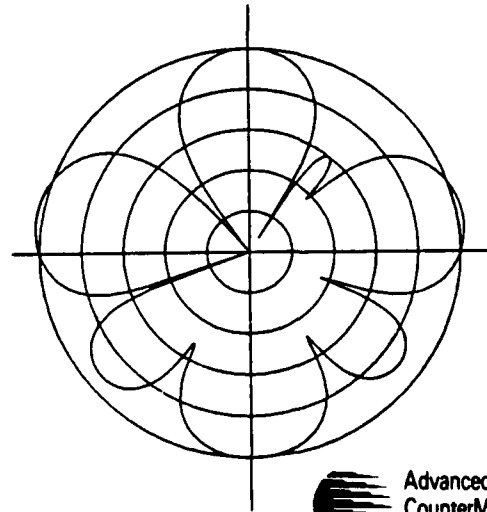
**3 ELEMENTS**



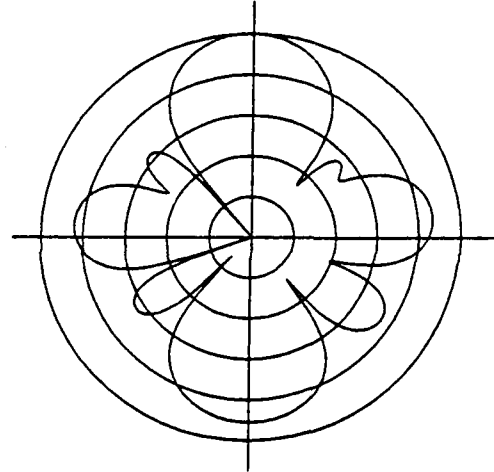
**4 ELEMENTS  
 CENTERED**



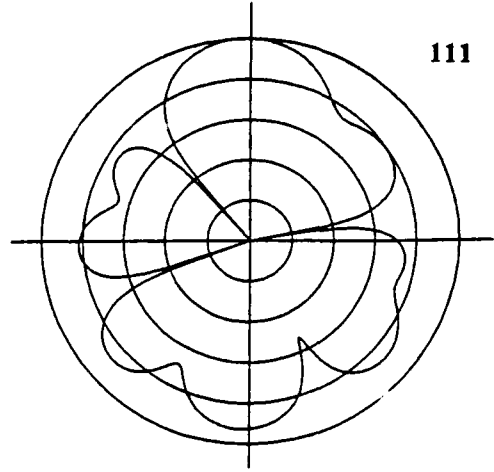
**4 ELEMENTS  
 NON-CENTERED**



**5 ELEMENTS  
 CENTERED**



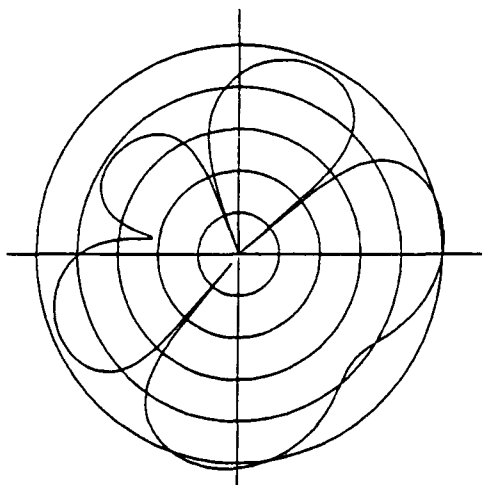
**7 ELEMENTS  
 CENTERED**



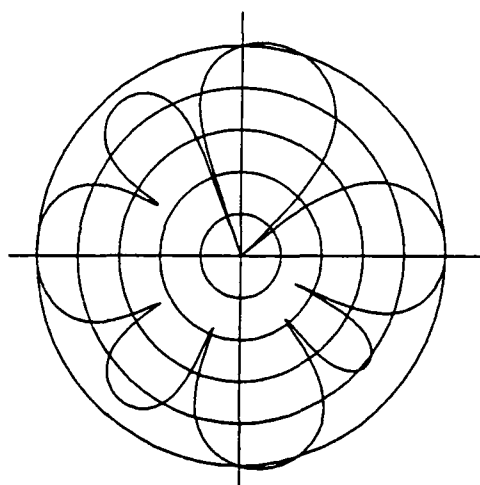
**7 ELEMENTS  
 NON-CENTERED**



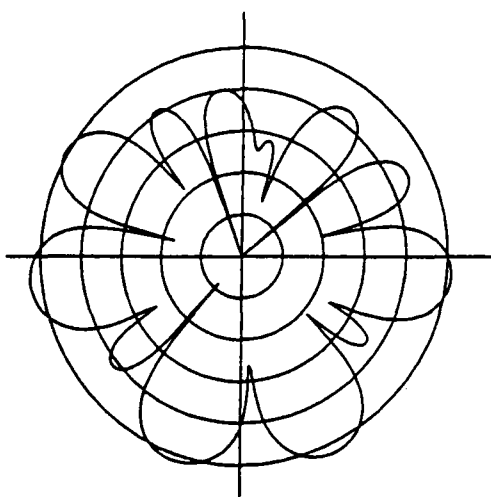
**Figure 30**      **RECEIVE ANTENNA PATTERNS vs. ARRAY DIAMETER**  
**(4 ELEMENT ANTENNA ARRAY)**



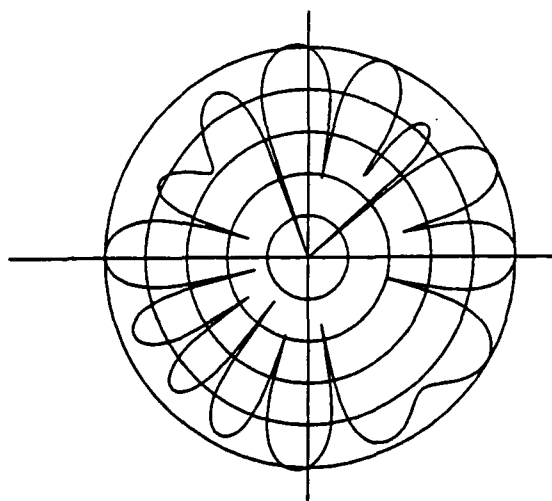
DIAMETER =  $\lambda_c$



DIAMETER =  $\lambda_c * \sqrt{2}$



DIAMETER =  $\lambda_c * 2$



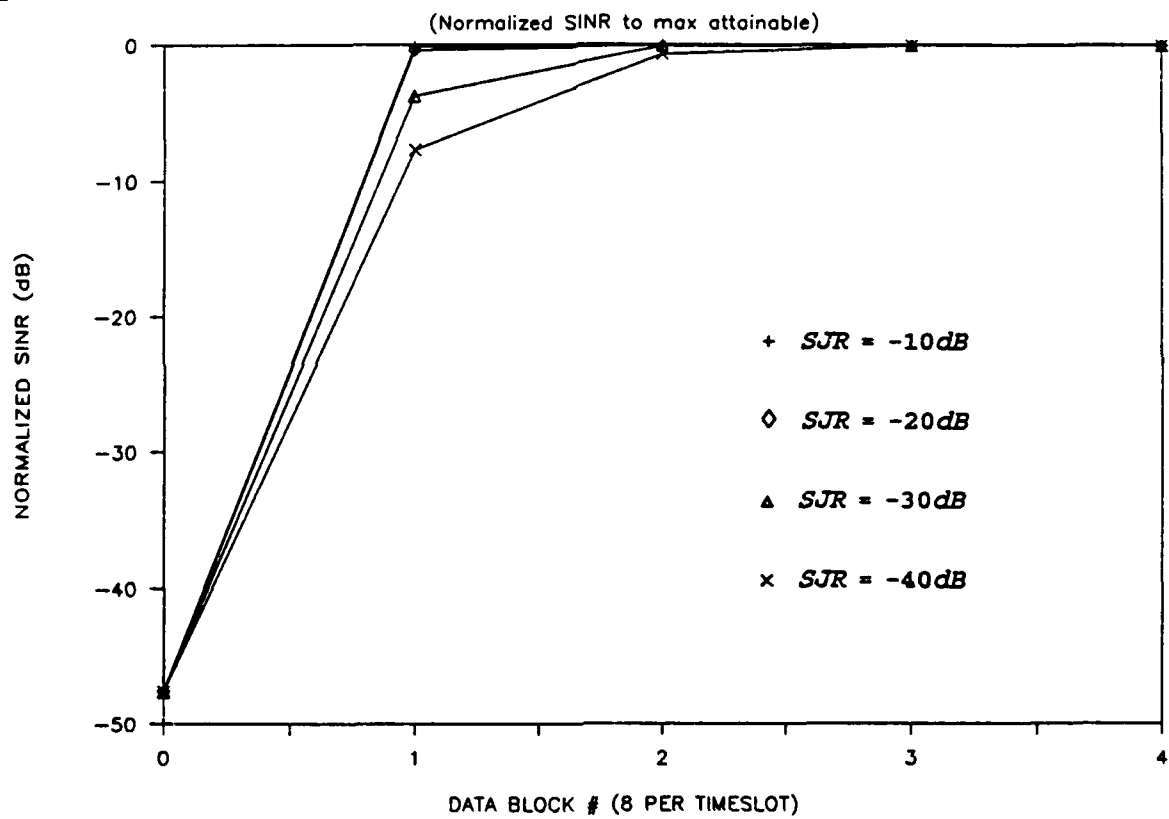
DIAMETER =  $\lambda_c * 2\sqrt{2}$

**Table 8**            **Output SINR for various jammer levels.**

SJR = -10		SJR = -20		SJR = -30		SJR = -40	
Blk	SINR (dB)						
0	-10.0	0	-20.0	0	-30.0	0	-40.0
1	37.5	1	27.2	1	13.9	1	-0.1
2	37.5	2	27.5	2	17.5	2	6.9
3	37.5	3	27.5	3	17.5	3	7.5
4	37.5	4	27.5	4	17.5	4	7.5
5	37.5	5	27.5	5	17.5	5	7.5
6	37.5	6	27.5	6	17.5	6	7.5
7	37.5	7	27.5	7	17.5	7	7.5
MAX	37.5	MAX	27.6	MAX	17.6	MAX	7.6

Figure 31

## CONVERGENCE TIME vs. JAMMER LEVEL



#### 4.3.4.3 SIMULATION RESULTS (continued)

##### Directive Communications, Antenna Patterns -

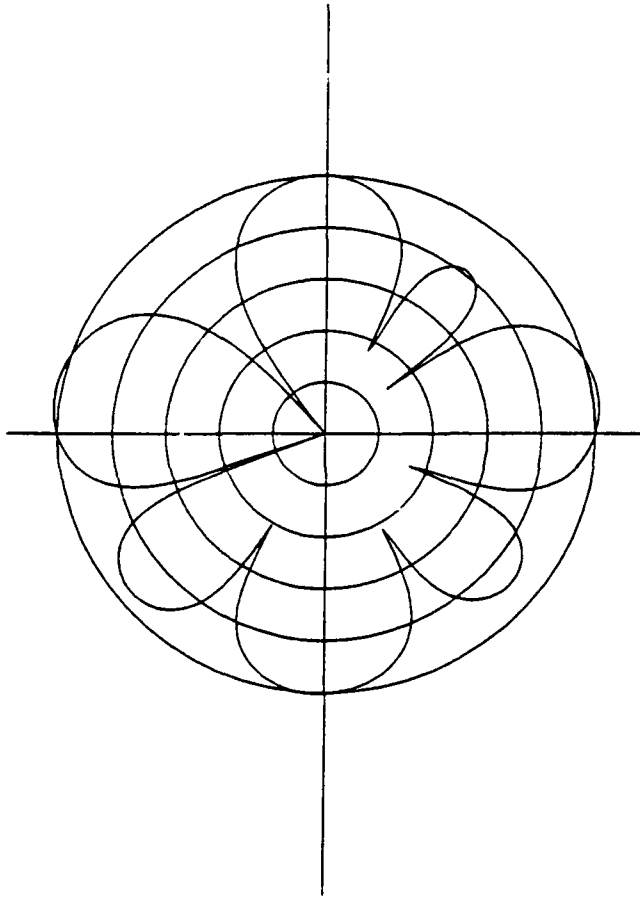
Retrodirective and directive antenna patterns were generated using the weights and aperture estimates. For the 4 element array which is non-centered with diameter  $\sqrt{2}\lambda_c$ , the receive antenna pattern, retrodirective antenna pattern, and retrodirective radiated power footprint are shown in Figure 32. In this figure, the antenna pattern grids are 10dB increments. The power footprints have a linear scale, and are normalized to the transmit direction of  $0^\circ$  (angle of intended receiver).

The antenna patterns and radiated power footprints in Figure 33 are for directive transmissions using different amounts of smoothing applied to the apertures. Here smoothing means each aperture estimate in subsequent visit to a particular frequency bin is incorporated into an on-going average of all prior aperture estimates in that bin (see Dominant Mode Block Update algorithm flow chart). The patterns clearly improve with more smoothing (more timeslots used to average). The ideal patterns were generated using the known apertures calculated in the Simulation Description, section 4.3.4.2, and are included for comparison.

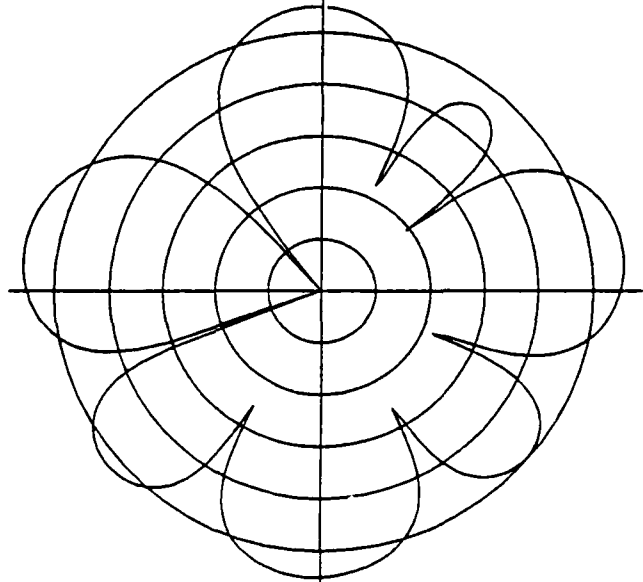
For each of the above cases, two jammers were present (simulation is of frequency bin 3). The arrival directions are  $40^\circ$  and  $110^\circ$ , and the SJR is -20dB for both.

Directive transmit patterns should improve when more elements are used. Simulation results shown in Figure 34 demonstrate this for 4, 7, and 19 elements. These patterns were generated using the known apertures. See Figure 28 for the geometry of the 19 element array. The intended receiver is assumed to be at  $0^\circ$  in all of the transmit cases analyzed.

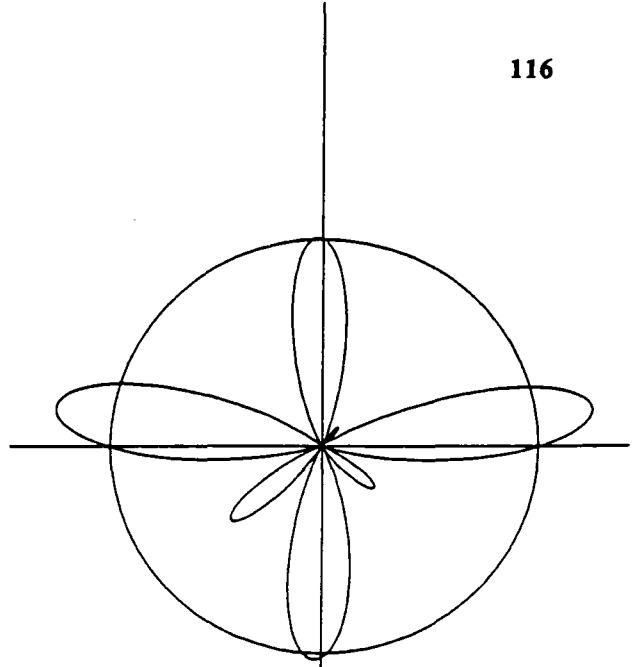
**Figure 32** 4 ELEMENT ANTENNA RECEIVE AND RETRODIRECTIVE TRANSMIT PATTERNS



**RECEIVE ANTENNA PATTERN**



**TRANSMIT ANTENNA PATTERN**

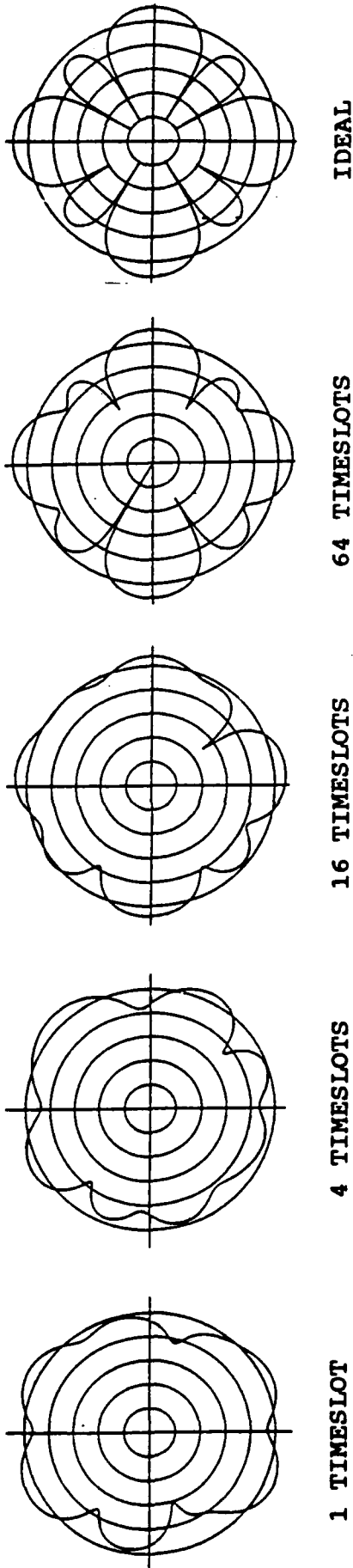


**TRANSMIT POWER FOOTPRINT**

**Figure 33**

**4 ELEMENT ANTENNA ARRAY  
(SMOOTHING APERTURE ESTIMATES)**

**DIRECTIVE TRANSMIT ANTENNA PATTERNS**



**DIRECTIVE TRANSMIT POWER FOOTPRINTS**

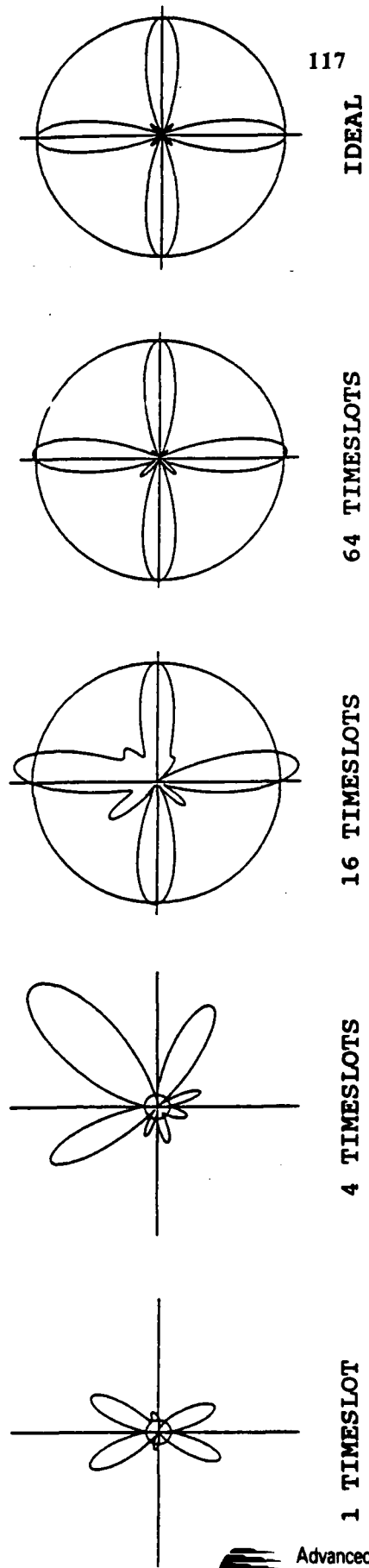
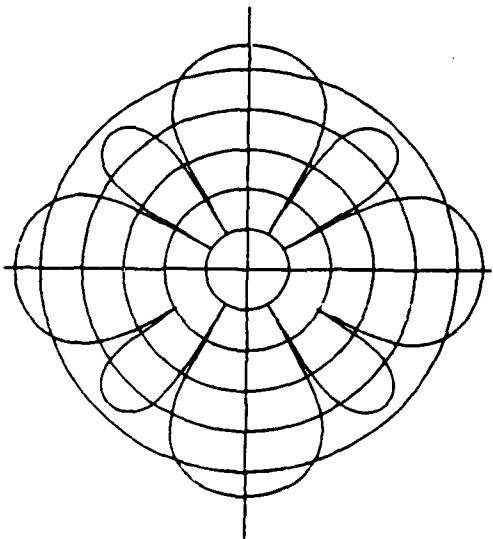


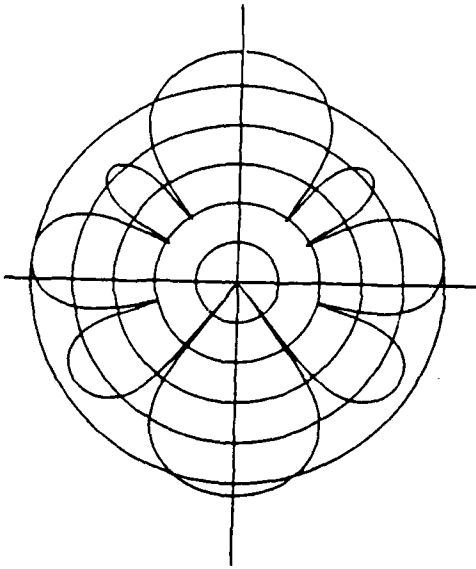
**Figure 34**

**DIRECTIVE TRANSMIT vs. NUMBER OF ELEMENTS**

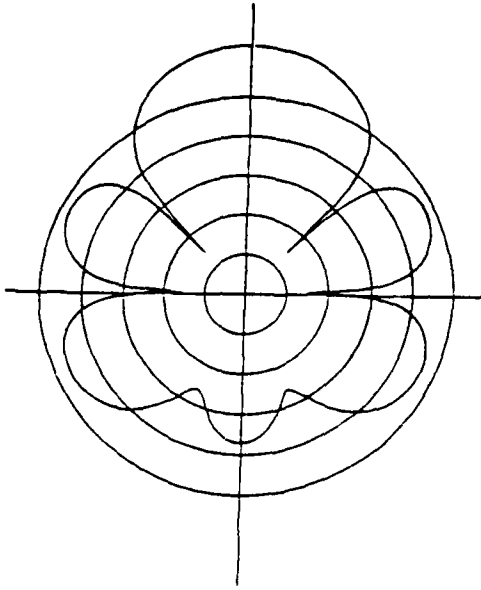
**DIRECTIVE TRANSMIT ANTENNA PATTERNS**



**4 ELEMENTS**

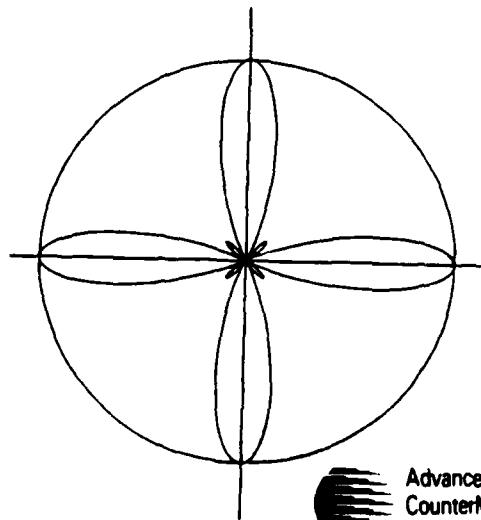


**7 ELEMENTS**

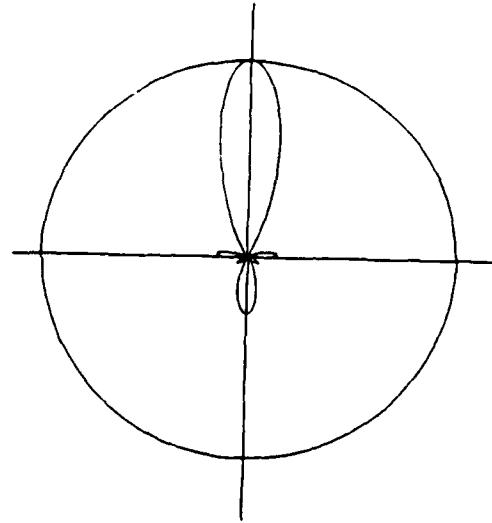


**19 ELEMENTS**

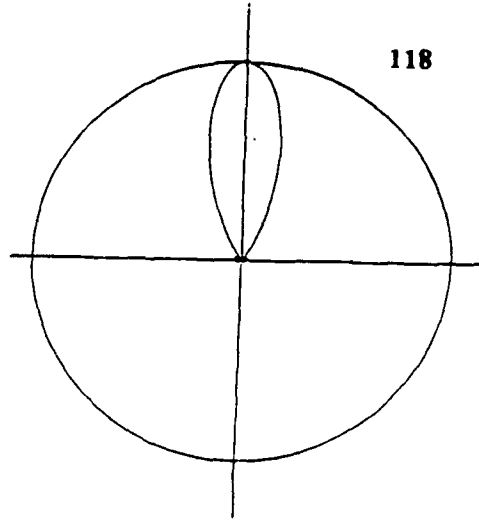
**DIRECTIVE TRANSMIT POWER FOOTPRINTS**



**4 ELEMENTS**



**7 ELEMENTS**



**118**

**19 ELEMENTS**

#### 4.3.4.3 SIMULATION RESULTS (continued)

##### Directive Communications, LPI -

The application of directive communications to an LPI system is described in sections 4.3.2.7 and 4.3.2.8. The results of the corresponding performance simulations are presented here.

Figure 35 shows a set of intercept footprints for four antenna arrays. Each set includes three cases: 1) both the receive and transmit arrays having isotropic antenna patterns (this is the baseline situation, provided for reference), 2) the receive array having an adapted pattern but the transmit array having an isotropic pattern, and 3) the receive array having an adapted pattern and the transmit array providing directive transmissions. The dramatic reduction in intercept footprint areas is evident in the shadings which represent these three situations.

The first example is a four element array with the sensors located on the circumference of a circle. In this case, the transmitter - receiver link is positioned relative to the array geometry such that virtually the largest possible intercept footprint results.

The second example shows the same array rotated 45 degrees. The resulting intercept footprint area drops significantly.

The third example also simulates a four element array, except in this case one of the sensors is located in the center of the array.

The fourth example is a seven element array. The expected reduction in intercept footprint area as the number of elements is increased is demonstrated by comparison of this example to the examples of the four element arrays.

The dependence of this area on the number of elements is further illustrated in figure 36, which shows the footprint area reduction versus the receiver to transmitter link direction for some of the examples.

##### Directive Communications, A/J -

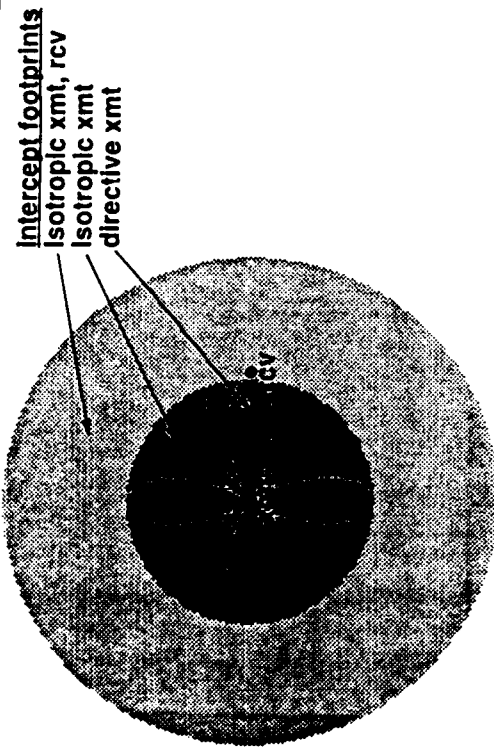
The application of directive communications to an A/J system is described in sections 4.3.2.7 and 4.3.2.8. The results of the corresponding performance simulations are presented here.

Figure 37 shows the A/J jammer footprints of the same arrays discussed above. The same situations are represented: 1) both the receive and transmit arrays having isotropic antenna patterns (this is the baseline situation, provided for reference), 2) the receive array having an adapted pattern but the transmit array having an isotropic pattern, and 3) the receive array having an adapted pattern and the transmit array providing directive transmissions. Again, the shadings illustrate the dramatic reduction in jammer footprint areas for these three situations.

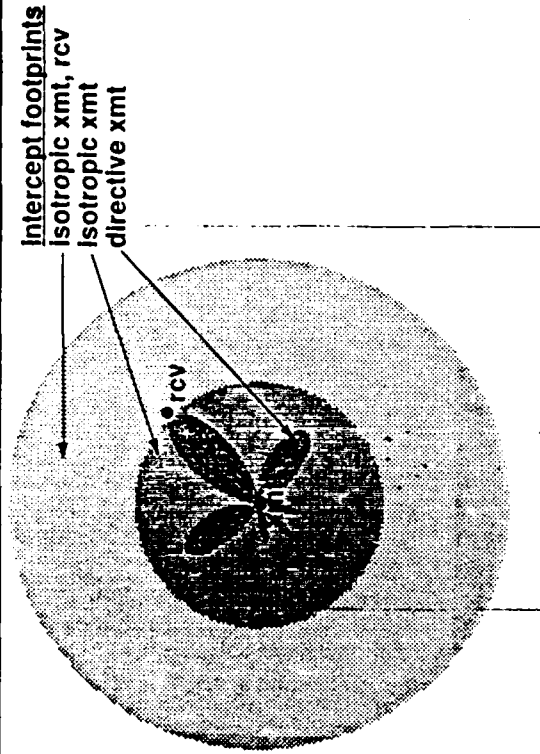
The first plot uses the four element array, all sensors on the circumference, with the array rotated 45 degrees from the original case. The second plot uses the four element array with one sensor at its center. The third plot represents the seven element array.

The areas are greatly reduced, and are difficult to see without changing scale. A close-up view of the critical areas for each of the previous three plots are shown in the fourth plot. Again, the dependence upon the number of elements in the array is demonstrated.

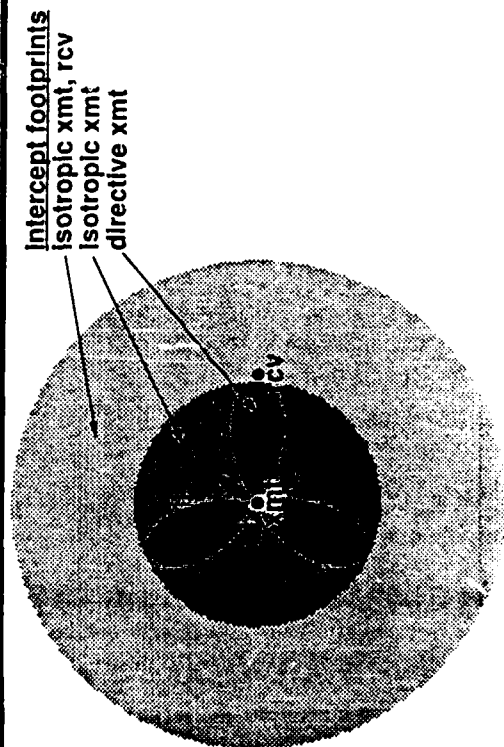
**Intercept Footprint,  
4-Element Circular Array**



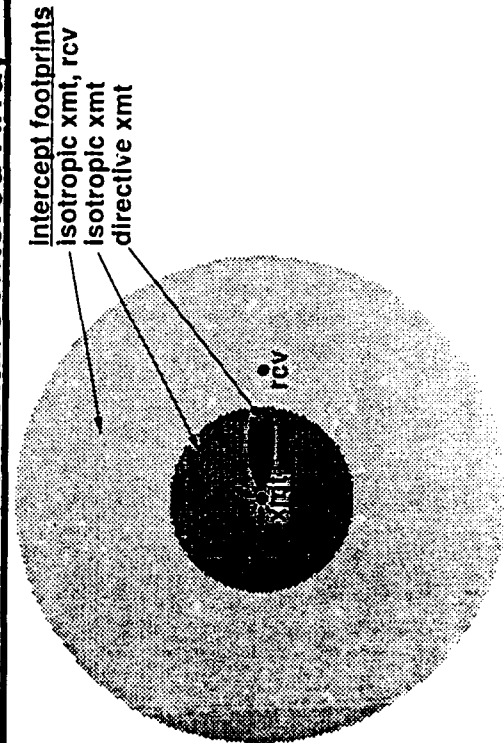
**Intercept Footprint, Same Array,  
45° Receiver Direction**



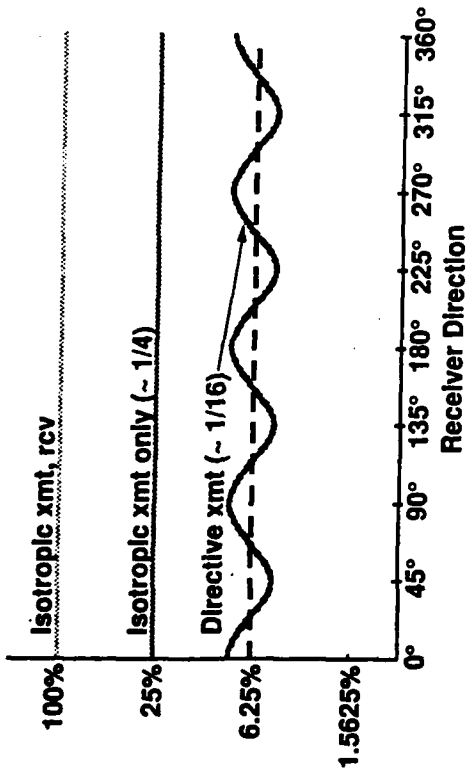
**Intercept Footprint,  
4-Element Circular/Centered Array**



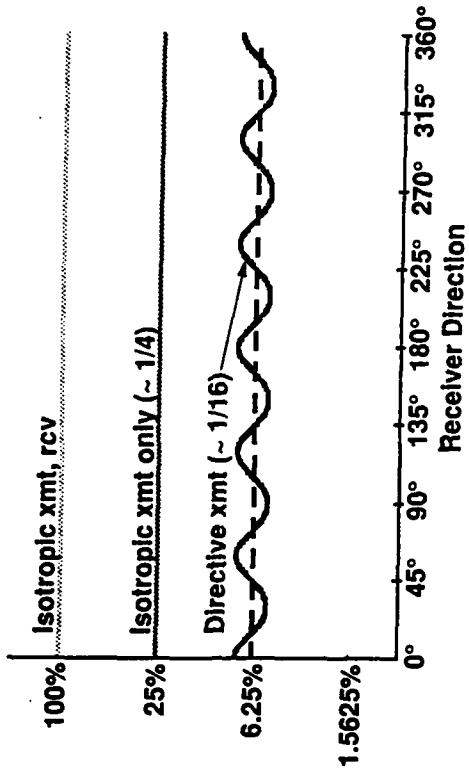
**Intercept Footprint,  
7-Element Circular/Centered Array**



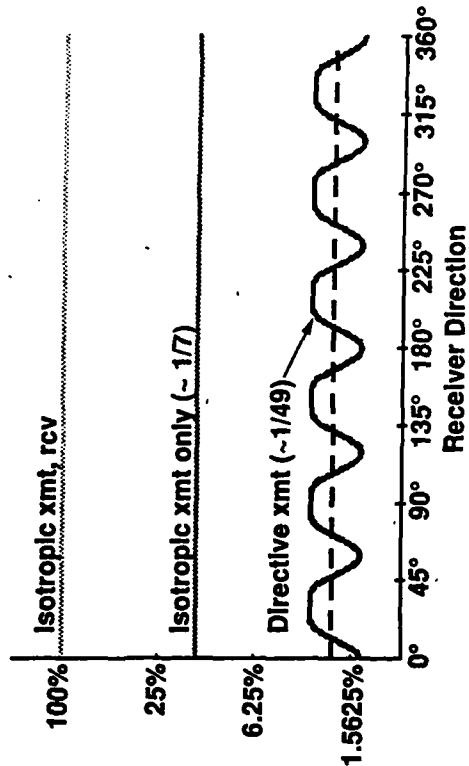
### Footprint Reduction vs. Rcvr Direction, 4-Element Circular Array



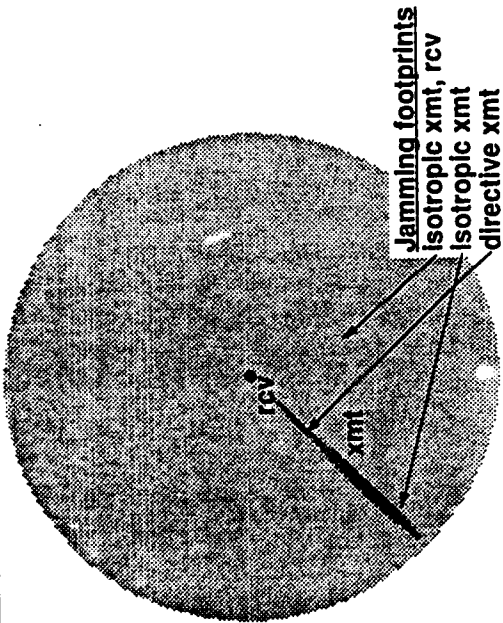
### Footprint Reduction vs. Rcvr Direction, 4-Element Circular/Centered Array



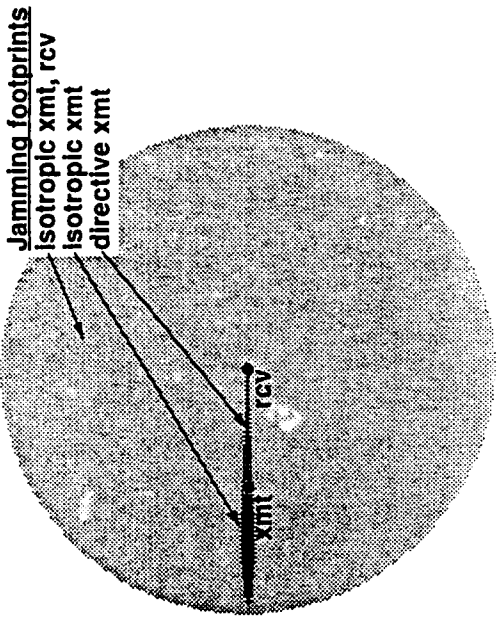
### Footprint Reduction vs. Rcvr Direction, 7-Element Circular/Centered Array



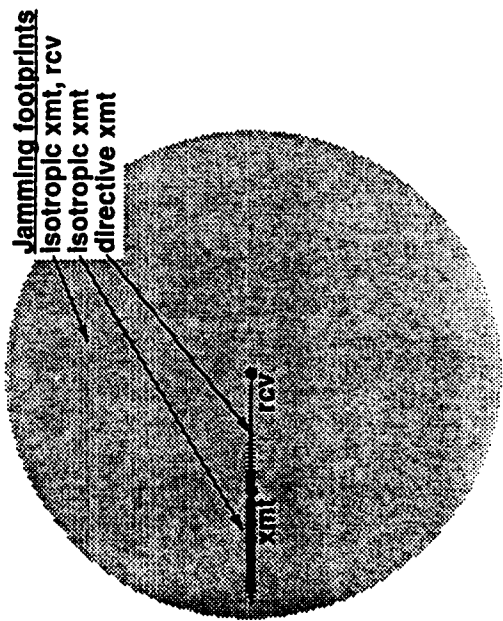
### Jamming Footprint, Same Array, 45° Receiver Direction



### Jamming Footprint, 4-Element Circular/Centered Array



### Jamming Footprint, 7-Element Circular/Centered Array



### Expansions of Jamming Footprints

- 4-element circular array
- 4-element circular/centered array
- 7 element circular/centered array

### 4.3.5 DOCUMENTATION

This Phase I SBIR effort has been well documented since the program's inception. Monthly reports, formally delivered to the Contracting Officer and informally to other technical representatives from the Government, have provided regular status reporting of technical accomplishments and cost / schedule issues. Five monthly reports have been provided, due the 20th of each month from September 1990 to January 1991. The last deliverable requirement of this SBIR program is this final report.

In addition to these reports, a proposal for a follow-on Phase II effort was submitted. This proposal is entitled "A Multi-Purpose Adaptive Array Processor Hardware Development for Frequency Hopped, Direct Sequence Spread Spectrum Radios" and is dated January 7, 1991.

## 4.4 ESTIMATES OF TECHNICAL FEASIBILITY / PERFORMANCE EVALUATIONS

### 4.4.1 INTRODUCTION

This study has addressed the application of adaptive array processing to ground based Army tactical radios. It was organized into three main tasks: algorithm development, architecture development, and computer modeling and performance simulation. The technical feasibility of the algorithm and architecture are discussed, and the results of the performance simulations are evaluated below.

### 4.4.2 ALGORITHM TECHNICAL FEASIBILITY

The algorithm developed under this study is the Dominant Mode Block Update algorithm. Its feasibility and application to FHSS and DSSS Army radios has been proven by derivation, a convergence and stability analysis, and performance analysis, and has been demonstrated by computer simulation.

The algorithm developed provides flexibility for customization to a specific communication network. The method for data collection is not entirely dictated by the algorithm; for example, the period or band that the off time data is acquired from can vary depending on the application. The equation which generates updates of the weight estimates can be implemented using on time data in vector ( $R_{xy}$ ) or matrix ( $R_1$ ) form. Monitoring critical points within the AAP and calculation of key parameters will allow modification to the adaptive process depending on the jamming scenario. For example, if on time data suggests that no SOI is present, the algorithm may cease adaptation and hold the weights at their last valid state. The signal levels internal to the AAP could be monitored and adjusted for optimal adaptation performance. The algorithm could adjust the variables which affect convergence time depending on the data collected, such as changing the value of  $u$  in the power method matrix  $A = R_0^{-1}R_1 - uI$ . If a specific Army radio is identified for operation with an AAP employing this algorithm, many operational features of the algorithm could be tailored to achieve specific goals.

The application of AAP to directive and retrodirective communications was addressed as well. Figures of merit for a fully adapted (receive and transmit) AAP system were identified for LPI and A/J applications: intercept footprint and maximum receiver input power, respectively. The analysis shows these figures of merit to be greatly improved over an isotropic communication system and to nearly approximate the optimal performance.

#### 4.4.3 ARCHITECTURE TECHNICAL FEASIBILITY

The feasibility of the architecture developed in this study is heavily supported in the architecture section of this report. That section includes examples of how every element of the AAP could be implemented in hardware; in many cases multiple implementations are available and the merits of those options are discussed. Examples of AAP elements and methods of implementation are given below:

- The complex weights could be implemented at RF, IF or baseband. If realized at baseband, digital or analog circuits could be used. The weights could be set using magnitude and phase adjustments or in-phase and quadrature adjustments. The suggested implementation is at RF (or IF, depending on application), with in-phase and quadrature adjustments.

- The statistical measurement circuits could be based on RF, IF or baseband multiplications; the sampled baseband data could be forwarded to a digital calculator which determines the signal statistics or the integrated statistical data could be sampled by the digital calculator. The architecture suggested allows for both IF multiplications (for cross-correlation vector measurements directly) and quadrature downconversions (for generating baseband data used in performing covariance matrix calculations). This provides all the data needed for employing a number of adaptation algorithms with very little added complexity.

- It is suggested that the weight calculations be done digitally; this is really the only valid option if the architecture is to support more than one radio or adaptation algorithm. Furthermore, a microprocessor based circuit is suggested, which would provide additional flexibility for the entire AAP system.

- All the major subassemblies are identified and discussed as well, but they are not unique to AAP applications. For example, the frequency synthesizer must be fast hopping - a multi-loop phase-locked loop synthesizer is suggested. The RF front ends, downconverter circuits, RF and IF chains, dc power supplies and the antenna array are also discussed, and descriptions of commercially available components for implementing them are provided.

- The key components, items such as SAW filters, termination insensitive mixers, quadrature multipliers, etc. are suggested for use and an explanation of their importance is given.

The performance of this architecture depends on the accuracies of several of its circuits: the statistical measurement circuits, the weight calculator, the complex weighting circuits, and the IF and RF amplitude and phase variations through various paths. These accuracies are greatly improved by calibration; components and procedures for implementing these calibrations are described in detail, and help assure the AAP system hardware feasibility.

A major advantage of this architecture over others is that it allows implementation of many algorithms, a flexibility that could be exploited in further development efforts.

#### 4.4.4 SIMULATED PERFORMANCE EVALUATION

This section provides an evaluation of the computer simulation results presented in section 4.3.4. All the following comments refer to simulated results, and underscore the significance of the results in the context of an operating communication system.

#### 4.4.4 SIMULATED PERFORMANCE EVALUATION (continued)

○ The fundamental operation of the AAP was verified - the output of the AAP approaches the maximum attainable SINR in all cases tested.

○ The AAP converges very quickly in all cases tested. Equating the results to the EPLRS format, convergence is achieved in less than 256 chips, or 85 usec (one chip is about 333 nsec). Although a timeslot lasts about 2 msec, the transmission occurs in a burst of about 800 usec. Thus, the maximum attainable SINR is achieved in about ten percent of the transmission time.

○ With this fast convergence speed, the AAP is ideal for frequency hopped applications. The simulations provided consistent results in a severe jamming environment, with a different mix of high level jammers at each frequency bin.

○ The improved performance expected by storing and recalling weights unique to each frequency bin was verified. Once the bin is visited and the weights converge, those weights provide a very good starting point for adaptation during the next visit to that bin.

○ The antenna patterns illustrate the depth of the nulls in the directions of jammers and the high gain maintained in the SOI direction (a "beam").

○ The AAP supports network communications as well as LPI communications. The direction of the SOI is not consistent in the network case, causing potential problems for algorithms attempting to maximize SINR. The worst case condition is to have the SOI direction during the present timeslot be the same as an inadvertant null from the previous timeslot. The impact: the SOI is partially rejected (30 dB or more) at the beginning of adaptation. This case was simulated, and the AAP achieved convergence at rates consistent with the results above.

○ A SOI is expected to be present during on time processing by the algorithm. If conditions are such that the level of the SOI is too low for detection, the previously optimized weights will slowly drift away from optimal. Although the amount of drift was demonstrated to be acceptable, the algorithm could easily be modified to cease adaptation under these conditions.

○ The anticipative method of collecting off time data was proven effective.

○ The use of cross-correlation vector measurements  $R_{xy}$  rather than auto-correlation matrix measurements  $R_{xx}$  for on time data collection was proven valid. This will speed adaptation in future hardware developments.

○ Some antenna array investigation was conducted but this effort was not sufficient in scope to state any verifiable conclusions.

○ The AAP achieved the maximum attainable SINR with consistently fast convergence times for multiple jammers and a range of SJR from -10 to -40 dB.

○ The use of adapted receive weights to calculate the transmit weights, for application to directive and retrodirective communications was verified. The transmit antenna patterns achieved approached the optimal.

○ The directive communication transmit weights require averaging of the receive aperture estimates over a number of timeslots. This is easy to implement and very affective.

#### 4.4.4 SIMULATED PERFORMANCE EVALUATION (continued)

○ For LPI applications, directive communications dramatically reduces the geographical area a reconnaissance receiver must be in to detect the transmission.

○ For A/J applications, directive communications dramatically increases the SOI power available to the intended receiver given a fixed transmit power.

#### 4.4.5 SUMMARY / CONCLUSIONS

This study has resulted in a number of unique developments and provides supporting proofs, justifications, and simulations.

○ A flexible algorithm was developed specifically for FHSS and DSSS systems which has been demonstrated and would allow application to various Army communication systems.

○ An extremely flexible architecture concept has been developed which would provide compatibility with Army tactical radios and allow implementation of a variety of adaptation algorithms.

○ The basic computer model and simulation programs are established for future studies, and were used in this phase to verify the suggested algorithm and architecture. The models allow many parameters to be variables, thereby providing flexibility to simulate environmental conditions, hardware limitations, and various algorithms and architectures.

The conclusion of this Phase I effort allows several options for further development:

○ A multi-purpose AAP hardware development which allows testing and verification of a variety of algorithms under real world conditions could be pursued. This hardware could be designed to be compatible with an existing Army radio. The Phase 2 proposal is based on development of this AAP hardware.

○ Additional study of the Dominant Mode Block Update algorithm could be undertaken.

○ Further development of the architecture suggested in this study, optimized for a specific Army radio, could be undertaken. Commitment to hardware could occur at a later date.

○ Additional study of the application of adaptive array processing to directive communications could be pursued. The primary application is low probability of intercept communication, which shows good promise.

○ Other, less directly related applications are also mentioned in the Phase 2 proposal for future development, including direction finding.

#### 4.5 LIST OF ALL TECHNICAL PUBLICATIONS

Other than the documents generated directly for this SBIR program (ie. monthly reports and this final report), there have been no technical documents generated as part of this contract. A proof showing some of the algorithms investigated to yield maximum likelihood estimates was started, and is expected to be submitted for publication at some later date. A preliminary abstract for this paper is provided below; when this paper is submitted for publication, the support of this study will be recognized and credited.[31]

#### 4.5 LIST OF ALL TECHNICAL PUBLICATIONS (continued)

##### Preliminary Abstract of Maximum Likelihood Estimator Proof -

A unifying framework for the design of blind adaptive signal extraction algorithms, based on maximum likelihood (ML) estimation of unknown signals with known modulation properties, is presented. The general ML estimator of a single signal of interest (SOI) with known properties is derived, under the assumption that the SOI is received by a narrowband antenna array in the presence of temporally-white complex-Gaussian interference with unknown spatial covariance. It is shown that the ML estimator admits a simple objective function if the SOI can be modelled as a member of a property set that encompasses all signals with the properties possessed by the transmitted SOI waveform or symbol sequence. This objective function is shown to have a Rayleigh Quotient form with a closed-form optimal solution if the property set is a linear subspace that is not spanned by the set of received data, for example, if the SOI is a time-limited, frequency-limited, FHSS or DSSS waveform. The objective function is also shown to reduce to a simple normalized least-squares form with an iteratively achievable optimal solution for a number of useful nonlinear property sets, for example, if the SOI waveform or symbol sequence has a constant modulus or a known modulus variation. Lastly, results are extended to more complicated environments where multiple SOIs are received in temporally-white complex-Gaussian interference, and where a single SOI is received in the presence of temporally-colored complex-Gaussian interference. Using these theoretical results, it is demonstrated that many of the blind and partially blind array adaptation algorithms developed to date can be interpreted as maximum likelihood estimation techniques.

#### 4.6 PERSONNEL SHOWING ADVANCED DEGREES EARNED WHILE ON PROJECT

None.

## 5. BIBLIOGRAPHY

- [1] B. Widrow, P. E. Mantey, L. J. Griffiths, B. B. Goode, "Adaptive Antenna Systems," *Proc. IEEE*, December 1967
- [2] J. G. Proakis, *Advances in Equalization of Intersymbol Interference*, Advances in Communications Systems, ed. A. V. Balakrishnan, A. J. Viterbi, N. Y. Academic Press, 1975
- [3] H. R. Rudin, Jr., "A Continuously-Adaptive Equalizer for General-Purpose Communications Channels," *BSTJ*, July-Aug. 1969
- [4] D. F. DiFonzo, W. S. Trachtman, A. E. Williams, "Adaptive Polarization Control for Frequency Reuse Systems," *COMSAT Technical Review*, vol. 6, Fall 1976
- [5] L. J. Griffiths, "A Simple Adaptive Algorithm for Real-Time Processing in Antenna Arrays," *Proc. IEEE*, vol. 57, Oct. 1969
- [6] O. L. Frost, "An Algorithm for Linearly-Constrained Adaptive Array Processing," *Proc. IEEE*, vol. 60, August 1972
- [7] B. G. Agee, "The Property Restoral Approach to Blind Adaptive Signal Extraction," Ph.D. Dissertation, Dept. of EECS, Univ. of Calif., Davis, 1989
- [8] B. G. Agee, S. V. Schell, W. A. Gardner, "Spectral Self-Coherence Restoral: A New Approach to Blind Adaptive Signal Extraction Using Antenna Arrays," *Proc. IEEE*, vol. 78, no. 4, pp. 753-767, April 1990
- [9] C. L. Nikias, M. R. Raghuveer, "Bispectrum Estimation: a Digital Signal Processing Framework," *Proc. IEEE*, vol. 75, no. 7, pp. 869-891, July 1987
- [10] G. B. Giannakis, "Cumulants: a Powerful Tool in Signal Processing," *Proc. IEEE*, vol. 75, no. 9, pp. 1333-1334, September 1987
- [11] D. N. Godard, "Self-Recovering Equalization and Carrier Tracking in Two-Dimensional Data Communication Systems," *IEEE Trans. Comm.*, vol. COM-28, pp. 1867-1875, November 1980
- [12] J. R. Treichler, B. G. Agee, "A New Approach to Multipath Correction of Constant Modulus Signals," *IEEE Trans. ASSP*, vol. ASSP-31, pp. 459-472, April 1983
- [13] J. R. Treichler, M. L. Larimore, "New Processing Techniques Based on the Constant Modulus Algorithm," in *IEEE Trans. ASSP*, pp. 420-431, April 1985
- [14] W. A. Sethares, G. A. Rey, C. R. Johnson, "Approaches to Blind Equalization of Signals With Multiple Modulus," in *Proc. 1989 Intl. Conf. on ASSP*, pp. 972-975, 1989
- [15] K. L. Reinhard, "Adaptive Antenna Arrays in Coded Communications Systems," Doctoral Dissertation, Ohio State University, 1973
- [16] R. T. Compton, "An Adaptive Array in a Spread Spectrum Communications System," *Proc. IEEE*, vol. 66, no. 3, pg. 289, March 1978

## 5. BIBLIOGRAPHY (continued)

- [17] D. M. DiCarlo, R. T. Compton, "Reference Loop Phase-Shift in Adaptive Arrays," *IEEE Trans. Aero. and Elect. Syst.*, vol. AES-14, no. 4, pg. 559, July 1978
- [18] Y. Bar-Ness, F. Haber, "Interference Canceller Array With Reference Generating Loop," *IEEE Trans. Aero. and Elect. Syst.*, vol. AES-21, no. 5, pp. 654-662, Sept. 1985
- [19] M. W. Ganz, R. T. Compton, "A Data-Derived Reference Signal Technique for Adaptive Arrays," *IEEE Trans. Comm.*, vol. 37, no. 9, pp. 975-983, Sept. 1989
- [20] K. Bakhru, D. J. Torrieri, "The Maximin Algorithm for Adaptive Arrays and Frequency-Hopping Communications," *IEEE Trans. Ant. and Prop.*, vol. AP-32, no. 9, pp. 919-928, Sept. 1984
- [21] D. J. Torrieri, K. Bakhru, "Frequency Compensation in Adaptive Antenna System for Frequency-Hopping Communications," *IEEE Trans. Aero. and Elect. Syst.*, vol. AES-23, no. 4, pp. 448-467, July 1987
- [22] D. J. Torrieri, K. Bakhru, "An Anticipative Adaptive Array for Frequency-Hopping Communications," *IEEE Trans. Aero. and Elect. Syst.*, vol. AES-24, no. 4, pp. 449-456, July 1988
- [23] B. G. Agee, "Property Restoral Beamforming Study: Final Report," Tech. Report No. AGI-88-11, AGI Engineering Consulting, Campbell, CA, November 1988
- [24] B. G. Agee, "Fast Acquisition of Burst and Transient Signals Using a Predictive Adaptive Beamformer," in *Proc. 1989 IEEE Military Communications Conference*, 1989
- [25] E. J. Kelly, "An Adaptive Detection Algorithm," *IEEE Trans. Aero. and Elect. Systems*, vol. AES-22, pp. 115-127, Mar. 1987
- [26] D. M. Dlugos, R. A. Scholtz, "Acquisition of Spread Spectrum Signals by an Adaptive Array," *IEEE Trans. ASSP*, vol. 37, no. 8, pp. 1253-1270, Aug. 1989
- [27] B. G. Agee, "The Least-Squares CMA: A New Technique for Rapid Correction of Constant Modulus Signals," in *Proc. 1986 Intl. Conf. on ASSP*, pp. 953-956, 1986
- [28] R. P. Gooch, J. Lundel, "The CM Array: An Adaptive Beamformer for Constant Modulus Signals," in *Proc. 1986 Intl. Conf. on ASSP*, 1986
- [29] B. G. Agee, "Blind Separation and Capture of Communication Signals Using a Multitarget Constant Modulus Beamformer," in *Proc. 1989 IEEE Military Communications Conference*, 1989
- [30] B. G. Agee, "Performance Evaluation of the Multitarget Modulus Restoral Algorithm Against the KEYSTROKE Data Set," Tech. Report No. AGI-90-04, AGI Engineering Consulting, Campbell, CA, April 1990
- [31] B. G. Agee, "Maximum-Likelihood Approaches to Blind Adaptive Signal Extraction Using Antenna Arrays, Part I: Extraction of Structured Waveforms," in preparation



**5. BIBLIOGRAPHY (continued)**

- [32] DiCarlo79, "Reference Loop Phase Shift in an N-element Adaptive Array," *IEEE Trans. Aero. and Elect. Syst.*, vol. AES-15, pp. 576-582, Jan. 1979
- [33] G. Strang, *Linear Algebra and Its Applications*, Orlando, FL: Harcourt, Brace & Jobanovich, 1988
- [34] J. H. Wilkinson, *The Algebraic Eigenvalue Problem*, Oxford Science Publications, 1965

**6. APPENDIXES**

None.